Observational Basics of Modern Cosmology (part II)

by Prof. M.V. Sazhin

Sternberg Astronomical Institute
Moscow State University
Russia

The Cosmology Today

Today cosmology is entered in “golden age”.

Several scientific organization were established which are specially devoted to cosmological investigations. Discussion on the cosmology became popular among community. All that provides us with hope that cosmology will be necessary element of mankind culture for a long time.

Three sources of success:

1. The development of astronomical observation;

2. The development of physical theory;

3. The moral courage of the scientists.

The observational basis of the Standard Cosmological Model

1. Expansion of our Universe

2. Existence of primordial radiation

3. The discovery of Large Scale Structure of our Universe

4. Light element abundance in our Universe

5. Anisotropy of the CMBR

5. Anisotropy of the CMBR

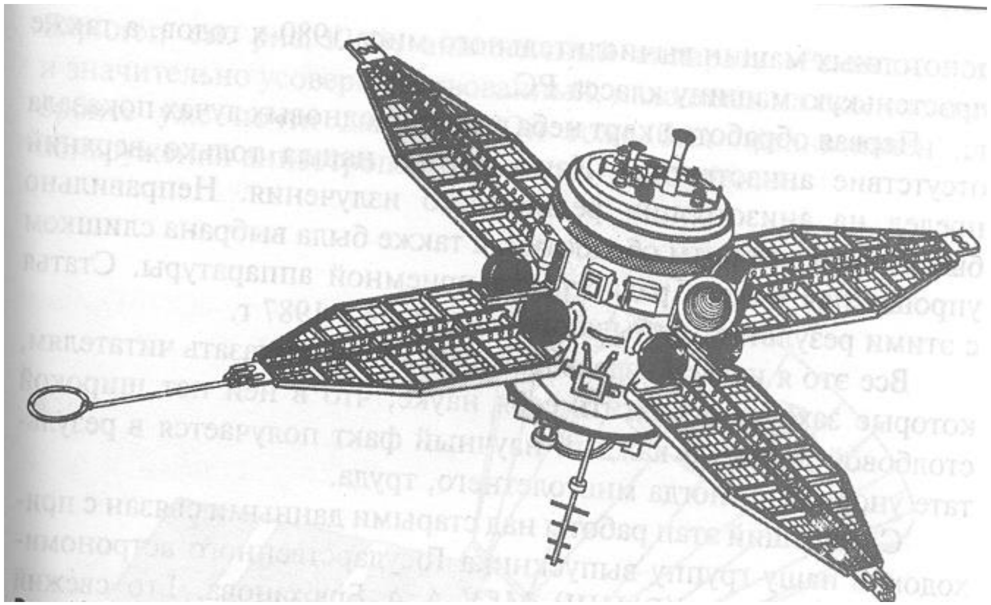

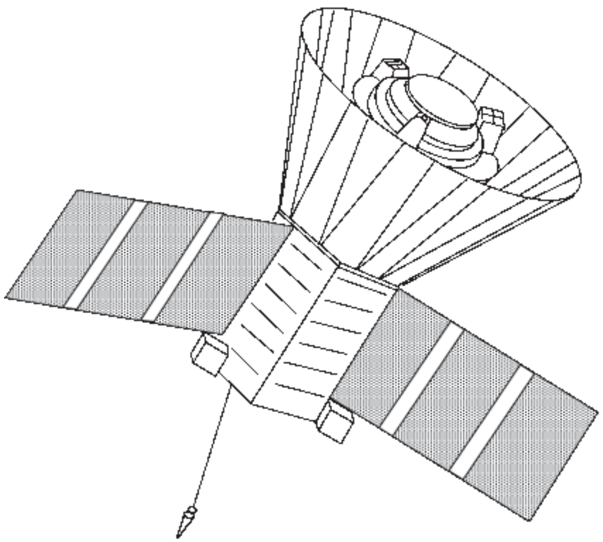

The last observational fact amoung the main is anisotropy of the CMBR.

The anisotropy was discovered in 1992.

Two groups announced the observation of the anisotropy signal. The first was the Relic group and the second was COBE.

Equation that describes the anisotropy of the CMBR

$$\frac{\delta T}{T} = -\frac{1}{2}\int \frac{\partial h_{ij}(t(\tau), x(\tau))}{\partial \tau} e^i e^j + \frac{1}{4}\frac{\delta \varepsilon_r}{\varepsilon} + \left(\frac{\vec{v}}{c}\vec{e}\right)_r$$

$$\frac{\delta T(\theta, \varphi)}{T} = \sum_{l,m} a_{lm} Y_{lm}(\theta, \varphi)$$

$$c_l = \frac{1}{2l+1}\sum_{m=-l}^{l} a_{lm}{}^2$$

$$c_l = \frac{c_0}{l(l+1)}$$ - **HZ-spectrum**

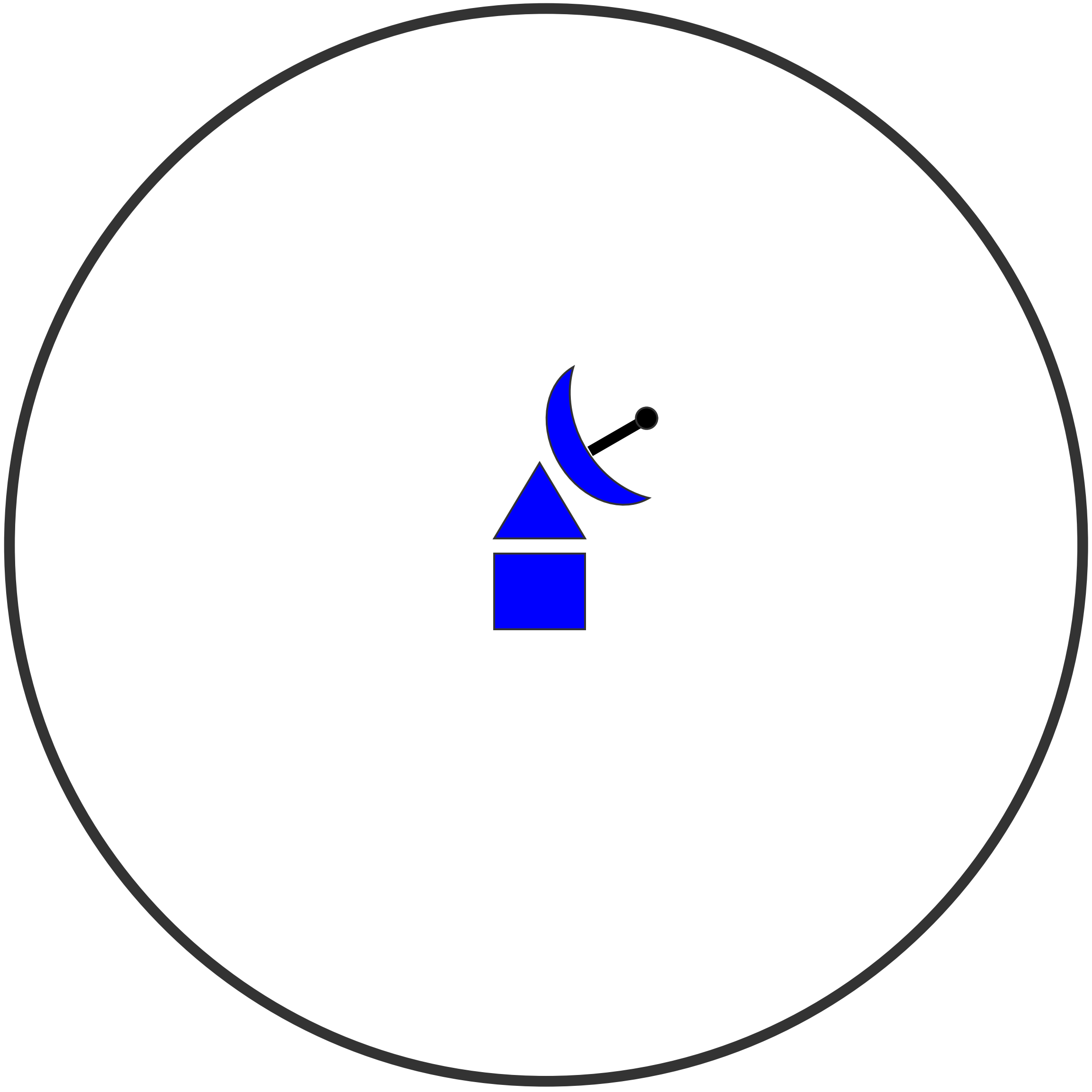

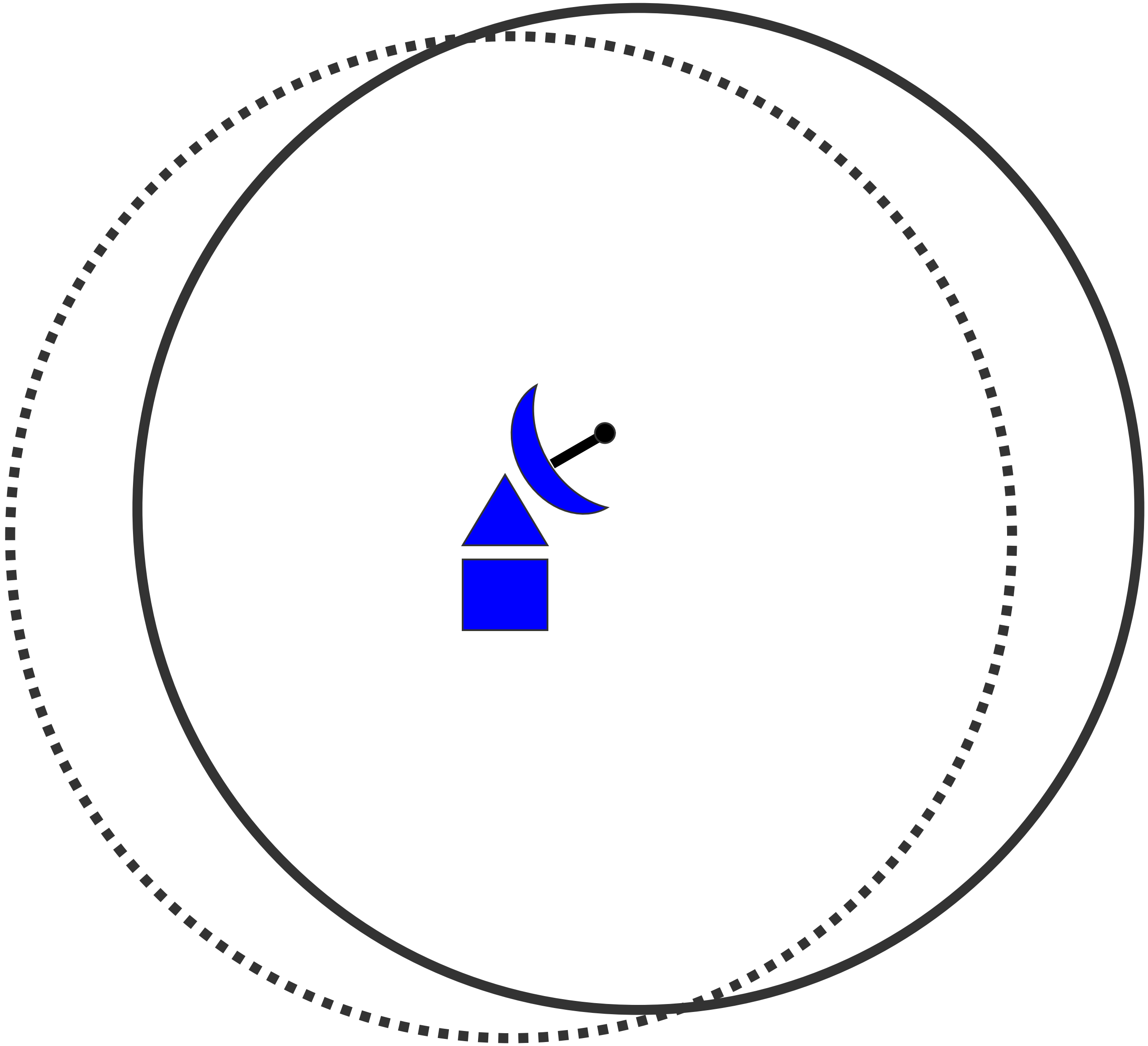

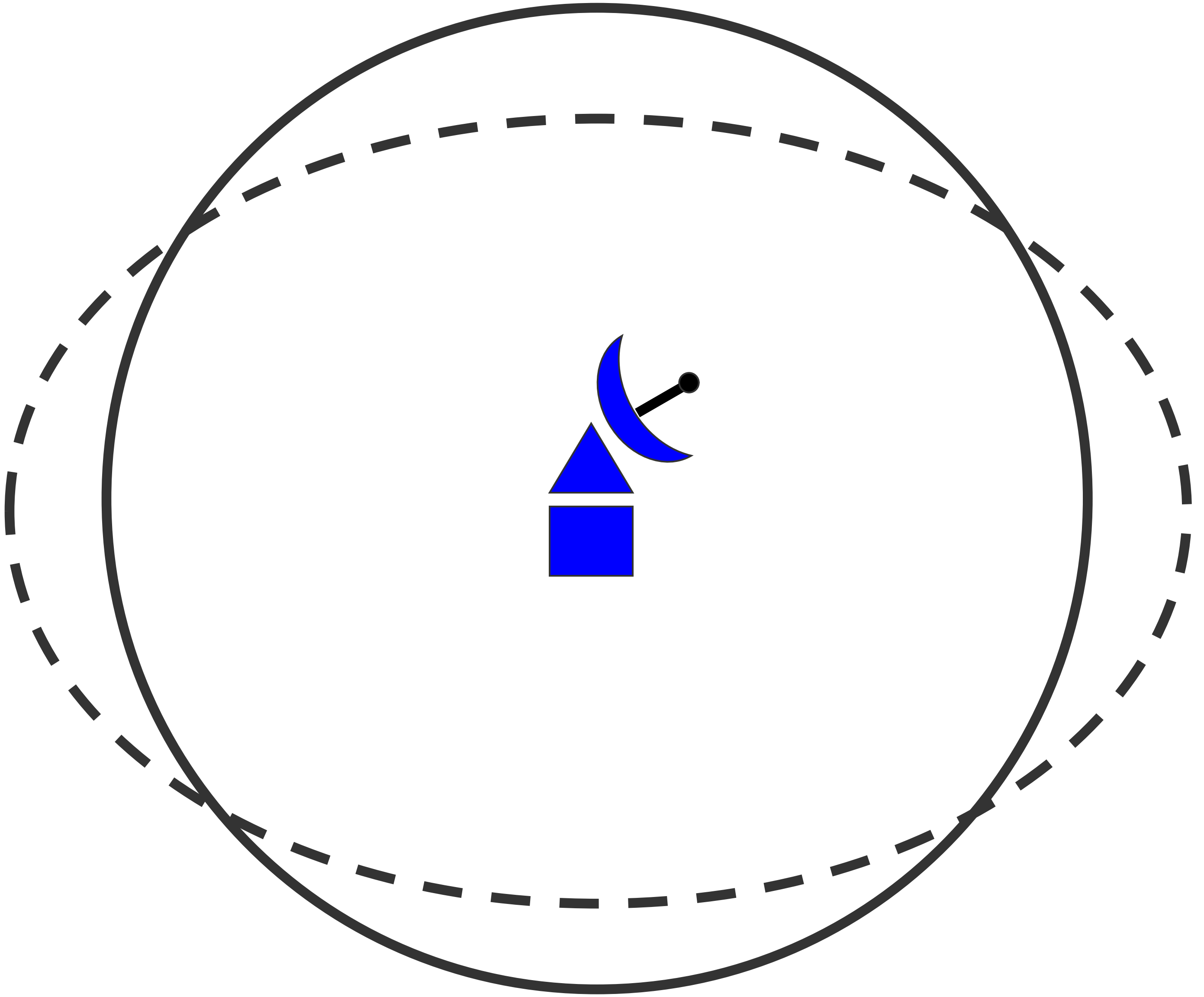

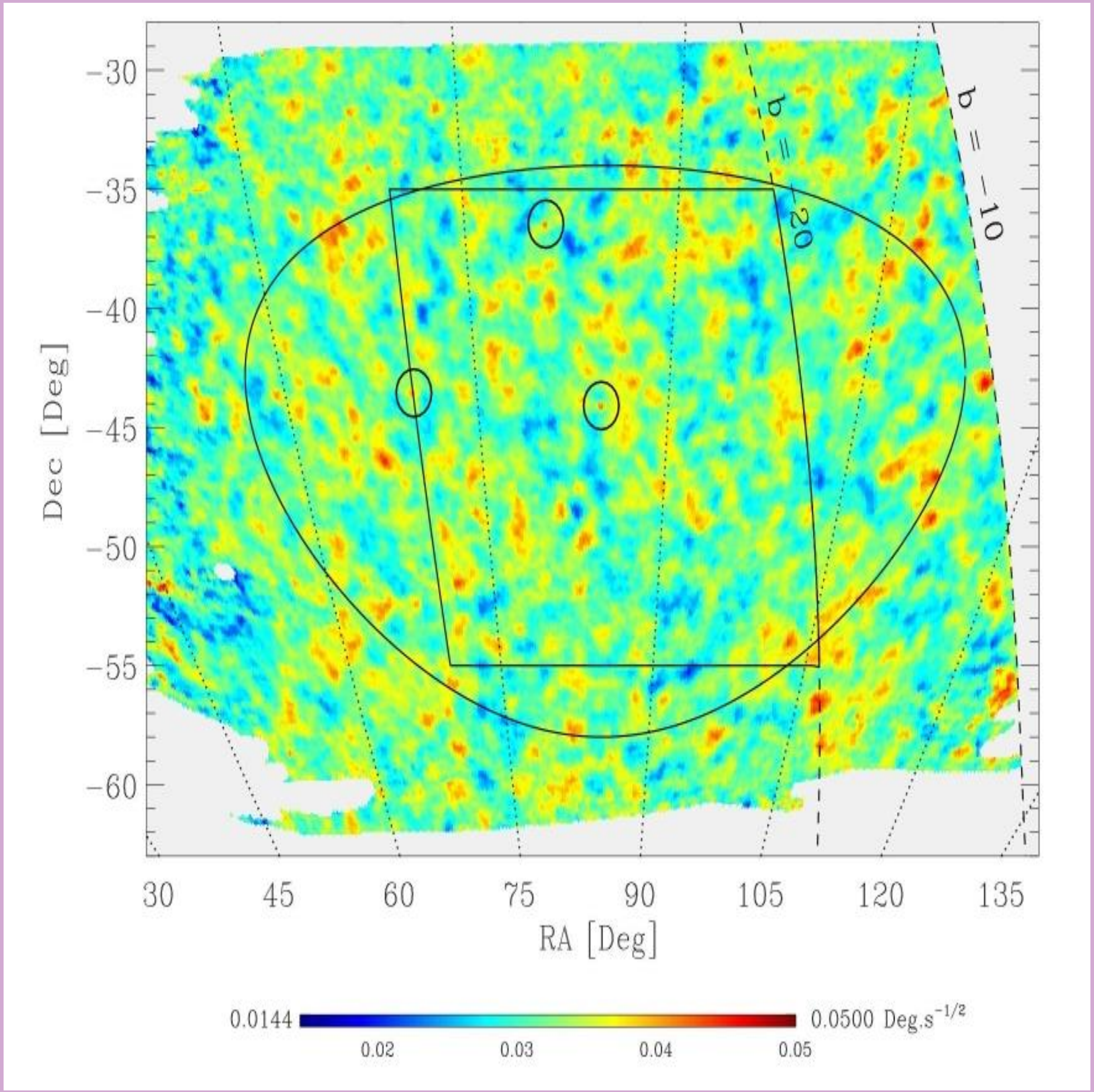

Part of the sky which was observed in Boomerang experiment

Total area is approximately 5% of the sky.

Boomerang

Boomerang

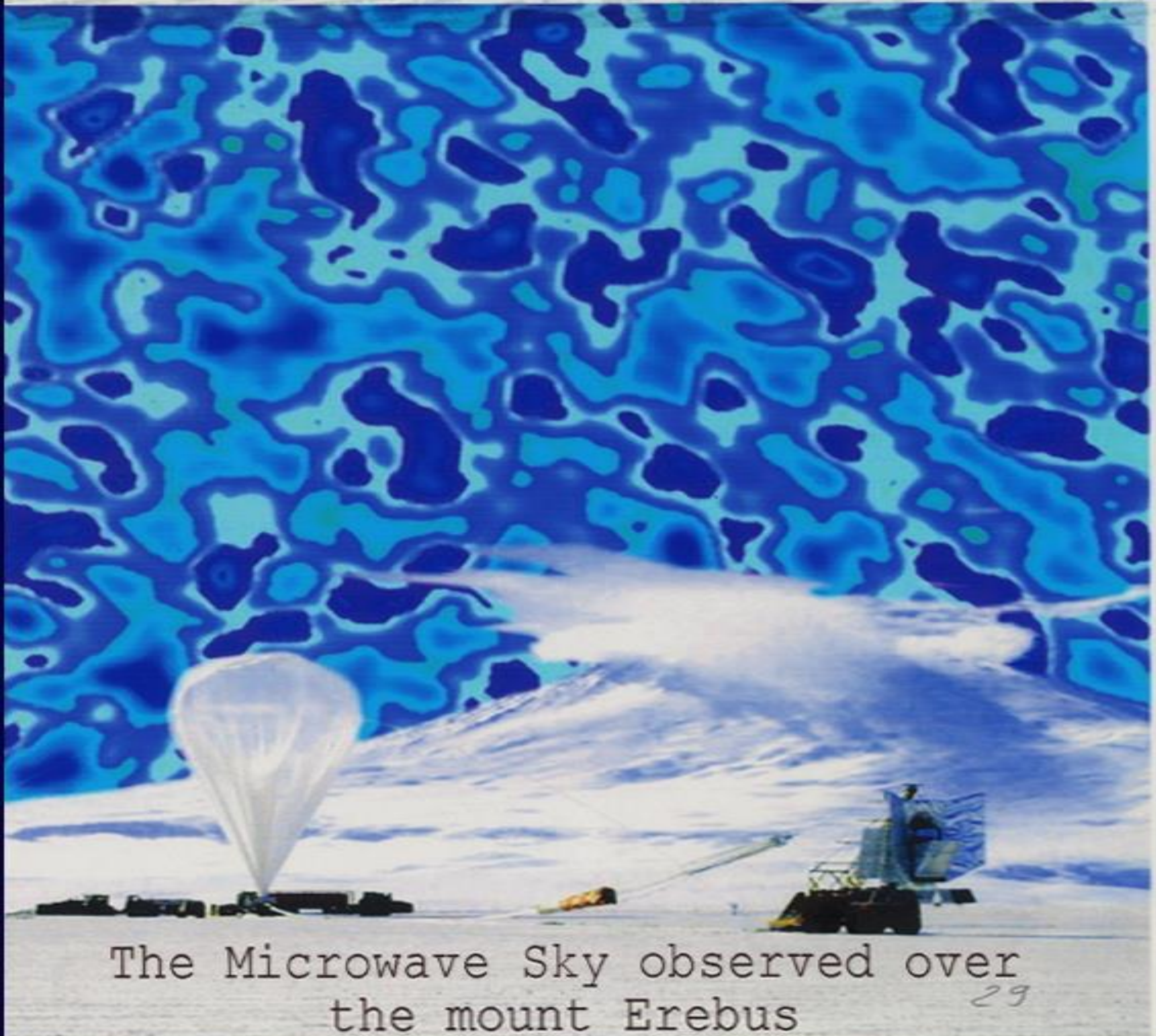

Angular spectrum of anisotropy obtained as a result of **Boomerang** experiment. Blue and red dots designate the same data value calculated with different methods.

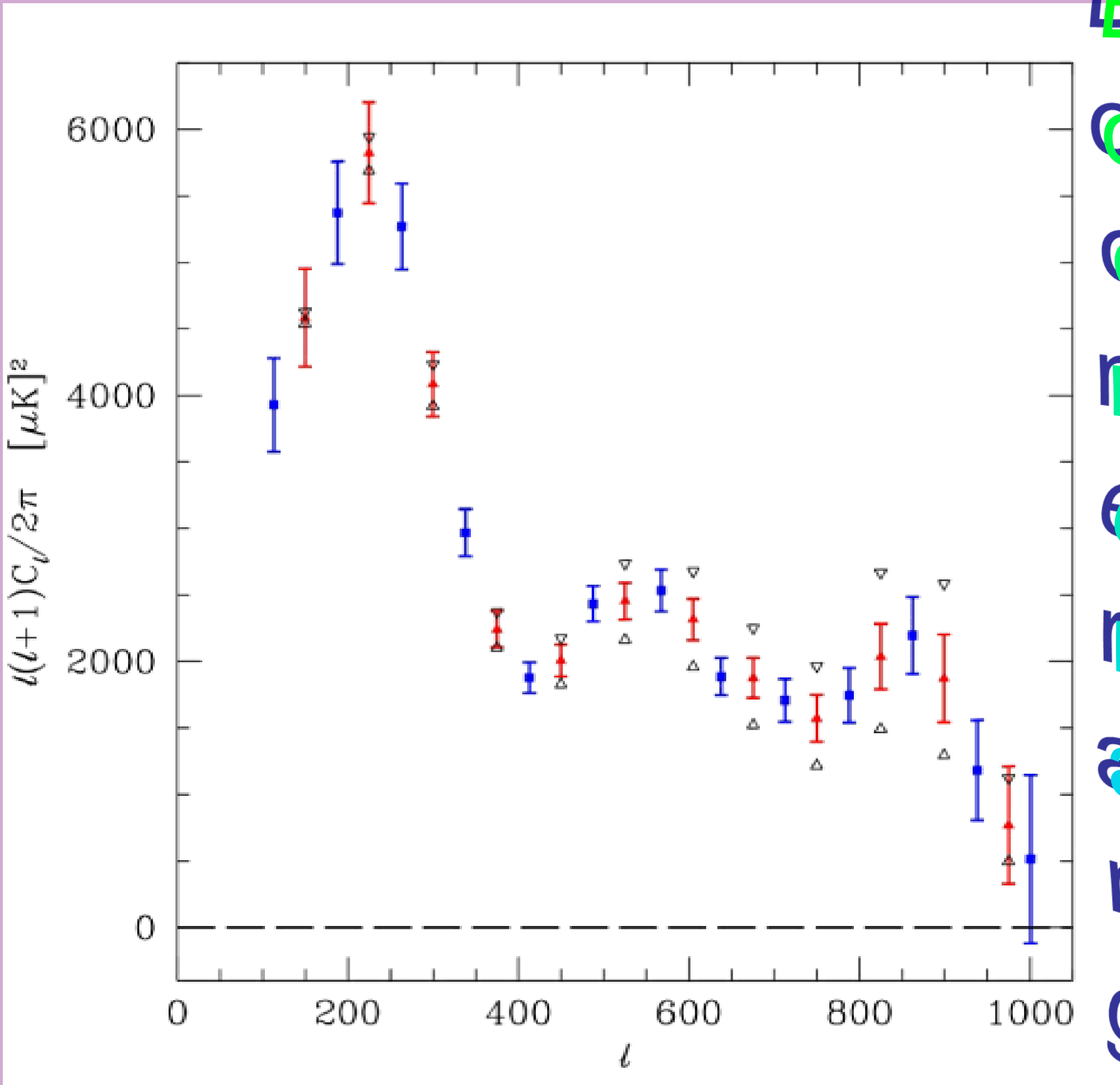

Boomerang

Experiment + models

The comparison between observational data *(dots with two error bars)* and theoretical predictions *(solid curve).*

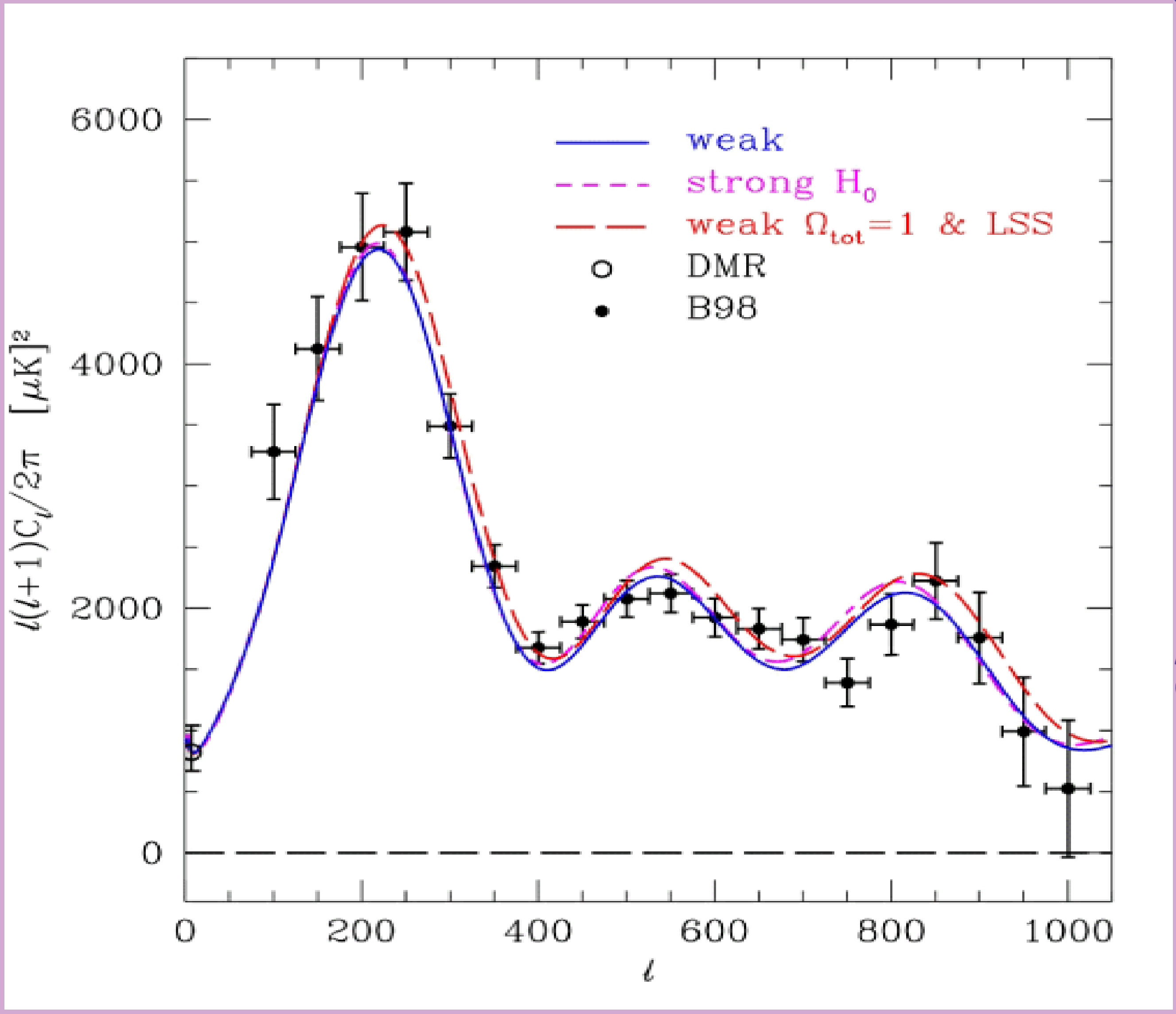

Boomerang

Polarization of the CMBR

Stoks' parameters:

$$I = I_l + I_r$$

$$Q = I_l - I_r$$

$$U = I_{12} + I_{21}$$

$$V = i\left(I_{21} - I_{12}\right)$$

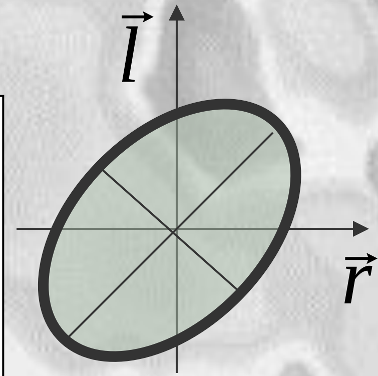

$$I = \sum_{l,m} a_{lm} Y_{lm}(\theta,\varphi)$$

$$Q \pm iU = \sum_{l,m} a_{lm}{}^{\pm 2} Y_{lm}{}^{\pm 2}(\theta,\varphi)$$

$$a_{lm}{}^{E} = \frac{1}{2}\left(a_{lm}{}^{+2} + a_{lm}{}^{-2}\right)$$

$$a_{lm}{}^{B} = \frac{i}{2}\left(a_{lm}{}^{+2} - a_{lm}{}^{-2}\right)$$

$$\frac{\partial \delta}{\partial \eta} + \frac{\partial \delta}{\partial x^{\alpha}} \cdot e^{\alpha} = \frac{1}{2}\frac{\partial h_{\alpha\beta}}{\partial \eta} e^{\alpha} e^{\beta} - \sigma_T N_e a(\eta) \times$$

$$\left(\delta - \oint P(\Omega, \Omega')\delta(\Omega')d\Omega'\right)$$

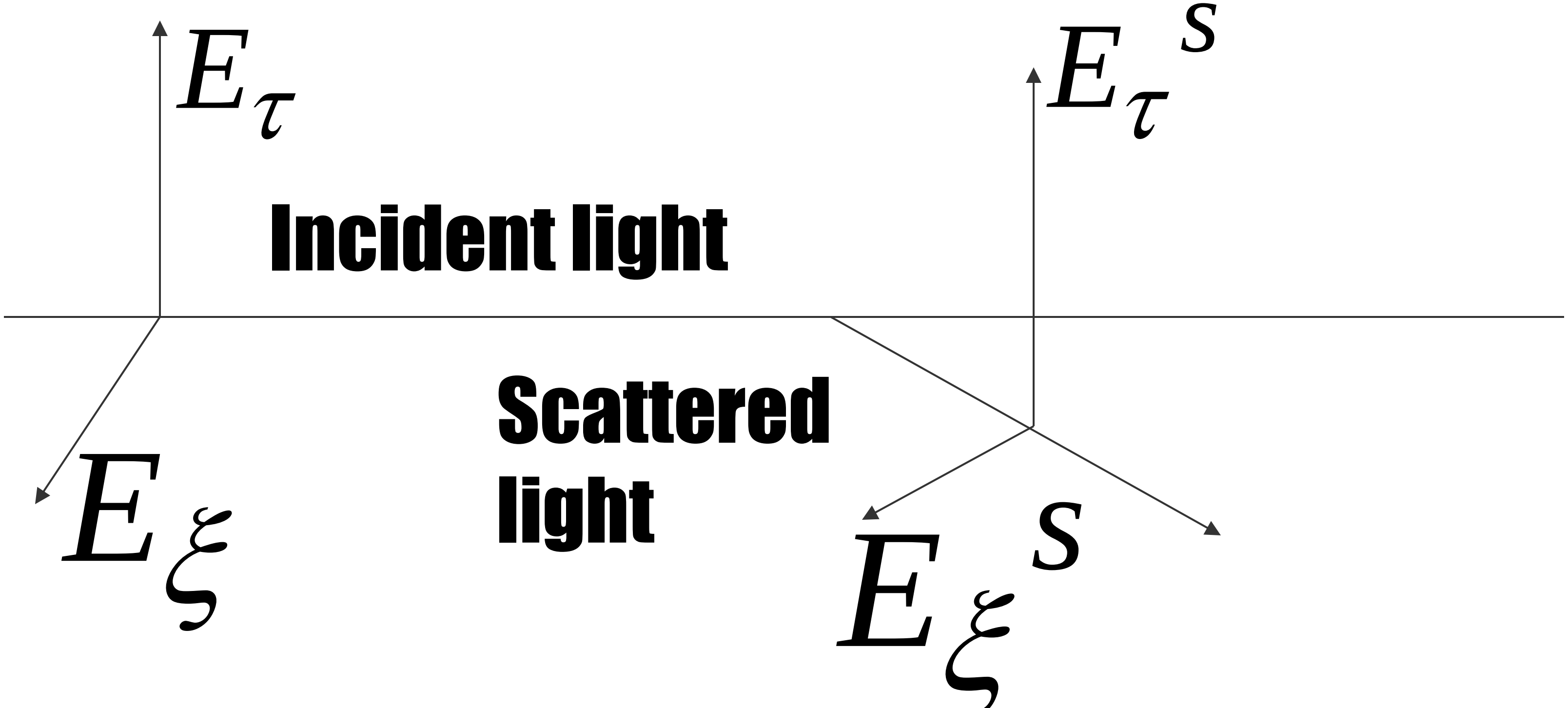

DASI

E and **B** polarization modes **(DASI)**

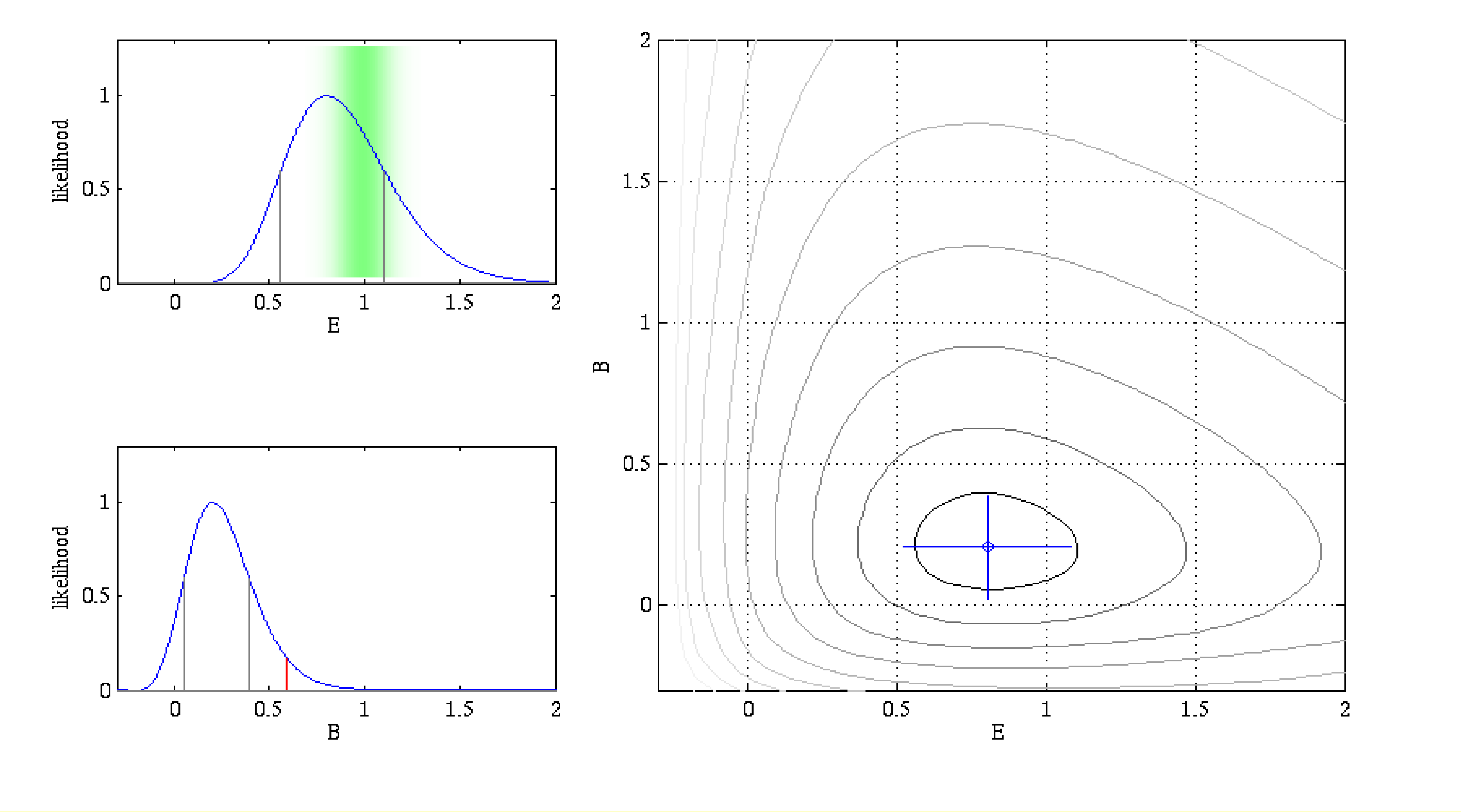

DASI

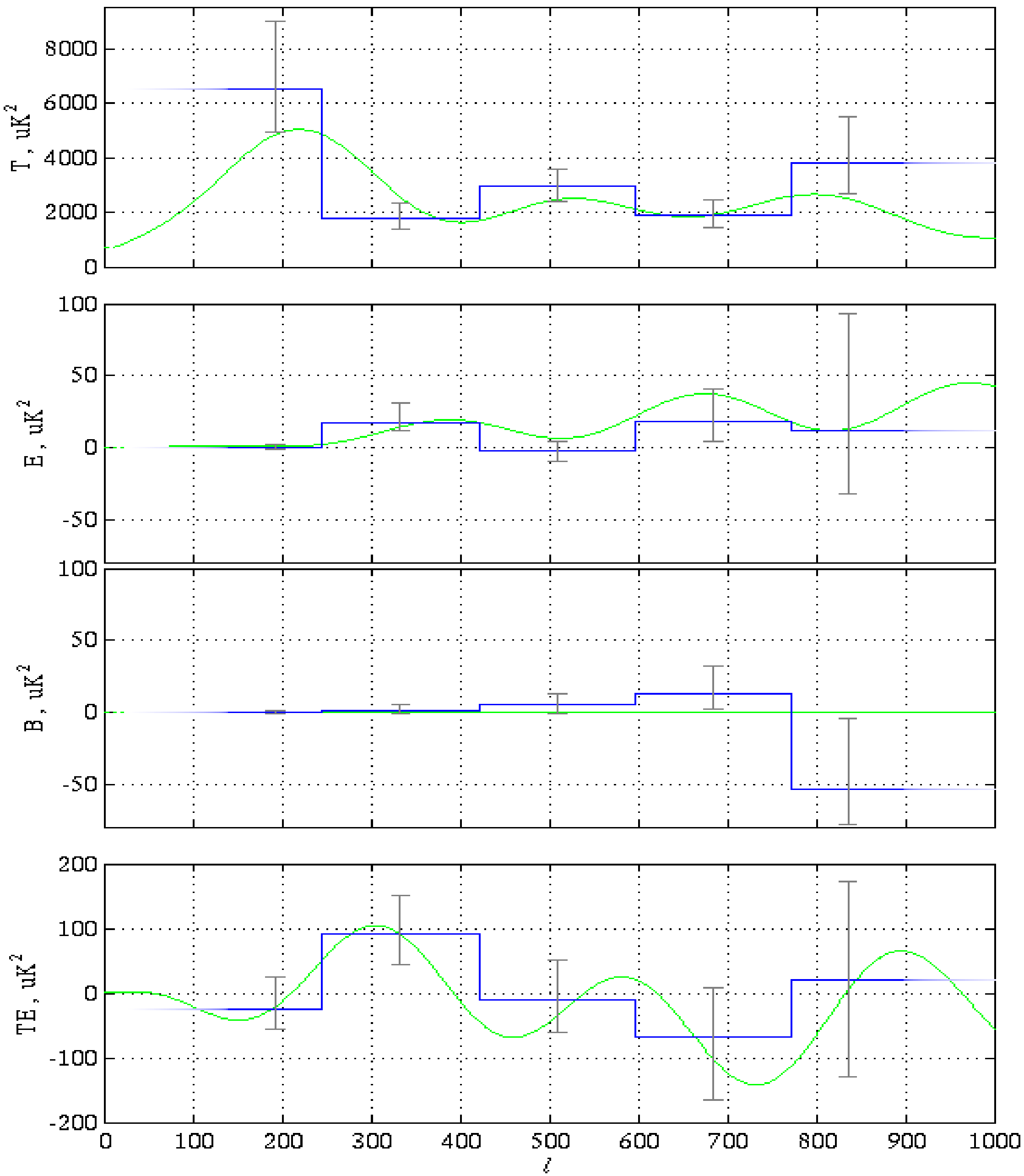

T, uK^2
8000
6000
4000
2000
0
E, uK^2
100
50
0
-50
B, uK^2
100
50
0
-50
TE, uK^2
200
100
0
-100
-200
0
100
200
300
400
500
600
700
800
900
1000
l

DASI

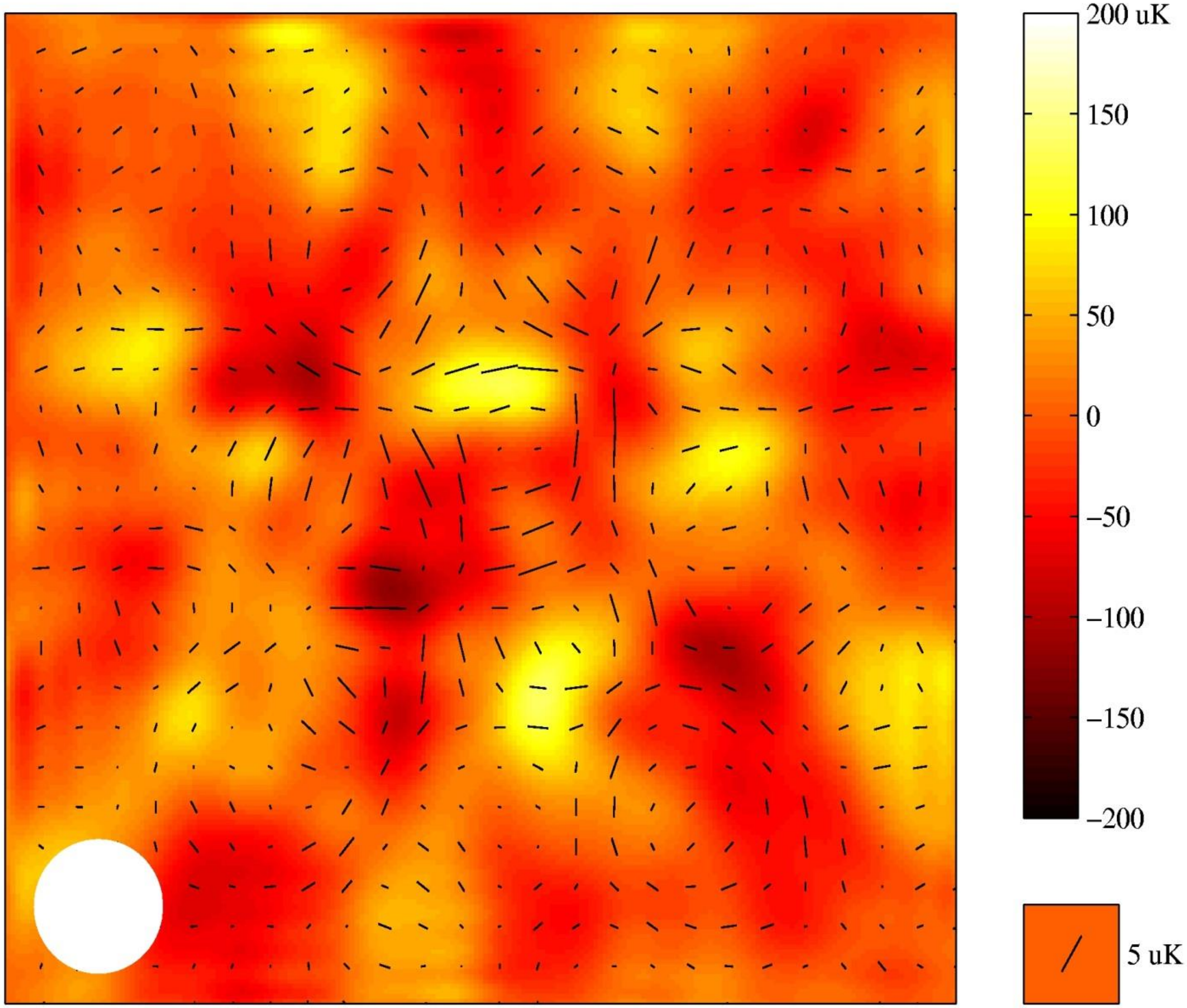

Map is 5 degrees square

DASI

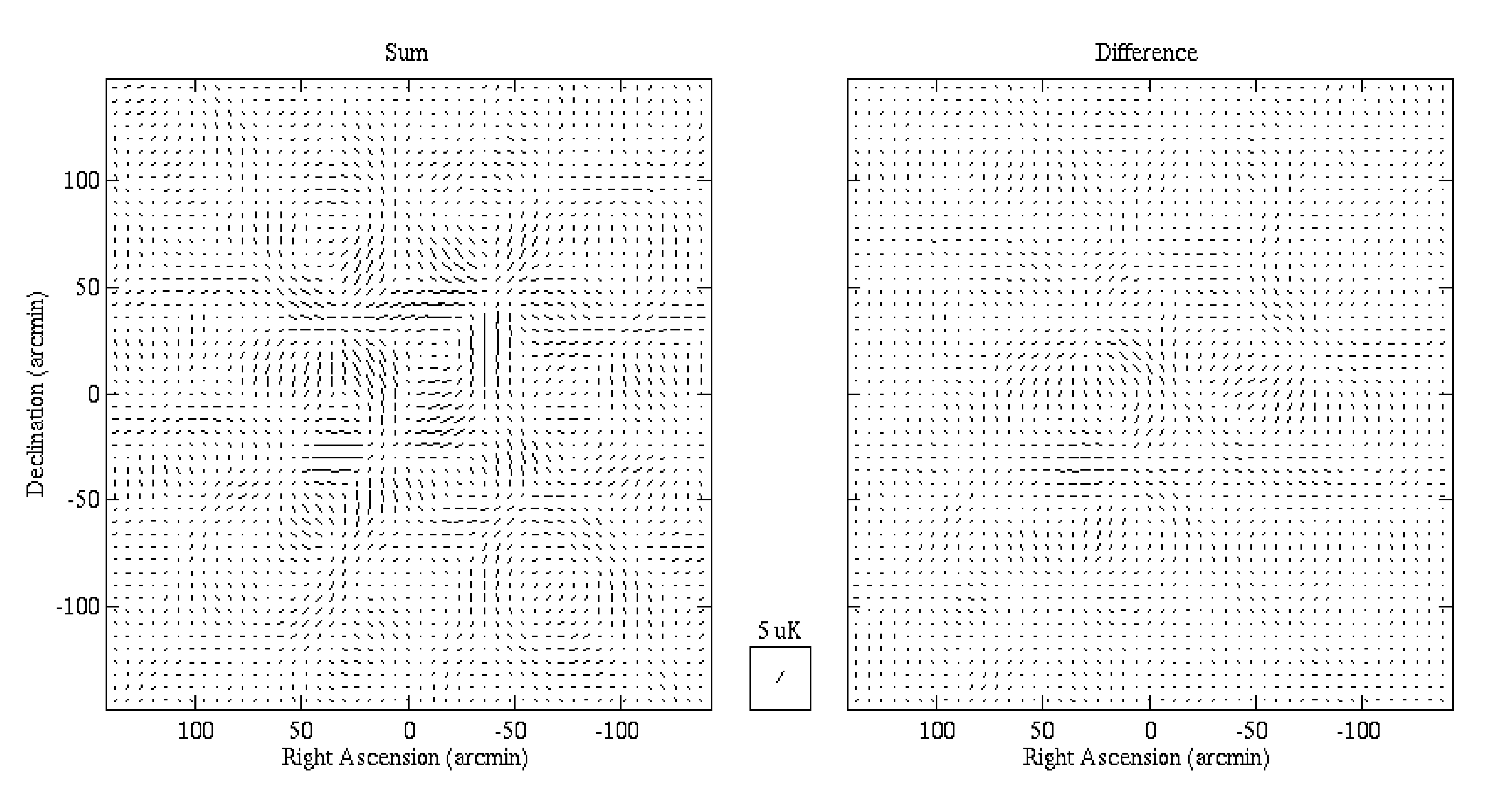

Sum
Difference
Declination (arcmin)
100
50
0
-50
-100
Right Ascension (arcmin)
5 uK

WMAP

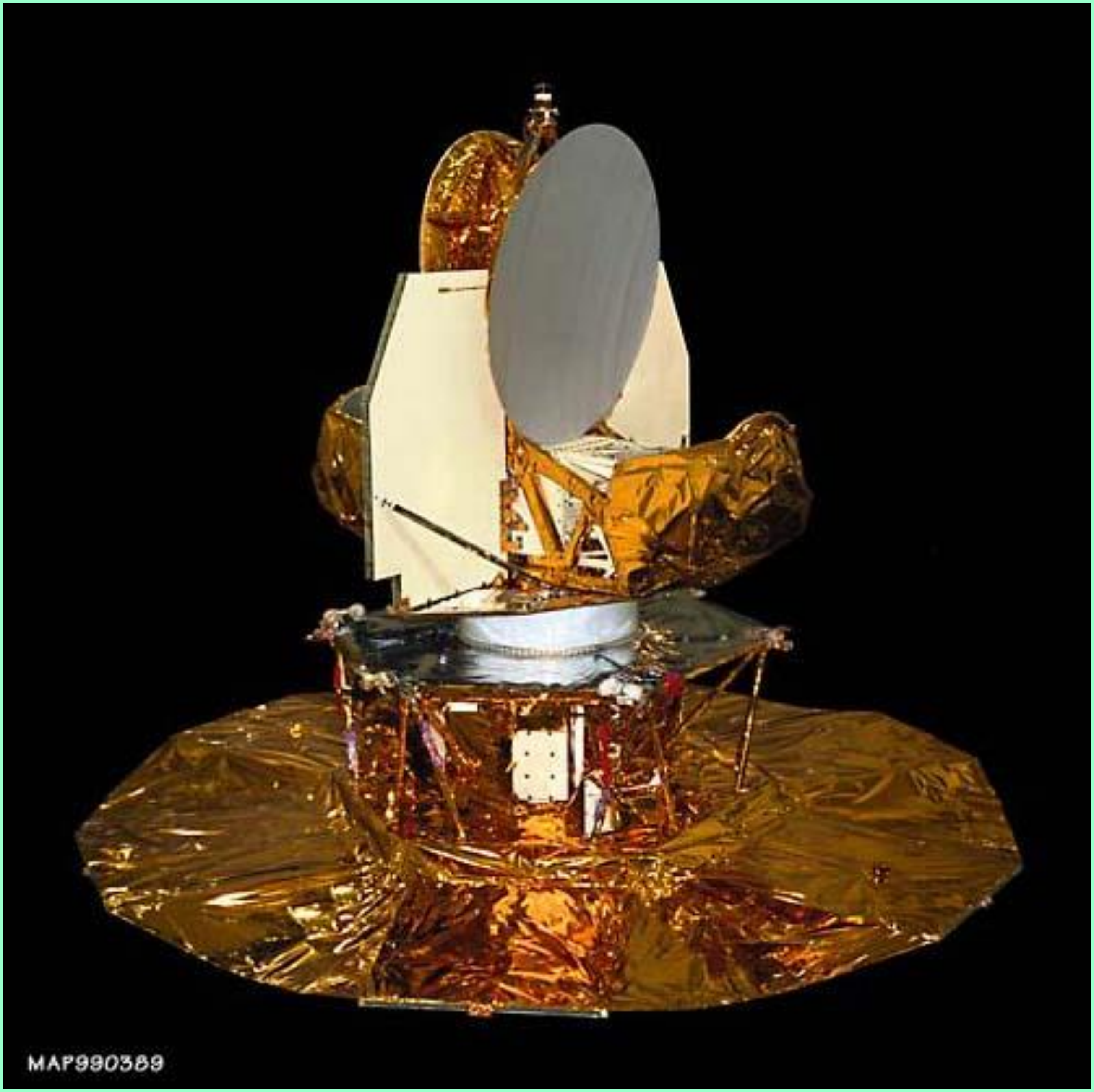

WMAP

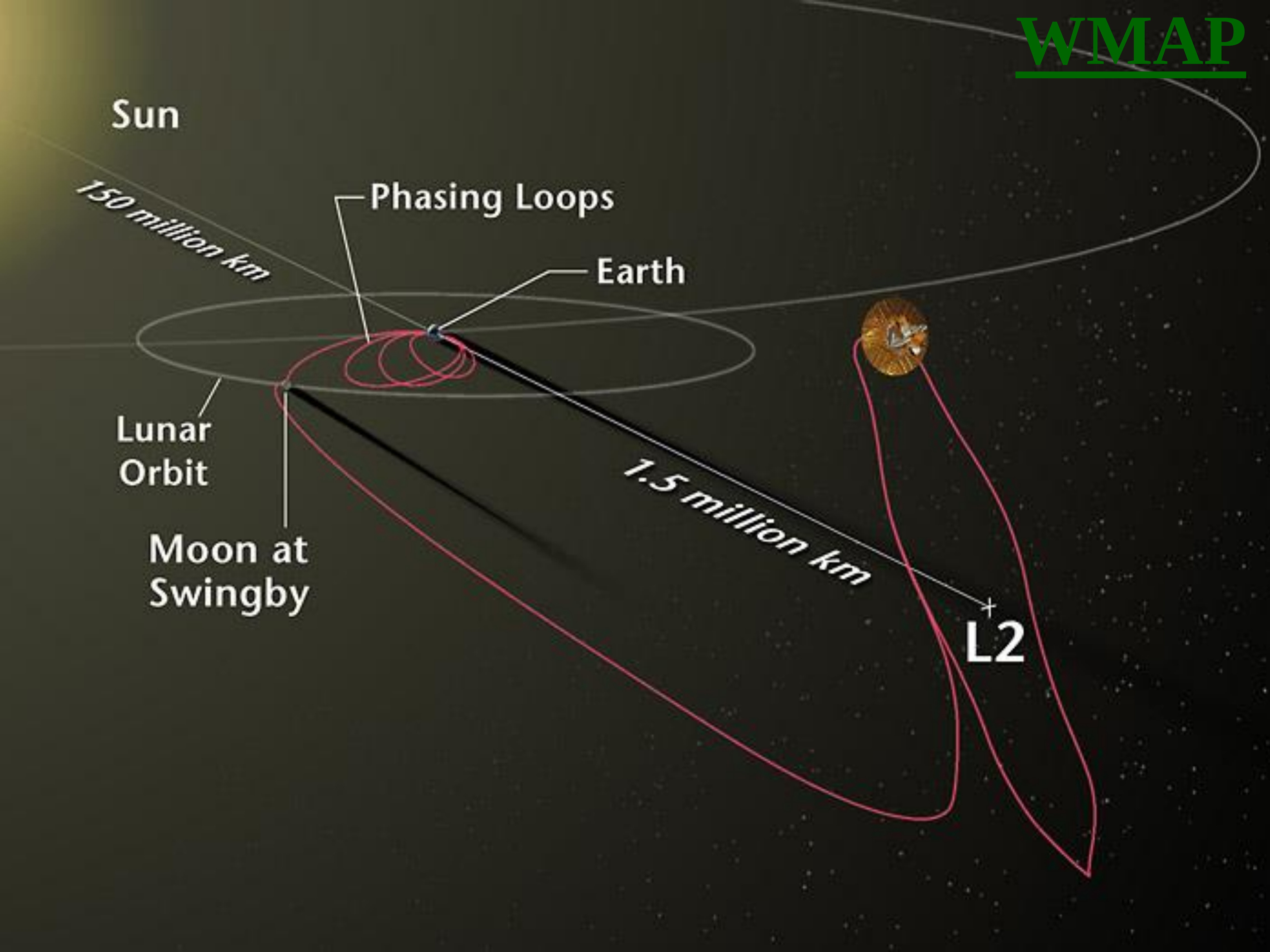

Sun
150 million km
Phasing Loops
Earth
Lunar Orbit
Moon at Swingby
1.5 million km
L2

WMAP

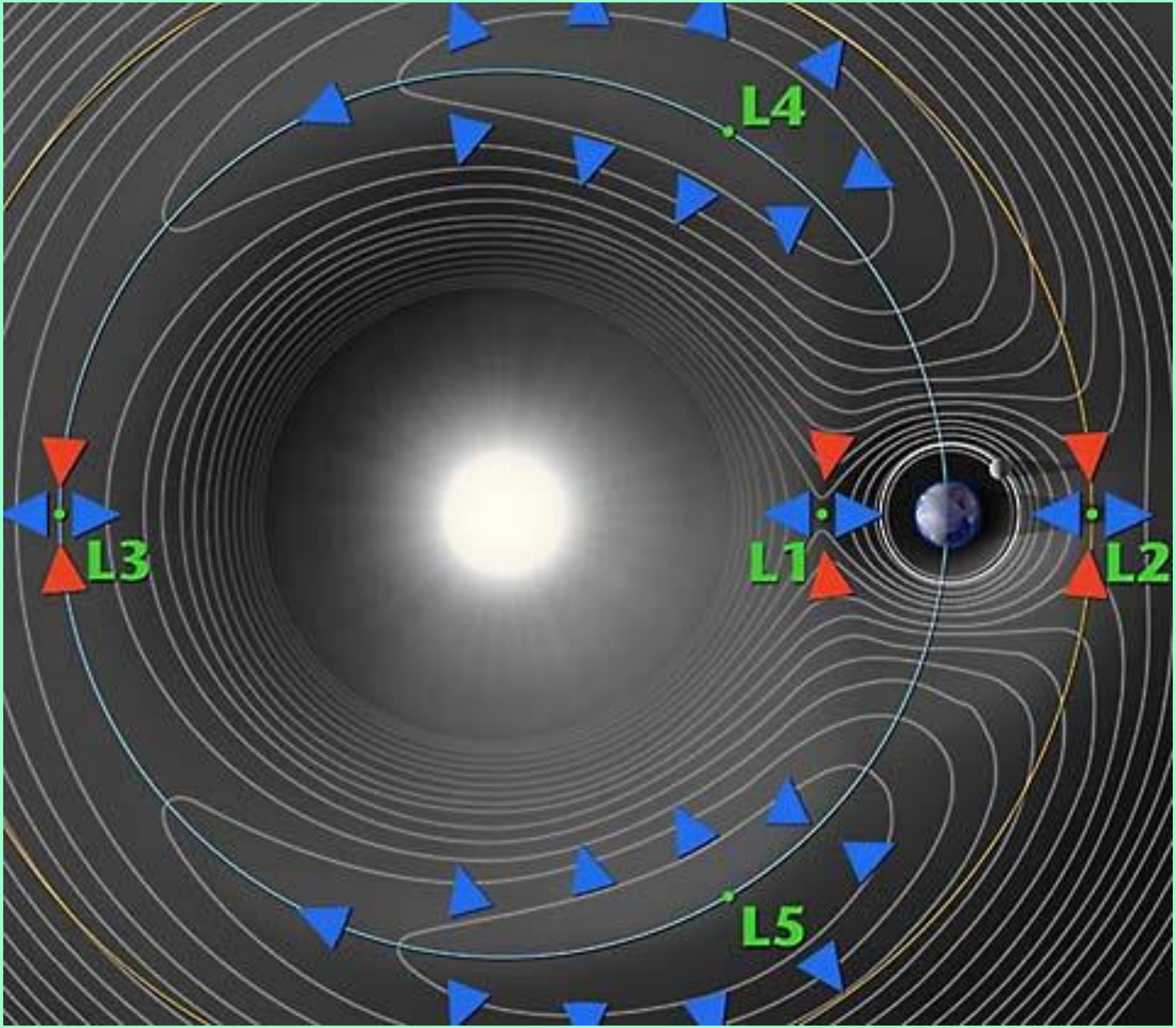

WMAP

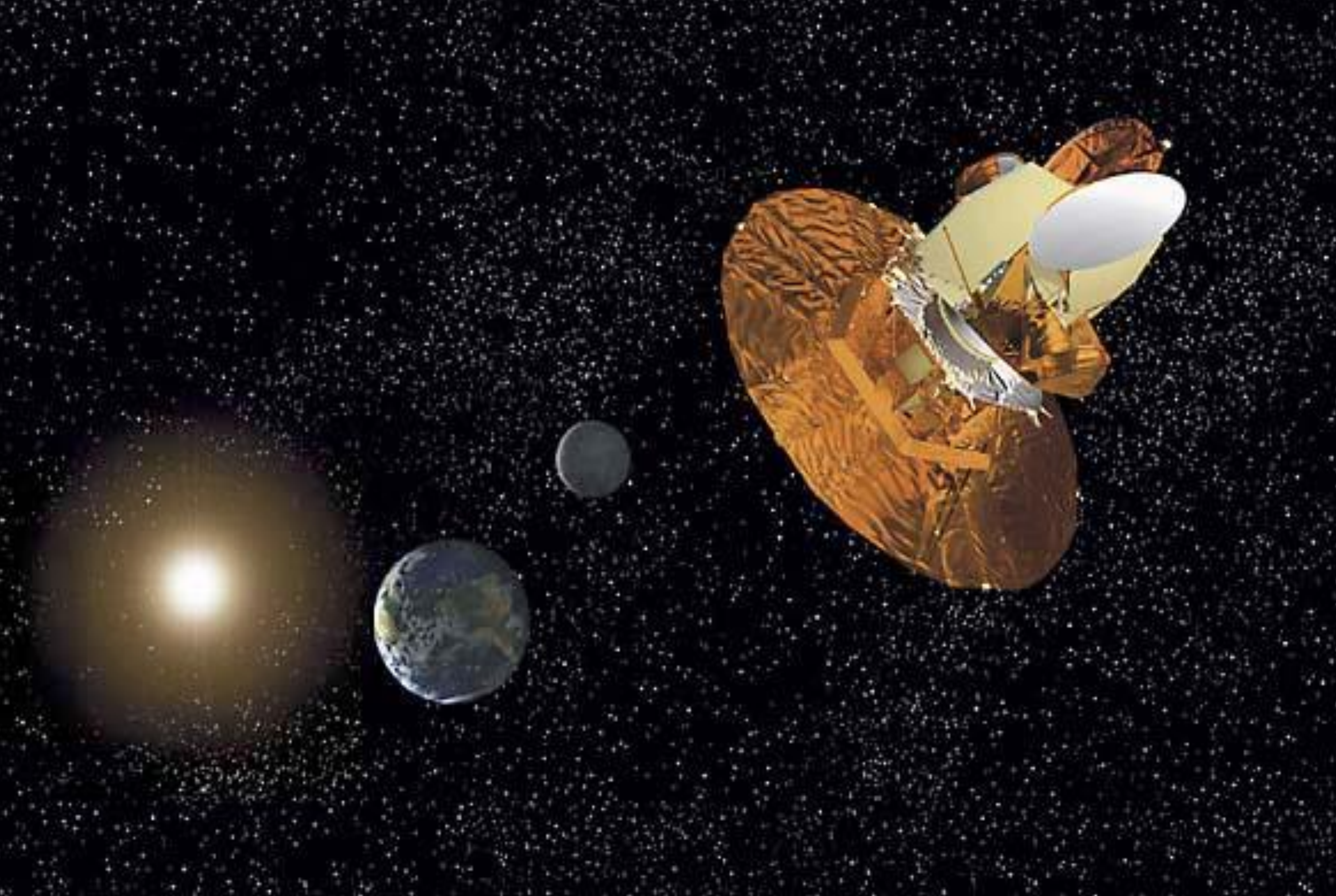

WMAP

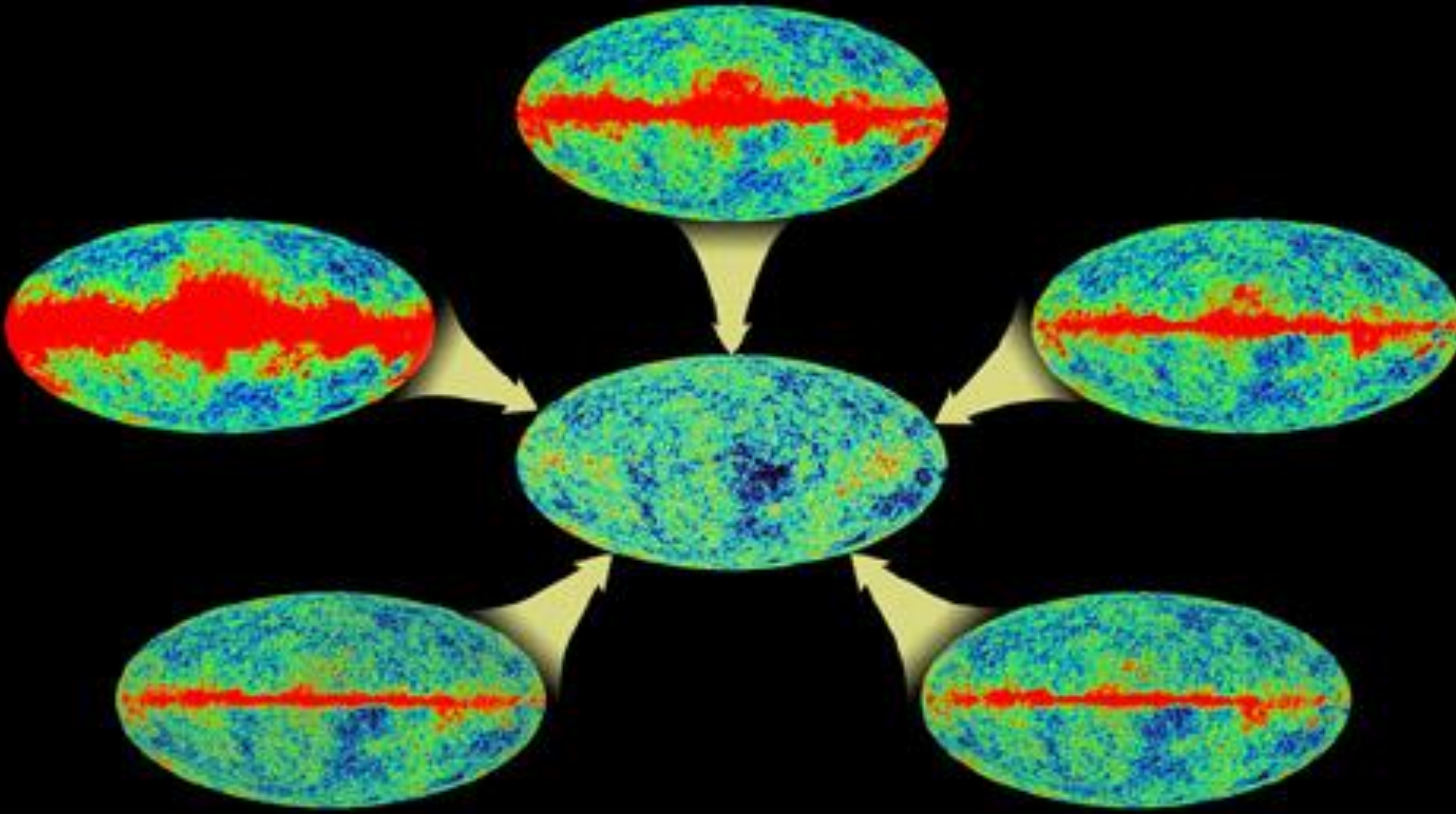

WMAP

Angular measure

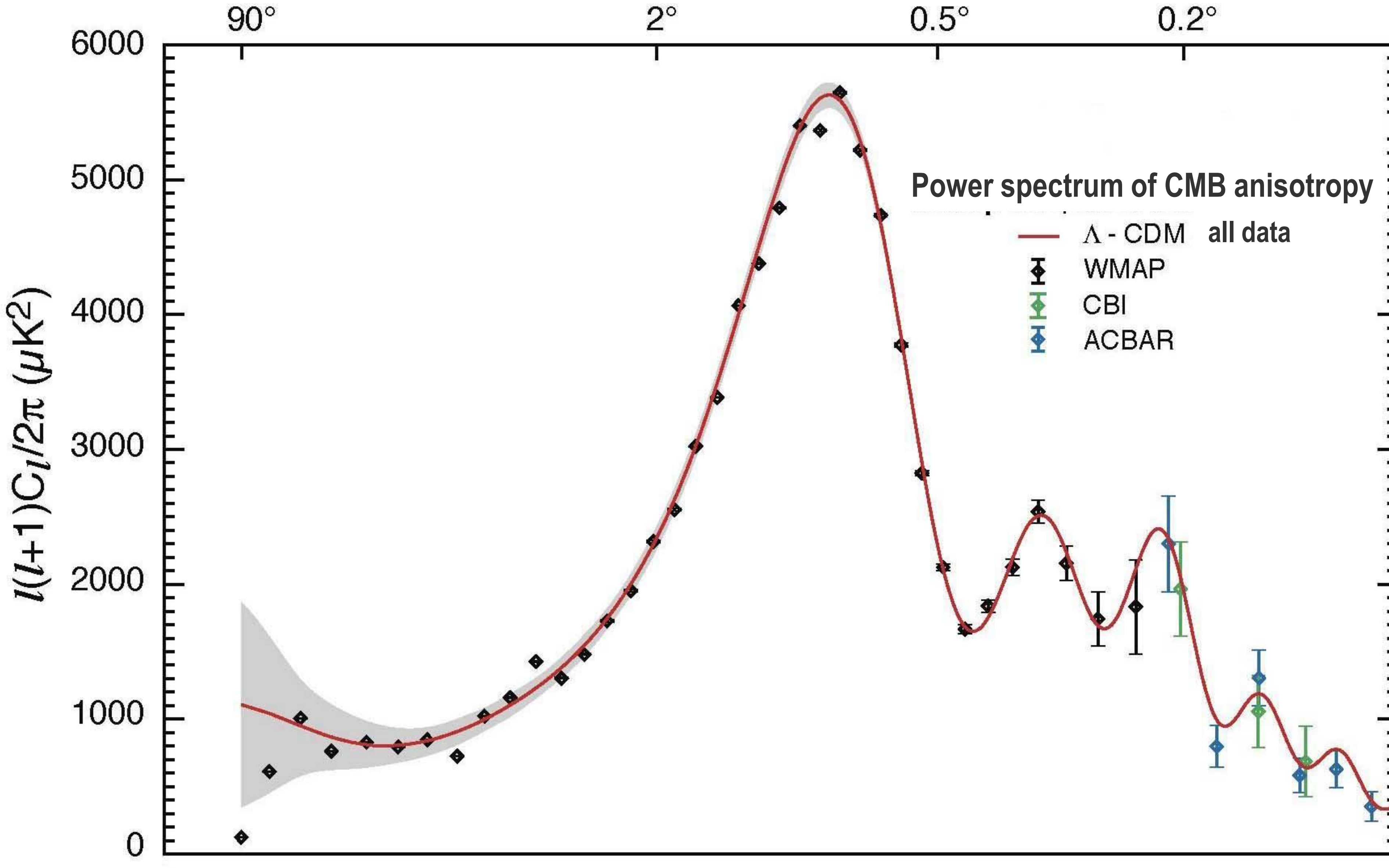

WMAP

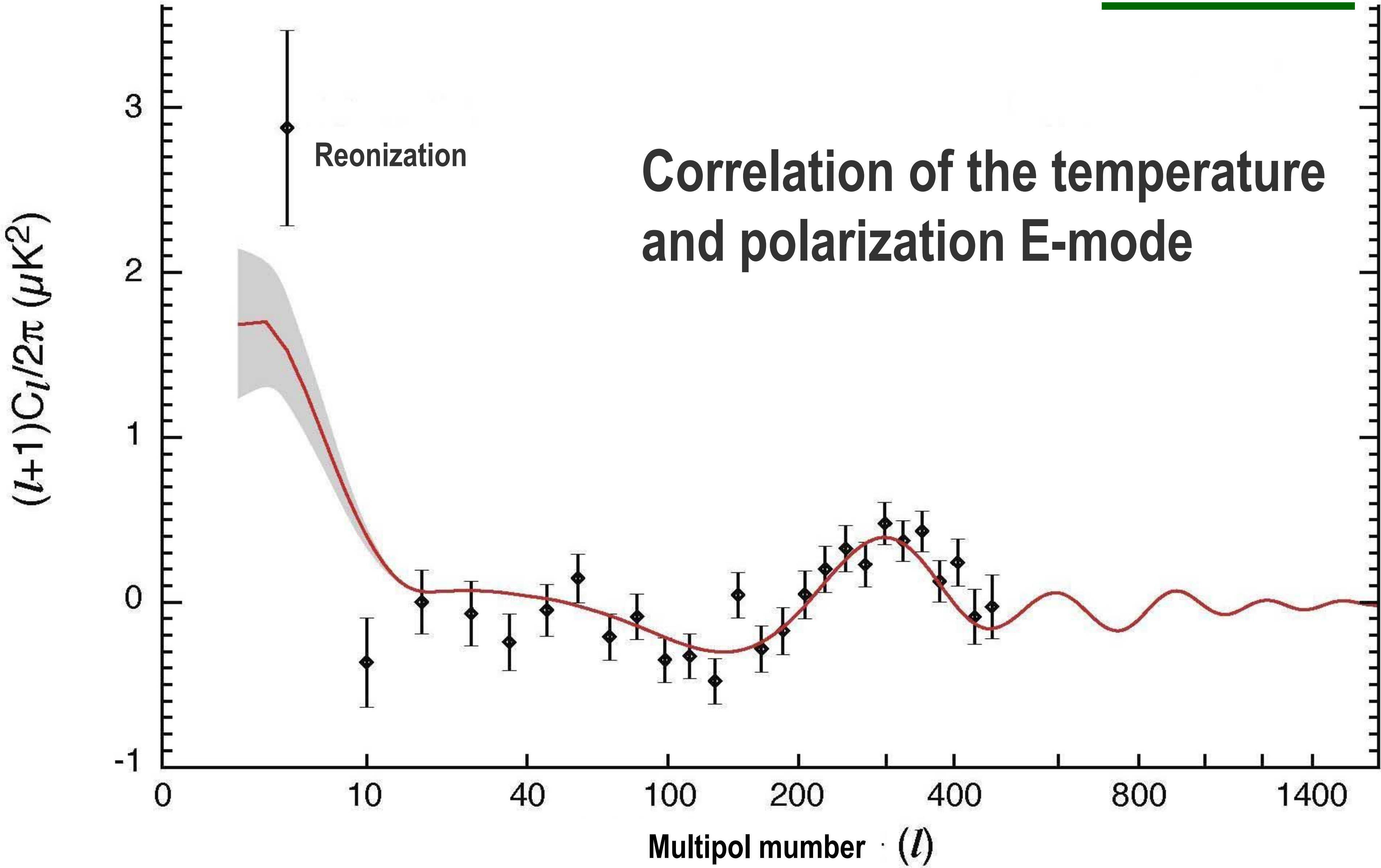
Reonization
Correlation of the temperature and polarization E-mode
$(l+1)C_l/2\pi\ (\mu K^2)$
3
2
1
0
-1
0
10
40
100
200
400
800
1400
Multipol mumber (l)

WMAP

Old Universe – *New* Numbers

$\Omega_{tot} = 1.02^{+0.02}_{-0.02}$

$w < -0.78$ (95% CL)

$\Omega_{\Lambda} = 0.73^{+0.04}_{-0.04}$

$\Omega_b h^2 = 0.0224^{+0.0009}_{-0.0009}$

$\Omega_b = 0.044^{+0.004}_{-0.004}$

$n_b = 2.5 \times 10^{-7}{}^{+0.1\times10^{-7}}_{-0.1\times10^{-7}}\ \mathrm{cm}^{-3}$

$\Omega_m h^2 = 0.135^{+0.008}_{-0.009}$

$\Omega_m = 0.27^{+0.04}_{-0.04}$

$\Omega_{\nu} h^2 < 0.0076$ (95%CL)

$m_{\nu} < 0.23$ eV (95% CL)

$T_{cmb} = 2.725^{+0.002}_{-0.002}$ K

$n_{\gamma} = 410.4^{+0.9}_{-0.9}\ \mathrm{cm}^{-3}$

$\eta = 6.1 \times 10^{-10}{}^{+0.3\times10^{-10}}_{-0.2\times10^{-10}}$

$\Omega_b \Omega_m^{-1} = 0.17^{+0.01}_{-0.01}$

$\sigma_8 = 0.84^{+0.04}_{-0.04}$ Mpc

$\sigma_8 \Omega_m^{0.5} = 0.44^{+0.04}_{-0.05}$

$A = 0.833^{+0.086}_{-0.083}$

$n_s = 0.93^{+0.03}_{-0.03}$

$dn_s/d\ln k = -0.031^{+0.016}_{-0.018}$

$r < 0.71$ (95% CL)

$z_{dec} = 1089^{+1}_{-1}$

$\Delta z_{dec} = 195^{+2}_{-2}$

$h = 0.71^{+0.04}_{-0.03}$

$t_0 = 13.7^{+0.2}_{-0.2}$ Gyr

$t_{dec} = 379^{+8}_{-7}$ kyr

$t_r = 180^{+220}_{-80}$ Myr (95% CL)

$\Delta t_{dec} = 118^{+3}_{-2}$ kyr

$z_{eq} = 3233^{+194}_{-210}$

$\tau = 0.17^{+0.04}_{-0.04}$

$z_r = 20^{+10}_{-9}$ (95% CL)

$\theta_A = 0.^{\circ}598^{+0.002}_{-0.002}$

$d_A = 14.0^{+0.2}_{-0.3}$ Gpc

$l_A = 301^{+1}_{-1}$

$r_s = 147^{+2}_{-2}$ Mpc

PLANCK

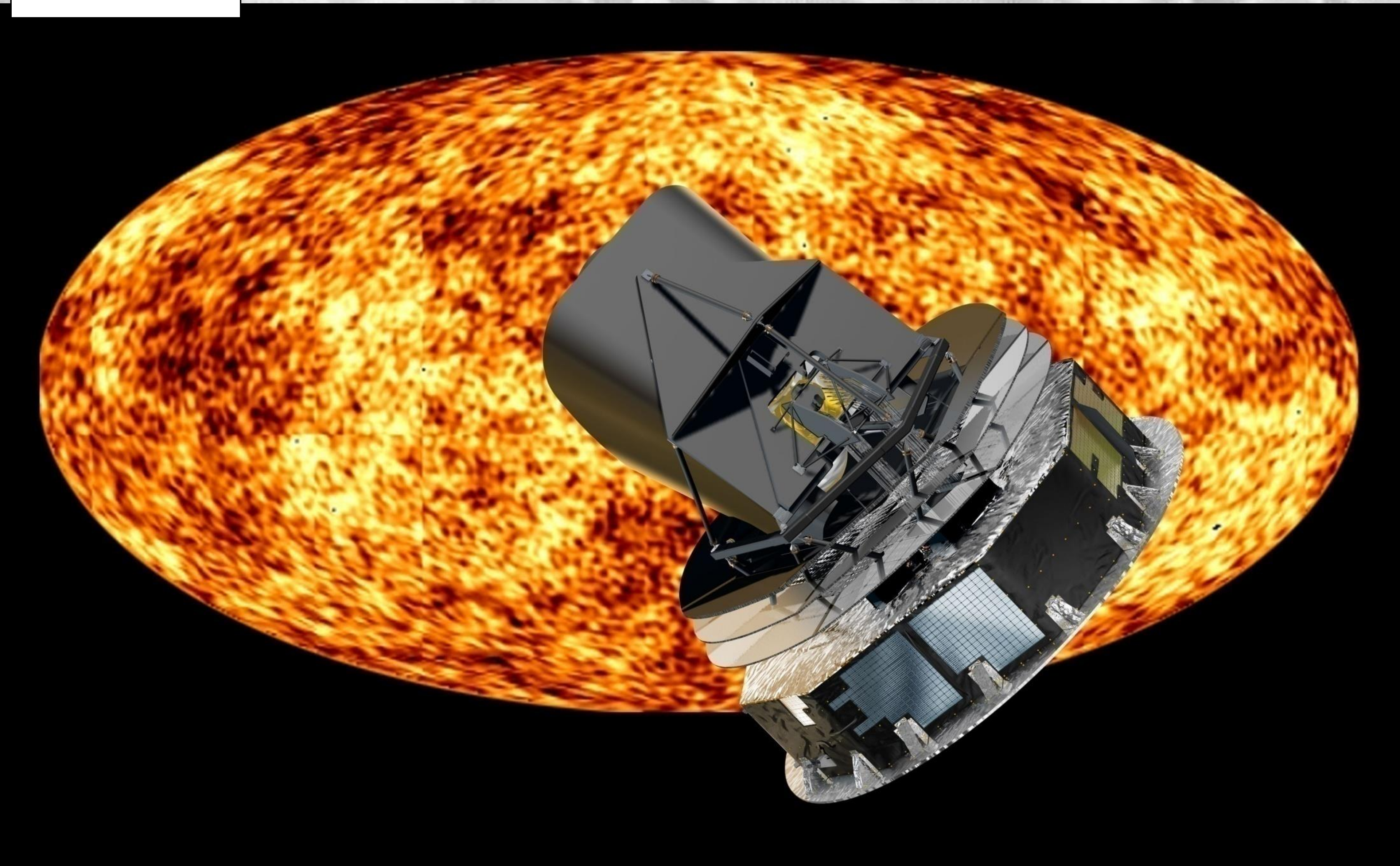

PLANCK

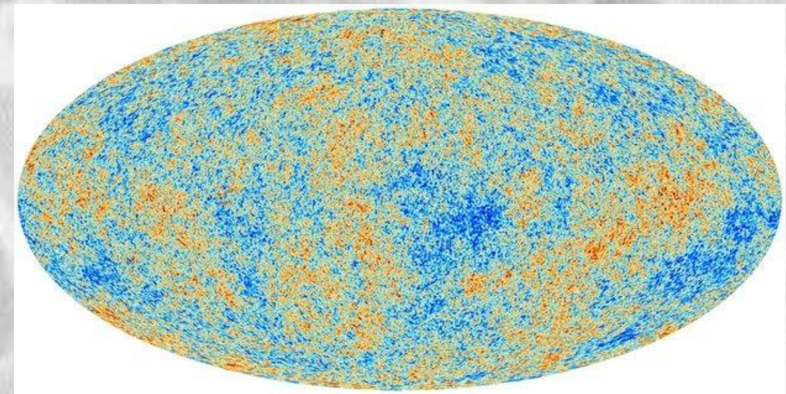

The European Space Agency's Planck satellite, dedicated to studying the early universe and its subsequent evolution, was launched on **14 May 2009** and has been surveying the microwave and submillimetre sky continuously since August 2009.

In March 2013, ESA and the Planck Collaboration publicly released the initial cosmology products based on the first 15.5 months of Planck operations, along with a set of scientific and technical papers and a web-based explanatory supplement. The science products include a set of **specialized maps of the cosmic microwave background**, **maps of Galactic** and **extragalactic extended foregrounds**, a **catalogue of compact Galactic and extragalactic sources**, and a **list of sources detected through the Sunyaev-Zeldovich**.

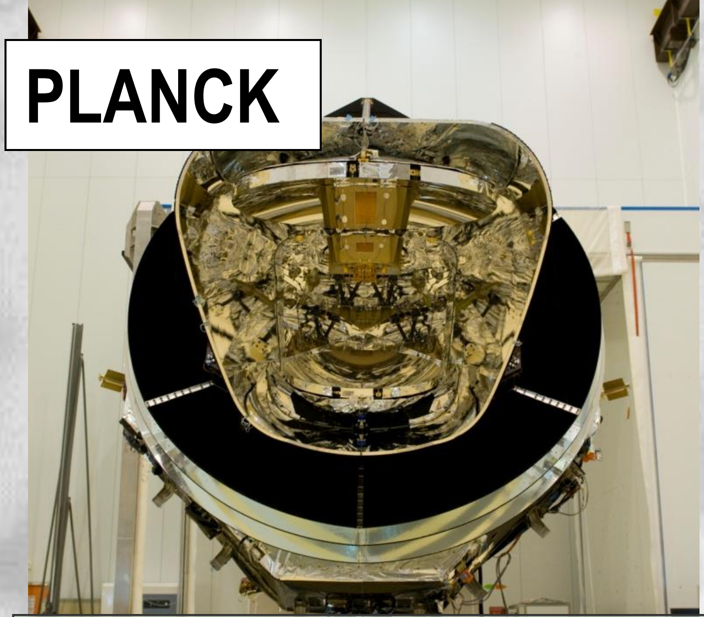

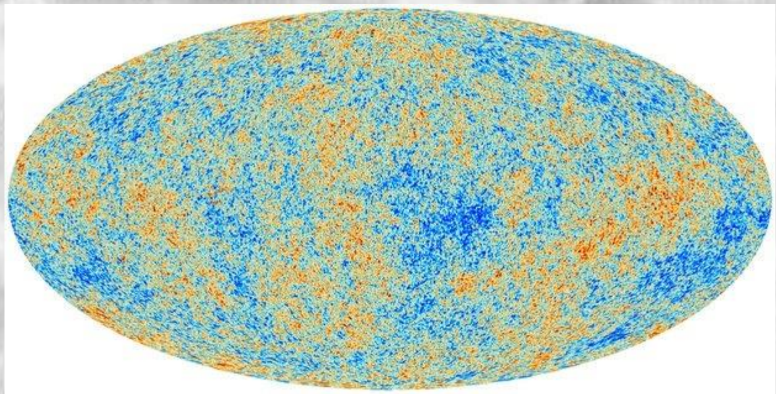

Scientific results include **robust support for the standard, six parameter Lambda-CDM** model of cosmology and improved measurements for the parameters that define this model, including a highly significant deviation from scale invariance of the primordial power spectrum.

Several large scale anomalies in the CMB temperature distribution detected earlier by WMAP are confirmed with higher confidence. Planck sets new limits on the number and mass of neutrinos, and has measured gravitational lensing of CMB anisotropies at 25sigma.

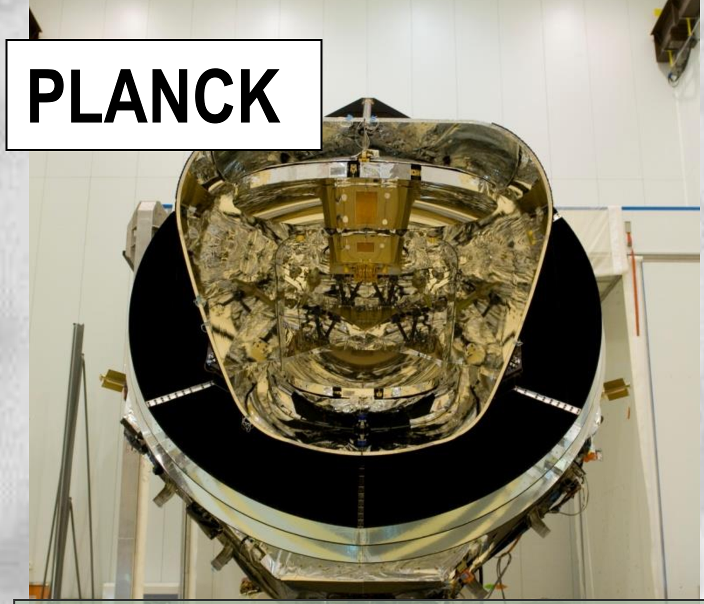

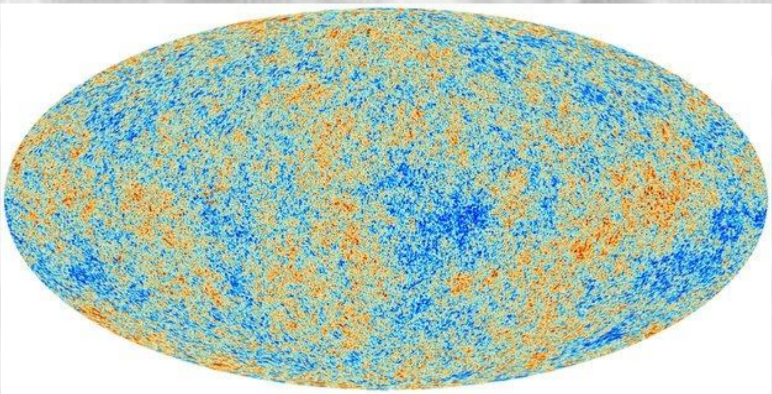

Planck finds **no evidence for non-Gaussian statistics of the CMB anisotropies**. There is some tension between Planck and WMAP results; this is evident in the power spectrum and results for some of the cosmology parameters. **In general, Planck results agree well with results from the measurements of baryon acoustic oscillations.** Because the analysis of Planck polarization data is not yet as mature as the analysis of temperature data, polarization results are not released. Planck team does, however, graphically illustrates the robust detection of the E-mode polarization signal around CMB hot- and cold-spots.

WMAP

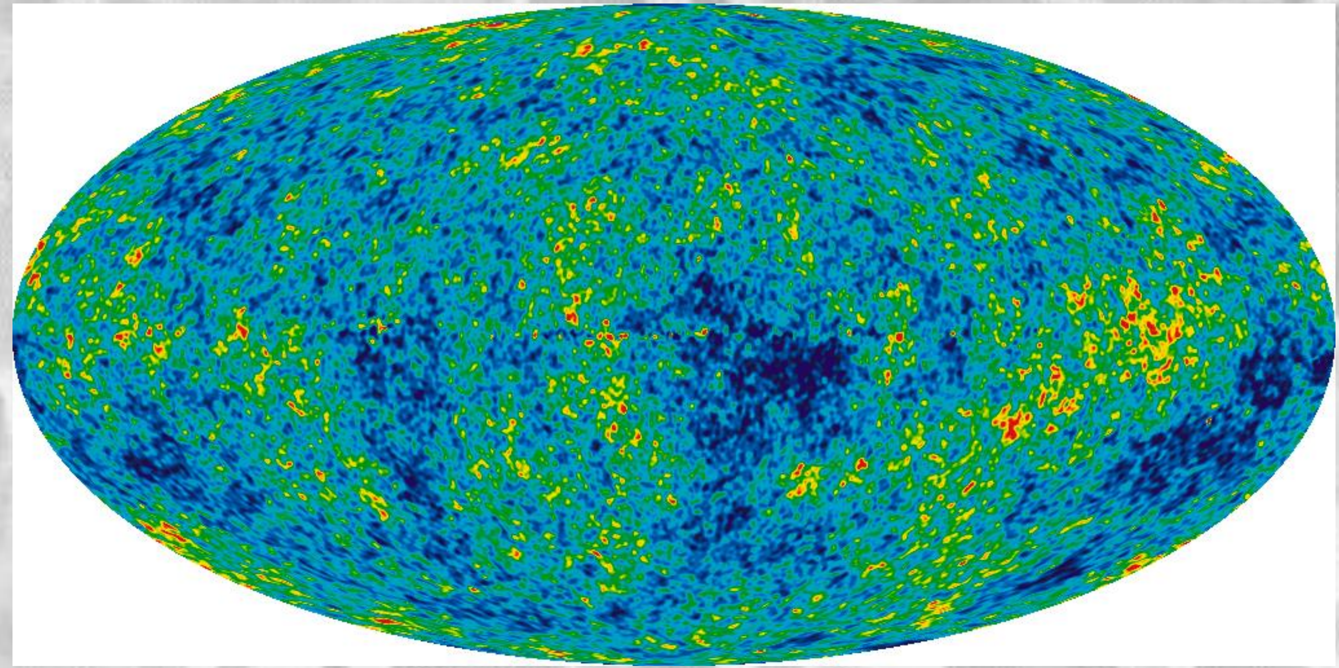

PLANCK

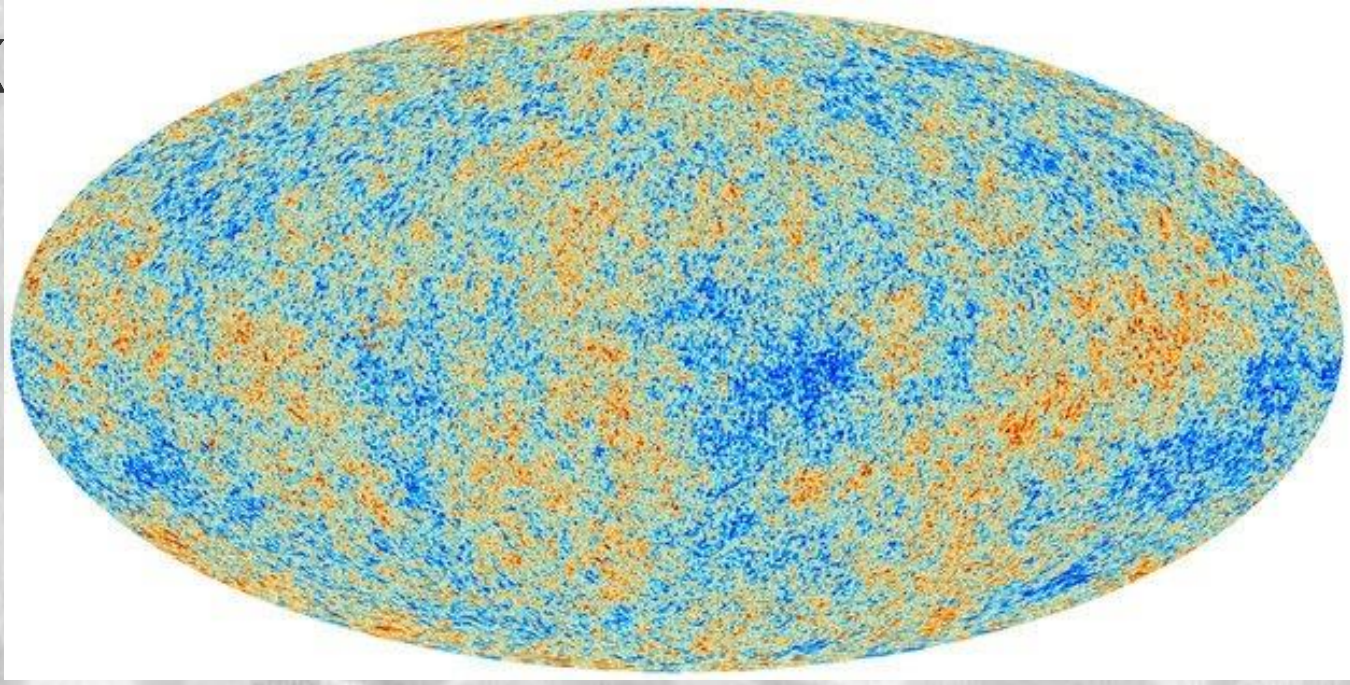

PLANCK

Size: 4.20 x 4.22 m (height x width)
Mass: 1.95 tonnes at launch
Reflector: 1.9 x 1.5 m primary reflector
Telescope mass: 205 kg with focal plane unit
Life time: A minimum of 15 months, limited by degradation of cooling system
Operation orbit: Lissajous orbit at an average distance of 400 000 km from L2
Forse: Hydrazine, 12 thrusters x 20 N each, 4 thrusters x 1 Newton each
Solar batt.: Flat, fixed triple-junction Gallium-Arsenide cell panels on rear of spacecraft, 13m2
Batt.: 39 Ah lithium ion batteries
Connection: 3 x low gain antennae 1 x medium gain antenna

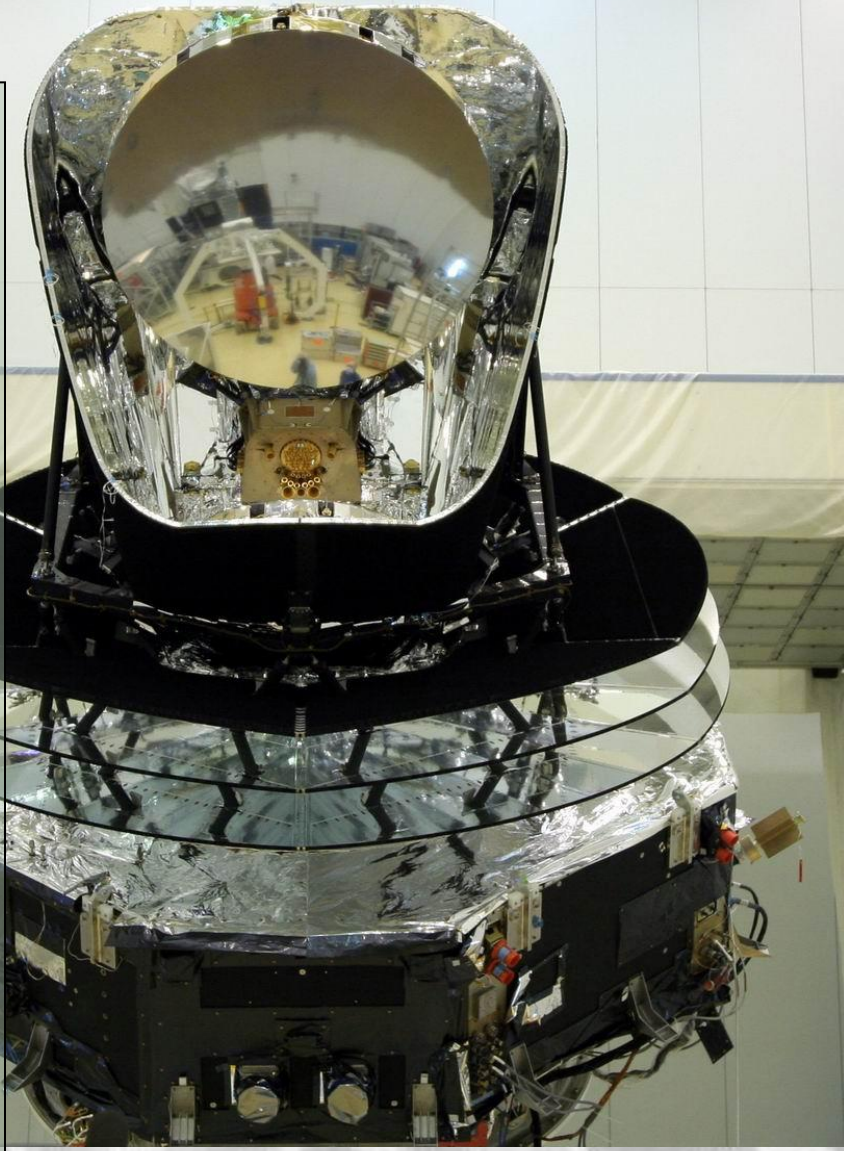

PLANCK

The Low Frequency Instrument (LFI)

Combined focal plane of Planck's two instruments

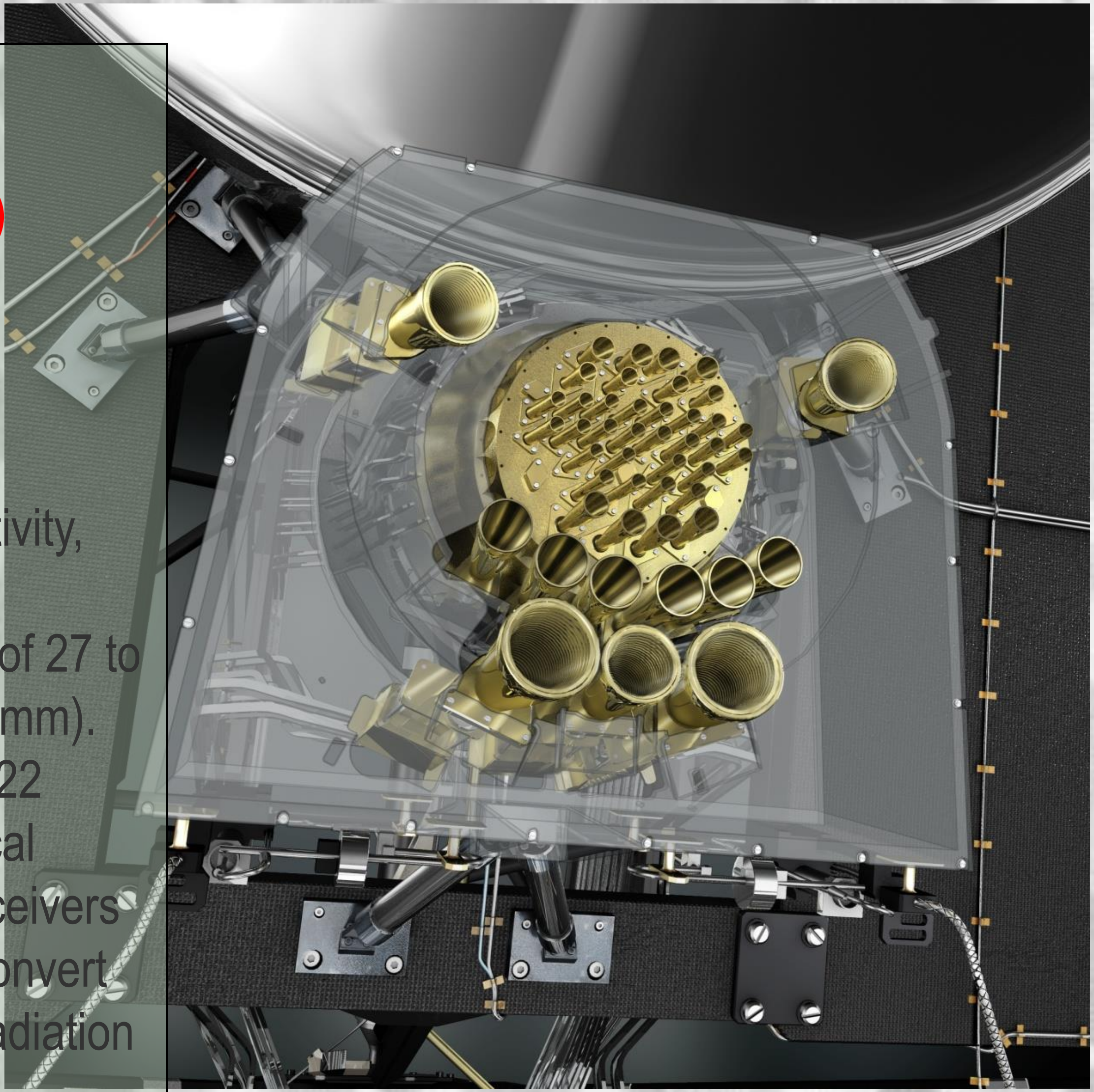

LFI is designed to produce high-sensitivity, multi-frequency measurements of the microwave sky in the frequency range of 27 to 77 GHz (wavelength range 11.1 to 3.9 mm). The instrument consists of an array of 22 tuned radio receivers located in the focal plane of the telescope. These radio receivers gather microwaves from the sky and convert them to a measure of the intensity of radiation at each frequency.

Principal Investigator: Nazzareno Mandolesi, Istituto di Astrofisica Spaziale e Fisica Cosmica, Bologna Italy.

PLANCK

The High Frequency Instrument (HFI)

HFI is designed to produce high-sensitivity, multi-frequency measurements of the diffuse radiation permeating the sky in all directions in the frequency range of 84 GHz to 1 THz (wavelength range 3.6 to 0.3 mm). The instrument consists of an array of 52 bolometric detectors placed in the focal plane of the telescope. Bolometric detectors are devices capable of detecting and measuring small amounts of thermal radiation.

The instruments are complementary and they work together to produce the overall mission results.

Principal Investigators (PI): Jean-Loup Puget (PI), Institut d'Astrophysique Spatiale in Orsay, France,
François Bouchet (co-PI), Institut d'Astrophysique de Paris, France.

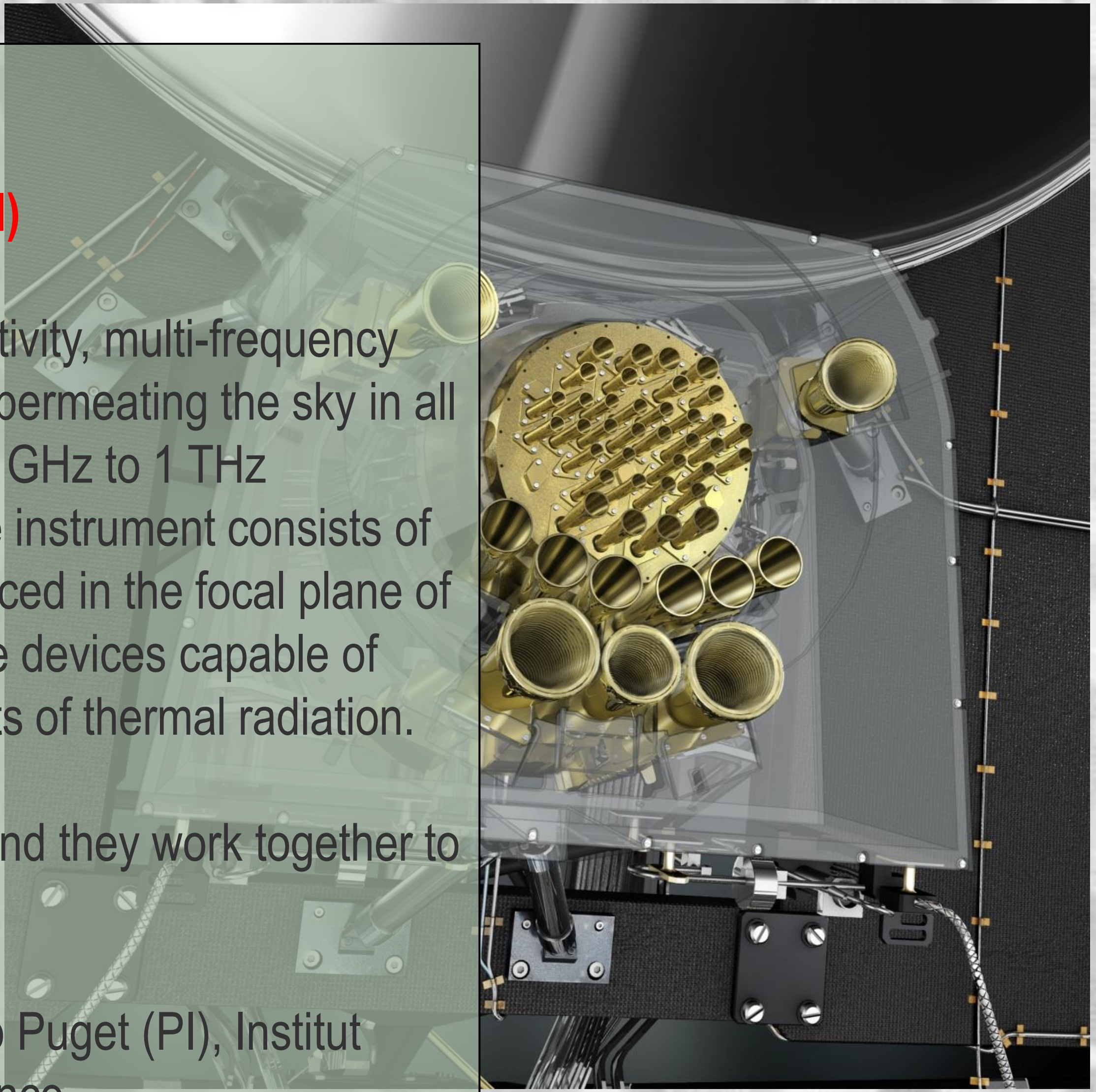

PLANCK in space

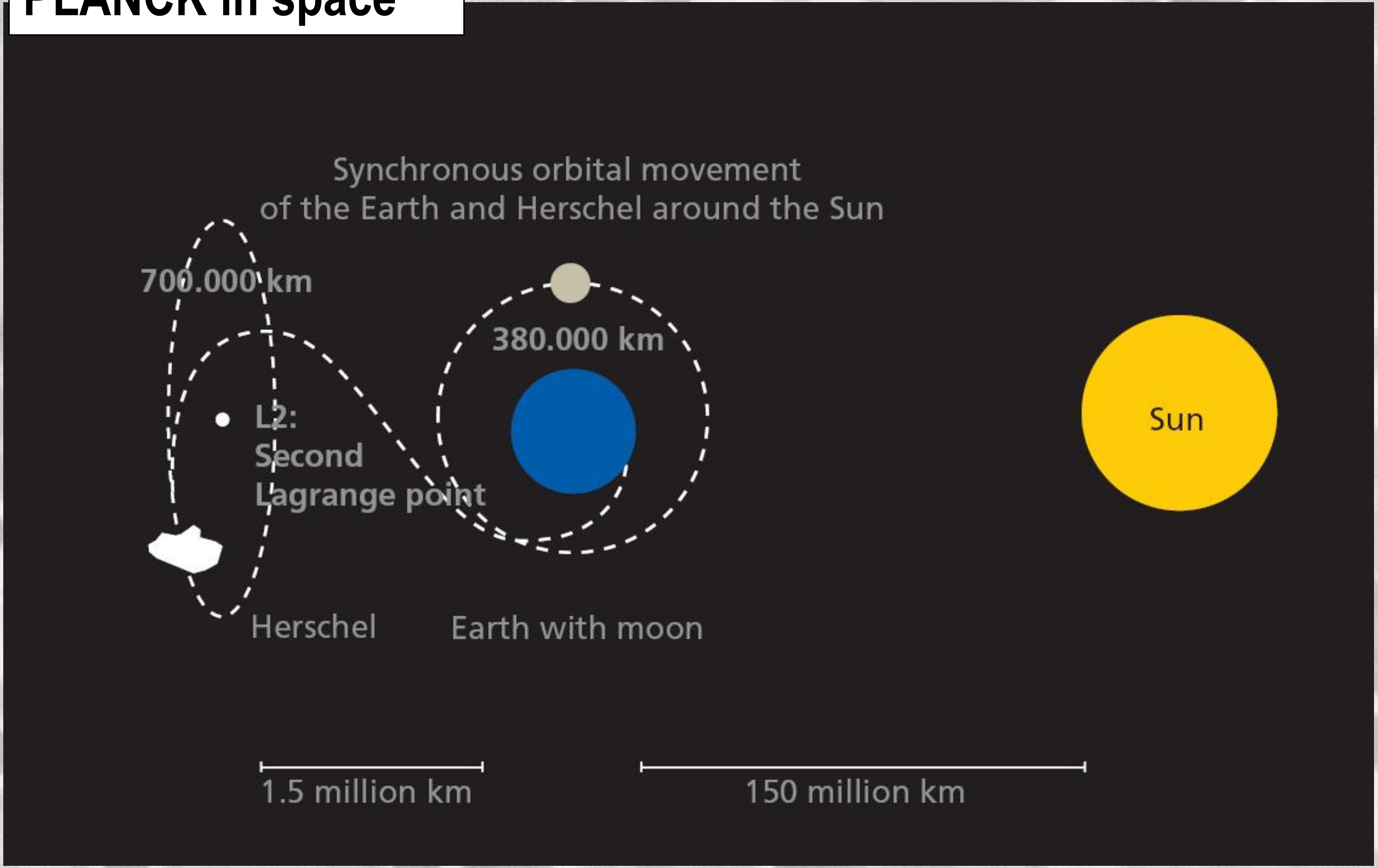

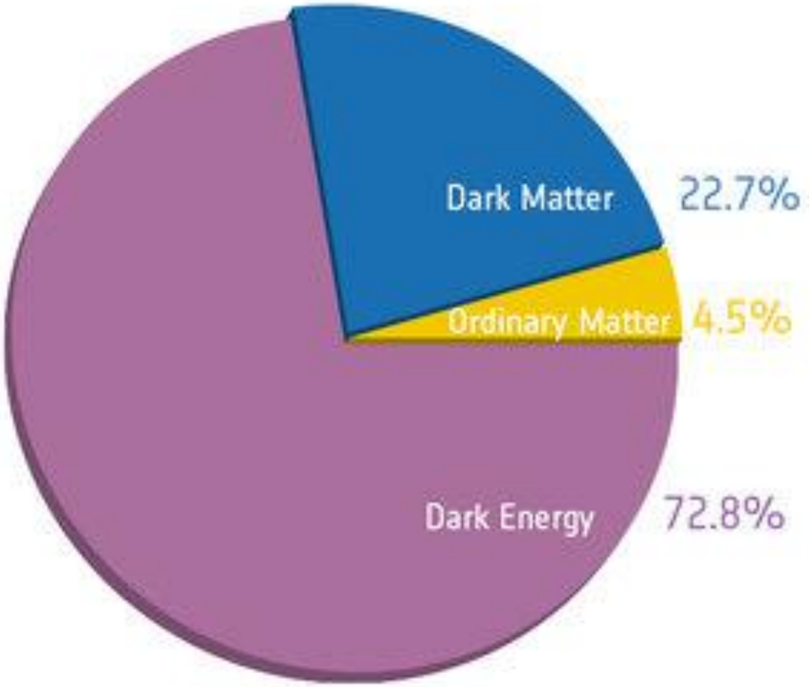
Dark Matter 22.7%
Ordinary Matter 4.5%
Dark Energy 72.8%

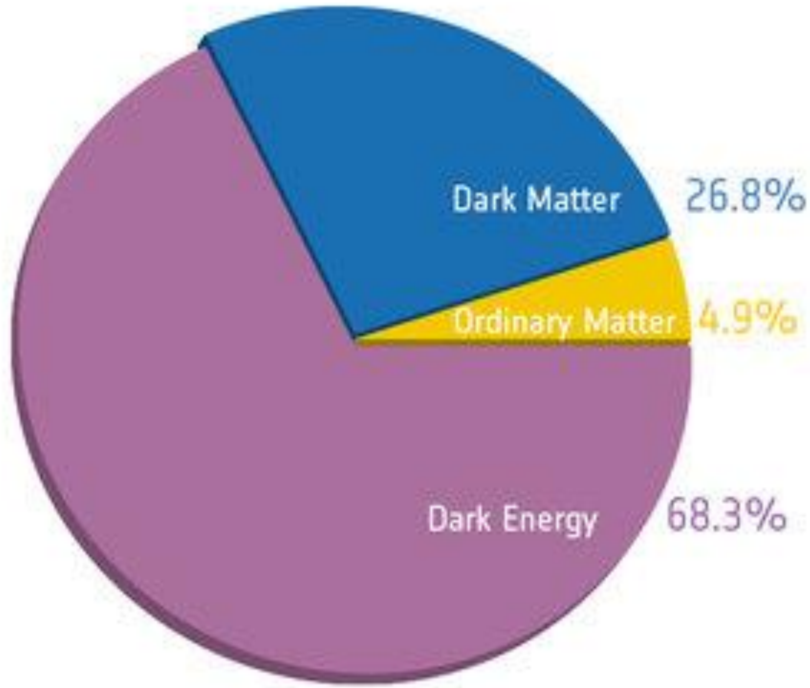
Dark Matter 26.8%
Ordinary Matter 4.9%
Dark Energy 68.3%

WMAP

PLANCK

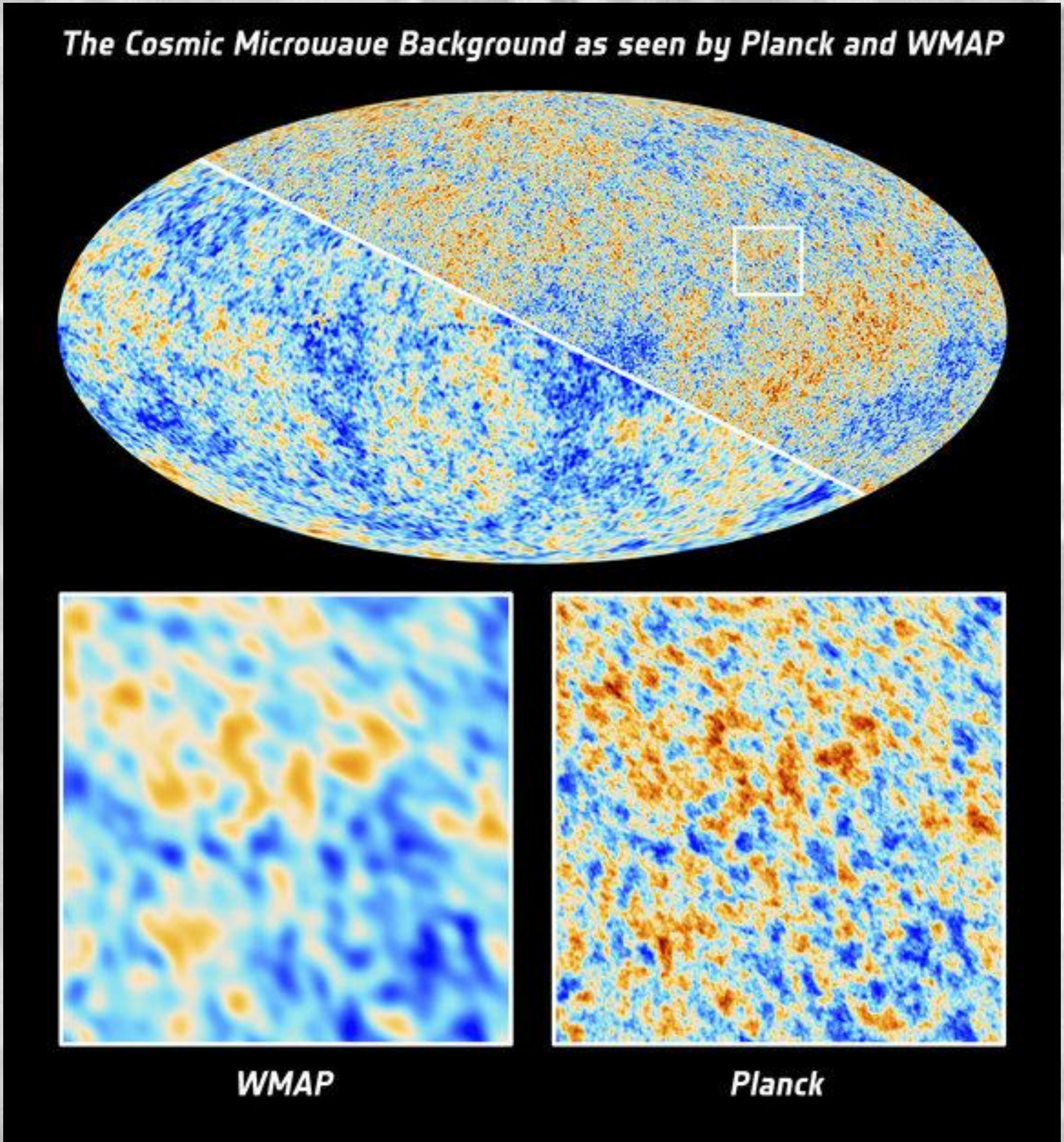
The Cosmic Microwave Background as seen by Planck and WMAP
WMAP
Planck

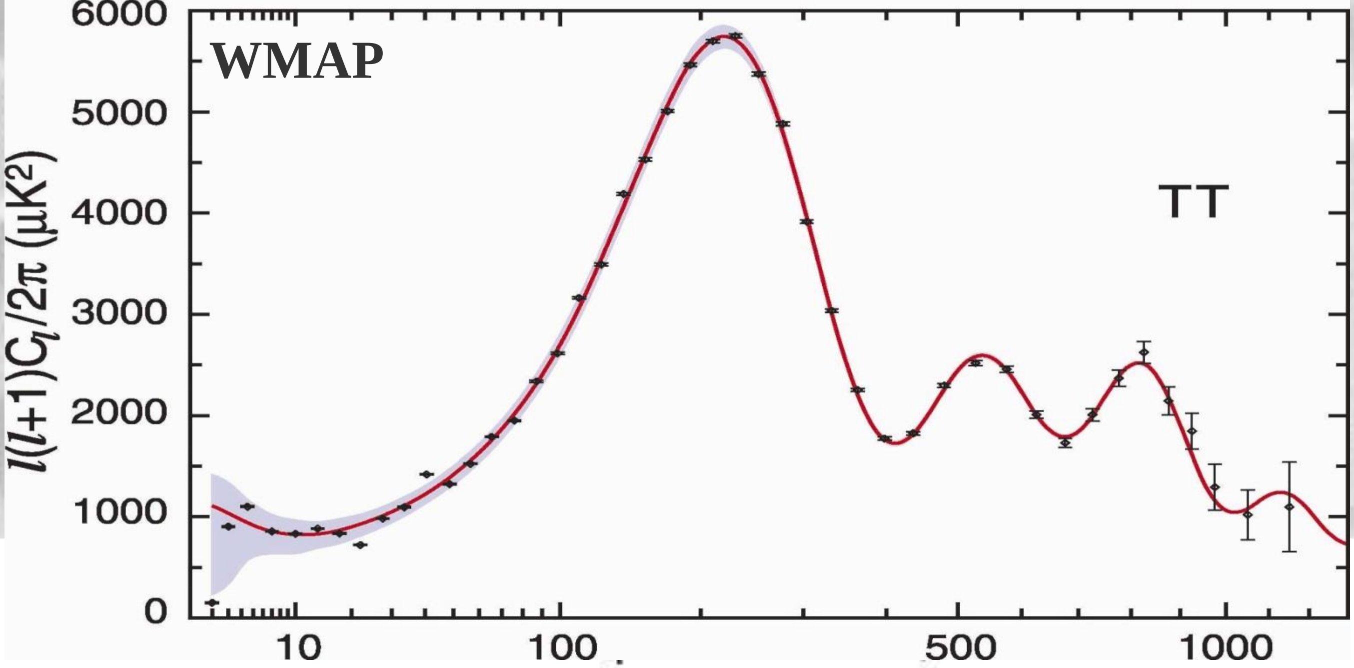
WMAP
TT
$l(l+1)C_l/2\pi$ (μK^2)
6000
5000
4000
3000
2000
1000
0
10
100
500
1000

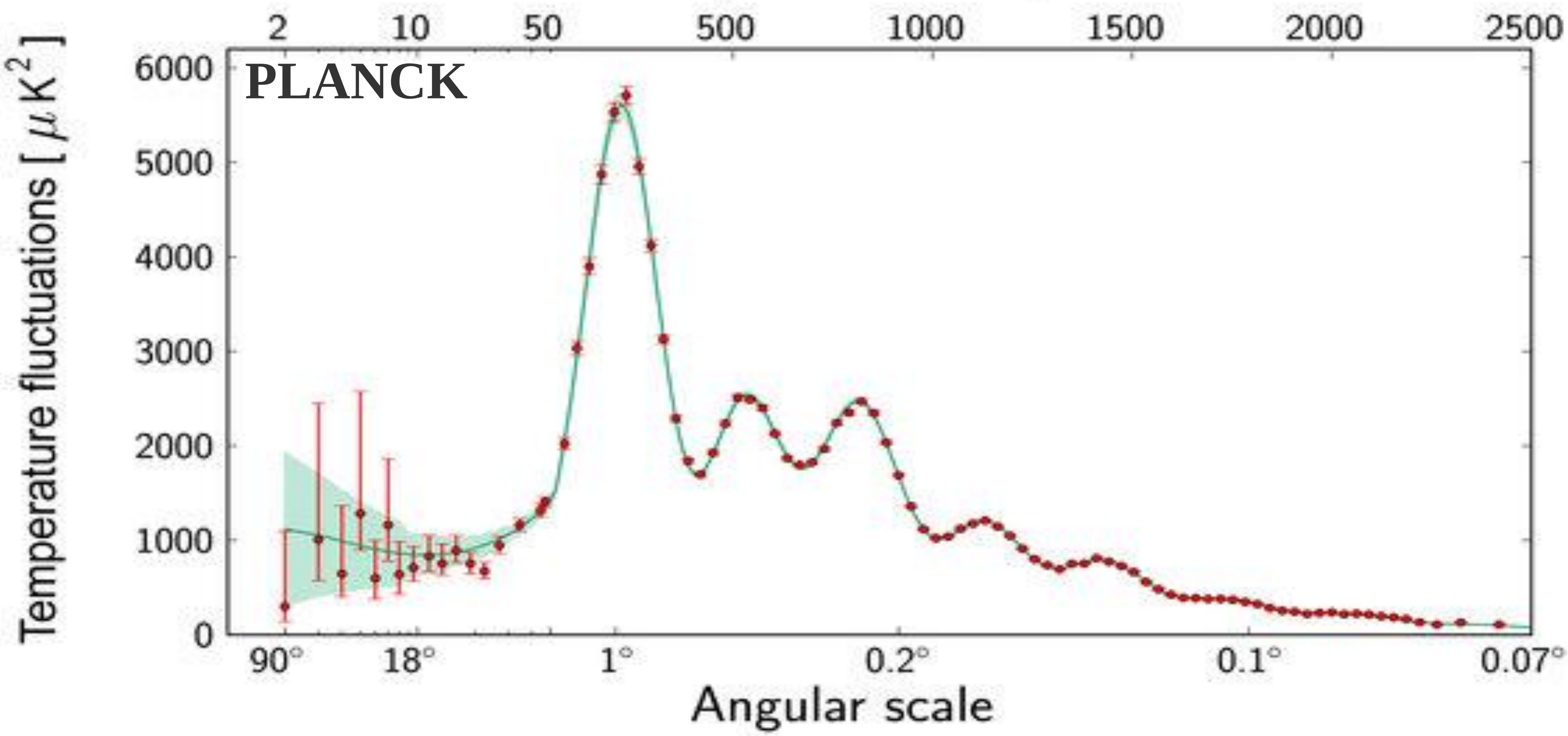
PLANCK
Temperature fluctuations [μK^2]
2
10
50
500
1000
1500
2000
2500
6000
5000
4000
3000
2000
1000
0
90°
18°
1°
0.2°
0.1°
0.07°
Angular scale

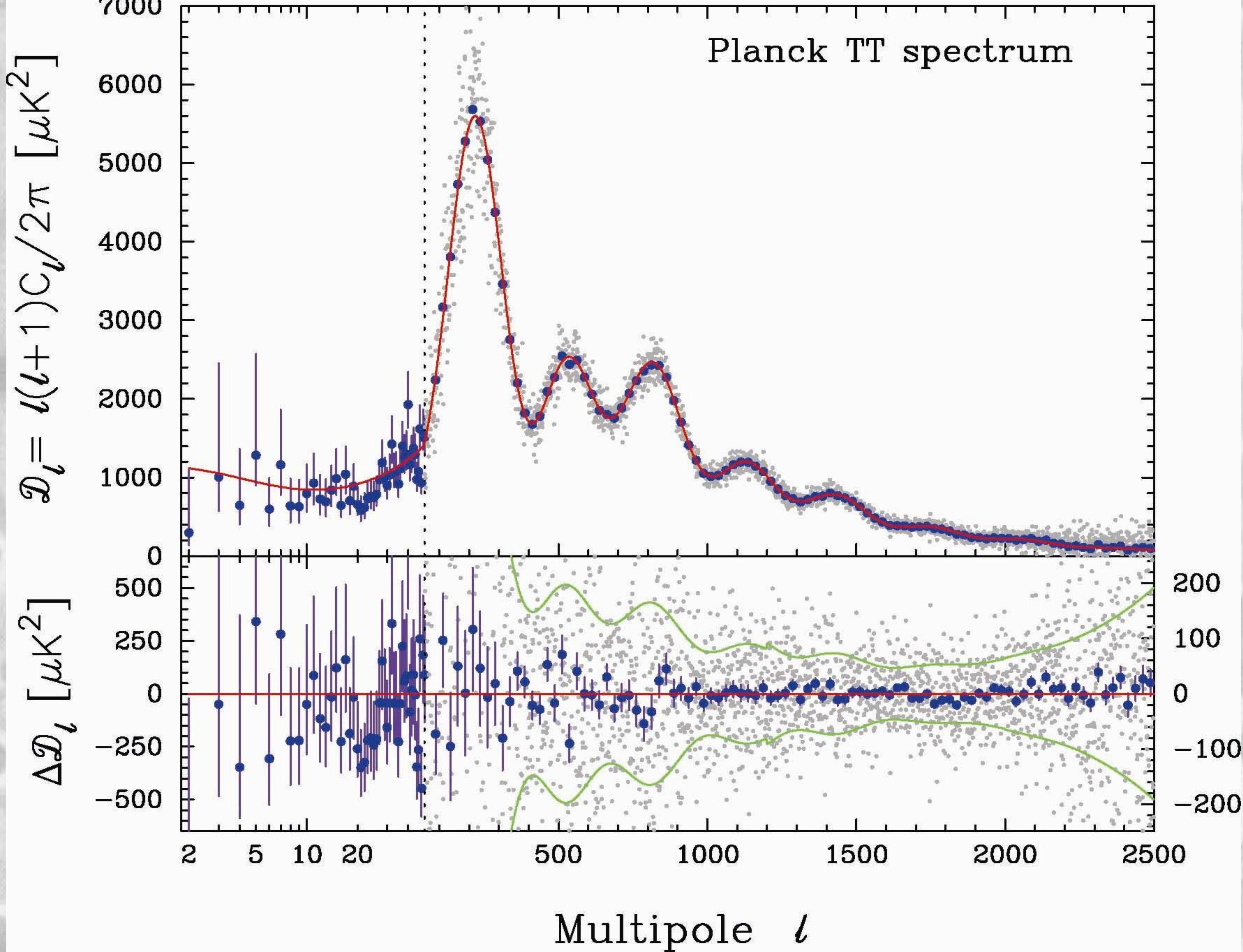

Planck TT spectrum
$\mathcal{D}_\ell = \ell(\ell+1)C_\ell/2\pi\ [\mu K^2]$
$\Delta\mathcal{D}_\ell\ [\mu K^2]$
Multipole ℓ
7000
6000
5000
4000
3000
2000
1000
0
500
250
0
−250
−500
200
100
0
−100
−200
2
5
10
20
500
1000
1500
2000
2500

Parameter	*Planck* Best fit	*Planck* 68% limits	*Planck*+lensing Best fit	*Planck*+lensing 68% limits	*Planck*+WP Best fit	*Planck*+WP 68% limits
$\Omega_b h^2$	0.022068	0.02207 ± 0.00033	0.022242	0.02217 ± 0.00033	0.022032	0.02205 ± 0.00028
$\Omega_c h^2$	0.12029	0.1196 ± 0.0031	0.11805	0.1186 ± 0.0031	0.12038	0.1199 ± 0.0027
$100\theta_{MC}$	1.04122	1.04132 ± 0.00068	1.04150	1.04141 ± 0.00067	1.04119	1.04131 ± 0.00063
τ	0.0925	0.097 ± 0.038	0.0949	0.089 ± 0.032	0.0925	$0.089^{+0.012}_{-0.014}$
n_s	0.9624	0.9616 ± 0.0094	0.9675	0.9635 ± 0.0094	0.9619	0.9603 ± 0.0073
$\ln(10^{10} A_s)$	3.098	3.103 ± 0.072	3.098	3.085 ± 0.057	3.0980	$3.089^{+0.024}_{-0.027}$
Ω_Λ	0.6825	0.686 ± 0.020	0.6964	0.693 ± 0.019	0.6817	$0.685^{+0.018}_{-0.016}$
Ω_m	0.3175	0.314 ± 0.020	0.3036	0.307 ± 0.019	0.3183	$0.315^{+0.016}_{-0.018}$
σ_8	0.8344	0.834 ± 0.027	0.8285	0.823 ± 0.018	0.8347	0.829 ± 0.012
z_{re}	11.35	$11.4^{+4.0}_{-2.8}$	11.45	$10.8^{+3.1}_{-2.5}$	11.37	11.1 ± 1.1
H_0	67.11	67.4 ± 1.4	68.14	67.9 ± 1.5	67.04	67.3 ± 1.2
$10^9 A_s$	2.215	2.23 ± 0.16	2.215	$2.19^{+0.12}_{-0.14}$	2.215	$2.196^{+0.051}_{-0.060}$
$\Omega_m h^2$	0.14300	0.1423 ± 0.0029	0.14094	0.1414 ± 0.0029	0.14305	0.1426 ± 0.0025
$\Omega_m h^3$	0.09597	0.09590 ± 0.00059	0.09603	0.09593 ± 0.00058	0.09591	0.09589 ± 0.00057
Y_P	0.247710	0.24771 ± 0.00014	0.247785	0.24775 ± 0.00014	0.247695	0.24770 ± 0.00012
Age/Gyr	13.819	13.813 ± 0.058	13.784	13.796 ± 0.058	13.8242	13.817 ± 0.048
z_*	1090.43	1090.37 ± 0.65	1090.01	1090.16 ± 0.65	1090.48	1090.43 ± 0.54
r_*	144.58	144.75 ± 0.66	145.02	144.96 ± 0.66	144.58	144.71 ± 0.60
$100\theta_*$	1.04139	1.04148 ± 0.00066	1.04164	1.04156 ± 0.00066	1.04136	1.04147 ± 0.00062
z_{drag}	1059.32	1059.29 ± 0.65	1059.59	1059.43 ± 0.64	1059.25	1059.25 ± 0.58
r_{drag}	147.34	147.53 ± 0.64	147.74	147.70 ± 0.63	147.36	147.49 ± 0.59
k_D	0.14026	0.14007 ± 0.00064	0.13998	0.13996 ± 0.00062	0.14022	0.14009 ± 0.00063
$100\theta_D$	0.161332	0.16137 ± 0.00037	0.161196	0.16129 ± 0.00036	0.161375	0.16140 ± 0.00034
z_{eq}	3402	3386 ± 69	3352	3362 ± 69	3403	3391 ± 60
$100\theta_{eq}$	0.8128	0.816 ± 0.013	0.8224	0.821 ± 0.013	0.8125	0.815 ± 0.011
$r_{drag}/D_V(0.57)$	0.07130	0.0716 ± 0.0011	0.07207	0.0719 ± 0.0011	0.07126	0.07147 ± 0.00091

Table 2. Cosmological parameter values for the six-parameter base ΛCDM model. Columns 2 and 3 give results for the *Planck* temperature power spectrum data alone. Columns 4 and 5 combine the *Planck* temperature data with *Planck* lensing, and columns 6 and 7 include *WMAP* polarization at low multipoles. We give best fit parameters as well as 68% confidence limits for constrained parameters. The first six parameters have flat priors. The remainder are derived parameters as discussed in Sect. 2. Beam, calibration parameters, and foreground parameters (see Sect. 4) are not listed for brevity. Constraints on foreground parameters for *Planck*+WP are given later in Table 5.

	Planck+WP		*Planck*+WP+highL		*Planck*+lensing+WP+highL		*Planck*+WP+highL+BAO	
Parameter	Best fit	68% limits	Best fit	68% limits	Best fit	68% limits	Best fit	68% limits
$\Omega_b h^2$	0.022032	0.02205 ± 0.00028	0.022069	0.02207 ± 0.00027	0.022199	0.02218 ± 0.00026	0.022161	0.02214 ± 0.00024
$\Omega_c h^2$	0.12038	0.1199 ± 0.0027	0.12025	0.1198 ± 0.0026	0.11847	0.1186 ± 0.0022	0.11889	0.1187 ± 0.0017
$100\theta_{MC}$	1.04119	1.04131 ± 0.00063	1.04130	1.04132 ± 0.00063	1.04146	1.04144 ± 0.00061	1.04148	1.04147 ± 0.00056
τ	0.0925	$0.089^{+0.012}_{-0.014}$	0.0927	$0.091^{+0.013}_{-0.014}$	0.0943	$0.090^{+0.013}_{-0.014}$	0.0952	0.092 ± 0.013
n_s	0.9619	0.9603 ± 0.0073	0.9582	0.9585 ± 0.0070	0.9624	0.9614 ± 0.0063	0.9611	0.9608 ± 0.0054
$\ln(10^{10} A_s)$	3.0980	$3.089^{+0.024}_{-0.027}$	3.0959	3.090 ± 0.025	3.0947	3.087 ± 0.024	3.0973	3.091 ± 0.025
A^{PS}_{100}	152	171 ± 60	209	212 ± 50	204	213 ± 50	204	212 ± 50
A^{PS}_{143}	63.3	54 ± 10	72.6	73 ± 8	72.2	72 ± 8	71.8	72.4 ± 8.0
A^{PS}_{217}	117.0	107^{+20}_{-10}	59.5	59 ± 10	60.2	58 ± 10	59.4	59 ± 10
A^{CIB}_{143}	0.0	< 10.7	3.57	3.24 ± 0.83	3.25	3.24 ± 0.83	3.30	3.25 ± 0.83
A^{CIB}_{217}	27.2	29^{+6}_{-9}	53.9	49.6 ± 5.0	52.3	50.0 ± 4.9	53.0	49.7 ± 5.0
A^{tSZ}_{143}	6.80	...	5.17	$2.54^{+1.1}_{-1.9}$	4.64	$2.51^{+1.2}_{-1.8}$	4.86	$2.54^{+1.2}_{-1.8}$
$r^{PS}_{143\times217}$	0.916	> 0.850	0.825	$0.823^{+0.069}_{-0.077}$	0.814	0.825 ± 0.071	0.824	0.823 ± 0.070
$r^{CIB}_{143\times217}$	0.406	0.42 ± 0.22	1.0000	> 0.930	1.0000	> 0.928	1.0000	> 0.930
γ^{CIB}	0.601	$0.53^{+0.13}_{-0.12}$	0.674	0.638 ± 0.081	0.656	0.643 ± 0.080	0.667	0.639 ± 0.081
$\xi^{tSZ\times CIB}$	0.03	...	0.000	< 0.409	0.000	< 0.389	0.000	< 0.410
A^{kSZ}	0.9	...	0.89	$5.34^{+2.8}_{-1.9}$	1.14	$4.74^{+2.6}_{-2.1}$	1.58	$5.34^{+2.8}_{-2.0}$
Ω_Λ	0.6817	$0.685^{+0.018}_{-0.016}$	0.6830	$0.685^{+0.017}_{-0.016}$	0.6939	0.693 ± 0.013	0.6914	0.692 ± 0.010
σ_8	0.8347	0.829 ± 0.012	0.8322	0.828 ± 0.012	0.8271	0.8233 ± 0.0097	0.8288	0.826 ± 0.012
z_{re}	11.37	11.1 ± 1.1	11.38	11.1 ± 1.1	11.42	11.1 ± 1.1	11.52	11.3 ± 1.1
H_0	67.04	67.3 ± 1.2	67.15	67.3 ± 1.2	67.94	67.9 ± 1.0	67.77	67.80 ± 0.77
Age/Gyr	13.8242	13.817 ± 0.048	13.8170	13.813 ± 0.047	13.7914	13.794 ± 0.044	13.7965	13.798 ± 0.037
$100\theta_*$	1.04136	1.04147 ± 0.00062	1.04146	1.04148 ± 0.00062	1.04161	1.04159 ± 0.00060	1.04163	1.04162 ± 0.00056
r_{drag}	147.36	147.49 ± 0.59	147.35	147.47 ± 0.59	147.68	147.67 ± 0.50	147.611	147.68 ± 0.45

Table 5. Best-fit values and 68% confidence limits for the base ΛCDM model. Beam and calibration parameters, and additional nuisance parameters for "highL" data sets are not listed for brevity but may be found in the Explanatory Supplement (Planck Collaboration ES 2013).

PLANCK

The science products include a set of specialized maps of the cosmic microwave background, maps of Galactic and extragalactic extended foregrounds, a catalogue of compact Galactic and extragalactic sources, and a list of sources detected through the Sunyaev-Zeldovich. Scientific results include robust support for the standard, six parameter Lambda-CDM model of cosmology and improved measurements for the parameters that define this model, including a highly significant deviation from scale invariance of the primordial power spectrum. Several large scale anomalies in the CMB temperature distribution detected earlier by WMAP are confirmed with higher confidence. Planck finds no evidence for non-Gaussian statistics of the CMB anisotropies.

There is some tension between Planck and WMAP results; this is evident in the power spectrum and results for some of the cosmology parameters. In general, Planck results agree well with results from the measurements of baryon acoustic oscillations. Because the analysis of Planck polarization data is not yet as mature as the analysis of temperature data, polarization results are not released. We do, however, graphically illustrate the robust detection of the E-mode polarization signal around

CMB hot- and cold-spots.

5. The new cosmic microwave background (CMB) temperature maps from Planck provide the highest-quality full-sky view of the surface of last scattering available to date. This allows us to detect possible departures from the standard model of a globally homogeneous and isotropic cosmology on the largest scales. We search for correlations induced by a possible non-trivial topology with a fundamental domain intersecting, or nearly intersecting, the last scattering surface **(at comoving distance ξ_{rec})**, both via a direct search for matched circular patterns at the intersections and by an optimal likelihood search for specific topologies. We consider flat spaces with cubic toroidal (T3), equal-sided chimney (T2) and slab (T1) topologies, three multi-connected spaces of constant positive curvature (dodecahedral, truncated cube and octahedral) and two compact negativecurvature spaces. These searches yield no detection of the compact topology with the scale below the diameter of the last scattering surface. For most compact topologies studied the likelihood maximized over the orientation of the space relative to the observed map shows some preference for multi-connected models just larger than the diameter of the last scattering surface. Since this effect is also present in simulated realizations of isotropic maps, we interpret it as the inevitable alignment of mild anisotropic correlations with chance features in a single sky realization; such a feature can also be present, in milder form, when the likelihood is marginalized over orientations. Thus marginalized, the limits on the radius R_i of the largest sphere inscribed in topological domain (at log-likelihood-ratio $\Delta \ln L > -5$ relative to a simply-connected flat Planck best-fit model) are: in a flat Universe, Ri > 0.92 ξ_{rec} for the T3 cubic torus;

$R_i > 0.71\xi_{rec}$ for the T2 chimney; $R_i > 0.50\ \xi_{rec}$ for the T1 slab; and in a positively curved Universe, $R_i > 1.03\ \xi_{rec}$ for the dodecahedral space; $R_i > 1.0\ \xi_{rec}$ for the truncated cube; and $R_i > 0.89\ \xi_{rec}$ for the octahedral space. The limit for the T3 cubic torus from the matched-circles search is, consistently, $R_i > 0.94\ \xi_{rec}$ at 99% confidence level.

6. Planck data have been used to provide stringent new constraints on cosmic strings and other defects. We describe forecasts of the CMB power spectrum induced by cosmic strings, calculating these from network models and simulations using line-of-sight Boltzmann solvers. We have studied:
Nambu-Goto cosmic strings, we have obtained a constraint on the string tension of

$G\mu/c^2 < 1.5\ 10^{-7}$ and $f_{10} < 0.015$ at 95% confidence

$\delta T \sim 9\ \mu K$ (1 s level)

For the abelian-Higgs field theory model we find,

$G\mu/c^2 < 3.2\ 10^{-7}$ and $f_{10} < 0.028$.

We have additionally obtained comparable constraints on f_{10} for models with semilocal strings and global textures. In terms of the effective defect energy scale these are somewhat weaker at

$G\mu/c^2 < 1.1\ 10^{-6}$.

8. The two fundamental assumptions of the standard cosmological model—that the **initial fluctuations are statistically isotropic and Gaussian**—are rigorously tested using maps of the CMB anisotropy from the Planck satellite.

9. We analyse the implications of the Planck data for cosmic inflation. The Planck nominal mission temperature anisotropy measurements, combined with the WMAP large-angle polarization, constrain the scalar **spectral index** to $n_s = 0.9603 \pm 0.0073$, ruling out exact scale invariance at over 5σ.

Planck establishes an upper bound on the tensor-to-scalar ratio at $r < 0.11$ (95% CL).

The Planck data shrink the space of allowed standard inflationary models, preferring potentials with $V'' < 0$.
Exponential potential models, the simplest hybrid inflationary models, and monomial potential models of degree $n \geq 2$ do not provide a good fit to the data.

12. Cosmological parameters.

Temperature and lensing-potential power spectra.We find that the Planck spectra at high multipoles ($l \geq 40$) are extremely well described by the standard spatially-flat six-parameter ΛCDM cosmology with a power-law spectrum of adiabatic scalar perturbations. Within the context of this cosmology, the Planck data determine the cosmological parameters to high precision: the angular size of the sound horizon at recombination, the physical densities of baryons and cold dark matter, and the scalar spectral index are estimated to be

$\theta_{MC} = (1.04147 \pm 0.00062) * 10^{-2}$,

$\Omega_b h^2 = 0.02205 \pm 0.00028$,

$\Omega_c h^2 = 0.1199 \pm 0.0027$, and

$n_s = 0.9603 \pm 0.0073$, respectively (68% errors).

For this cosmology, we find a low value of the Hubble constant,

$H_0 = 67.3 \pm 1.2$ km s^{-1} Mpc^{-1},

and a high value of the matter density parameter,

$\Omega_m = 0.315 \pm 0.017$.

These values are in tension with recent direct measurements of H_0 and the magnitude-redshift relation for Type Ia supernovae, but are in excellent agreement with geometrical constraints from baryon acoustic oscillation (BAO) surveys. Including curvature, we find that the Universe is consistent with spatial flatness to percent level precision using Planck CMB data alone. We use high-resolution CMB data together with Planck to provide greater control on extragalactic foreground components in an investigation of extensions to the six-parameter Lambda-CDM model. We present selected results from a large grid of cosmological models, using a range of additional astrophysical data sets in addition to Planck and high-resolution CMB data. None of these models are favoured over the standard six-parameter Lambda-CDM cosmology. The deviation of the scalar spectral index from unity is insensitive to the addition of tensor modes and to changes in the matter content of the Universe. We find a 95% upper limit of $r_{0.002} < 0.11$ on the tensor-to-scalar ratio.

There is no evidence for additional neutrino-like relativistic particles beyond the three families of neutrinos in the standard model. Using BAO and CMB data, we find Neff = 3.30 ± 0.27 for the effective number of relativistic degrees of freedom, and an upper limit of 0.23 eV for the sum of neutrino masses. Our results are in excellent agreement with big bang nucleosynthesis and the standard value of Neff = 3.046. We find no evidence for dynamical dark energy; using BAO and CMB data, the dark energy equation of state parameter is constrained to be w = -1.13 +0.13 -0.10.

We also use the Planck data to set limits on a possible variation of the fine-structure constant, dark matter annihilation and primordial magnetic fields.

Despite the success of the six-parameter ΛCDM model in describing the Planck data at high multipoles, we note that this cosmology does not provide a good fit to the temperature power spectrum at low multipoles. The unusual shape of the spectrum in the multipole range 20 < l < 40 was seen previously in the WMAP data and is a real feature of the primordial CMB anisotropies.

The poor fit to the spectrum at low multipoles is not of decisive significance, but is an “anomaly” in an otherwise self-consistent analysis of the Planck temperature data.

New Discoveries of last century

1. DARK MATTER IN OUR UNIVERSE

2. DARK ENERGY IN OUR UNIVERSE

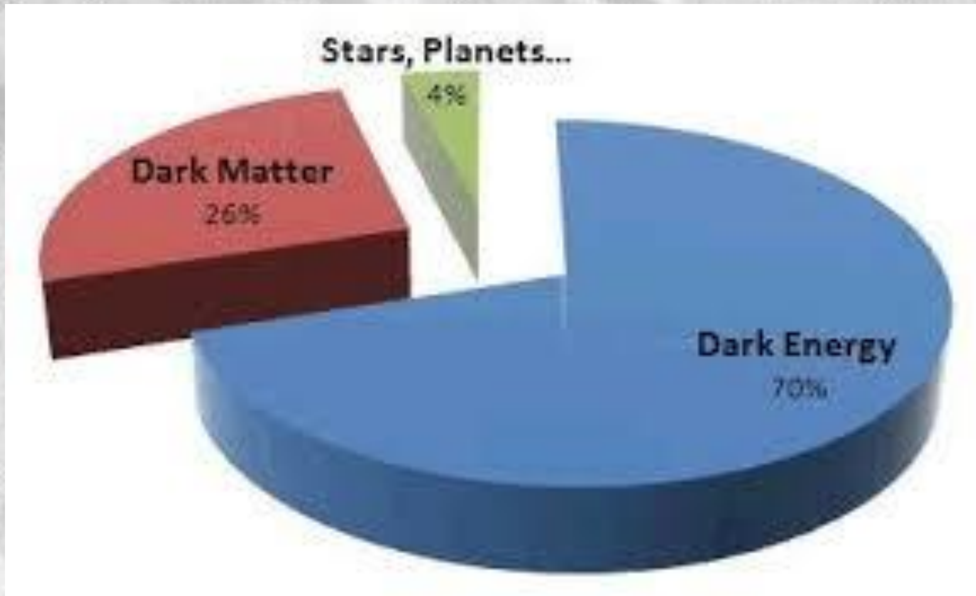

Dark Matter

Dark matter is a type of matter which was introduced to astrophysics to account for a large part of the total mass in the Universe. Dark matter cannot be seen directly with telescopes; its interaction in the electromagnetic sector of interaction is negligible. Its existence are supposed from its gravitational effects on visible matter.

The sources: classical baryonic paradigm

The universe contains some 100 billion galaxies, each with billions of stars, giant gas & dust clouds, and perhaps scads of planets and moons and other little bits of cosmic flotsam.

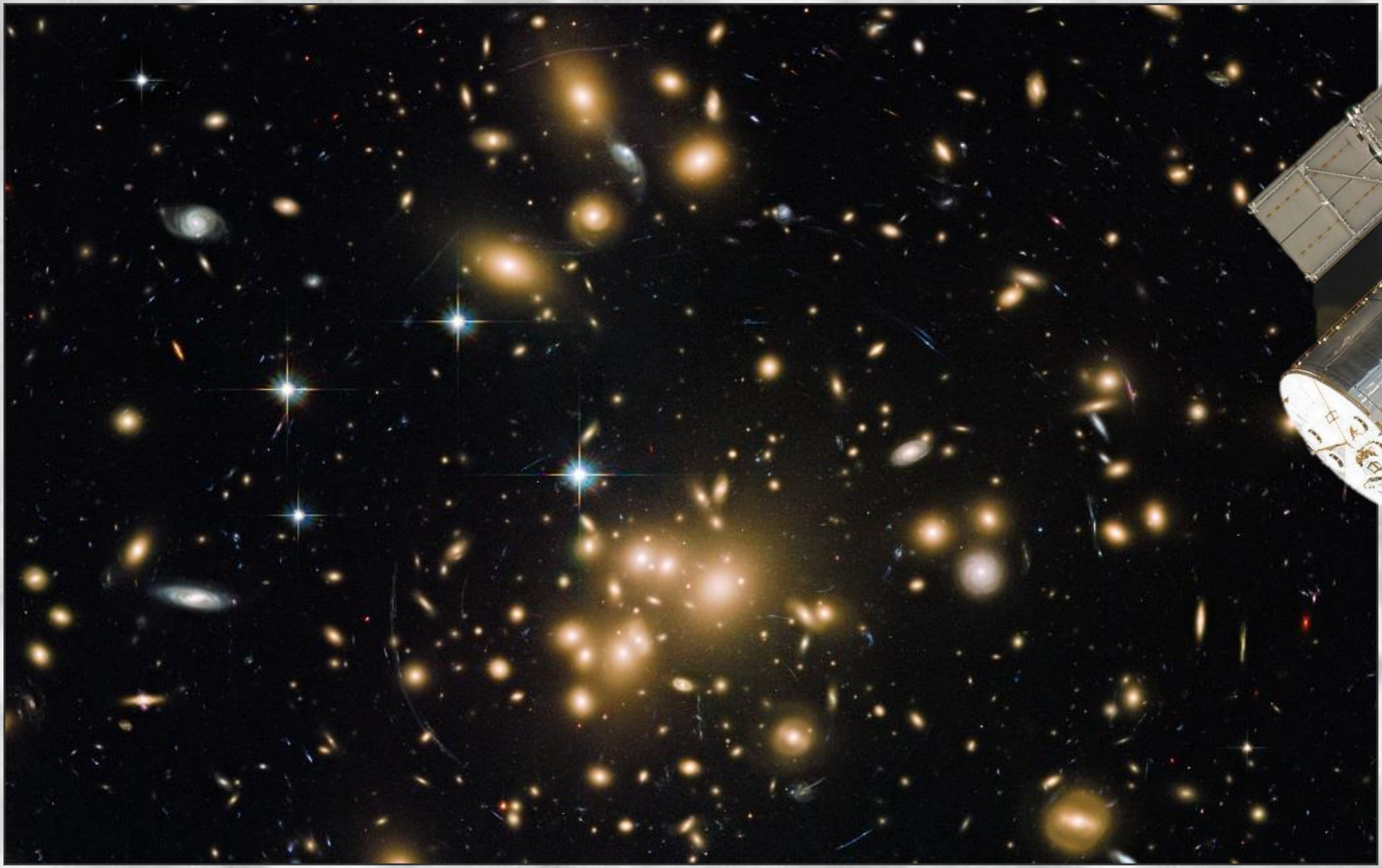

Galaxy cluster Abell 1689 in Virgo;
HST images

And now *new philosophy calls all in doubt*

John Donne

Recent discoveries claim that everything we see is like the tip of the cosmic iceberg

V. van Gogh
The Cafe Terrace on the Place du Forum - Arles

A new paradigm on stage: the dark cosmos

About 95% of cosmic matter/energy
seems to be in some unknown ″dark″ form

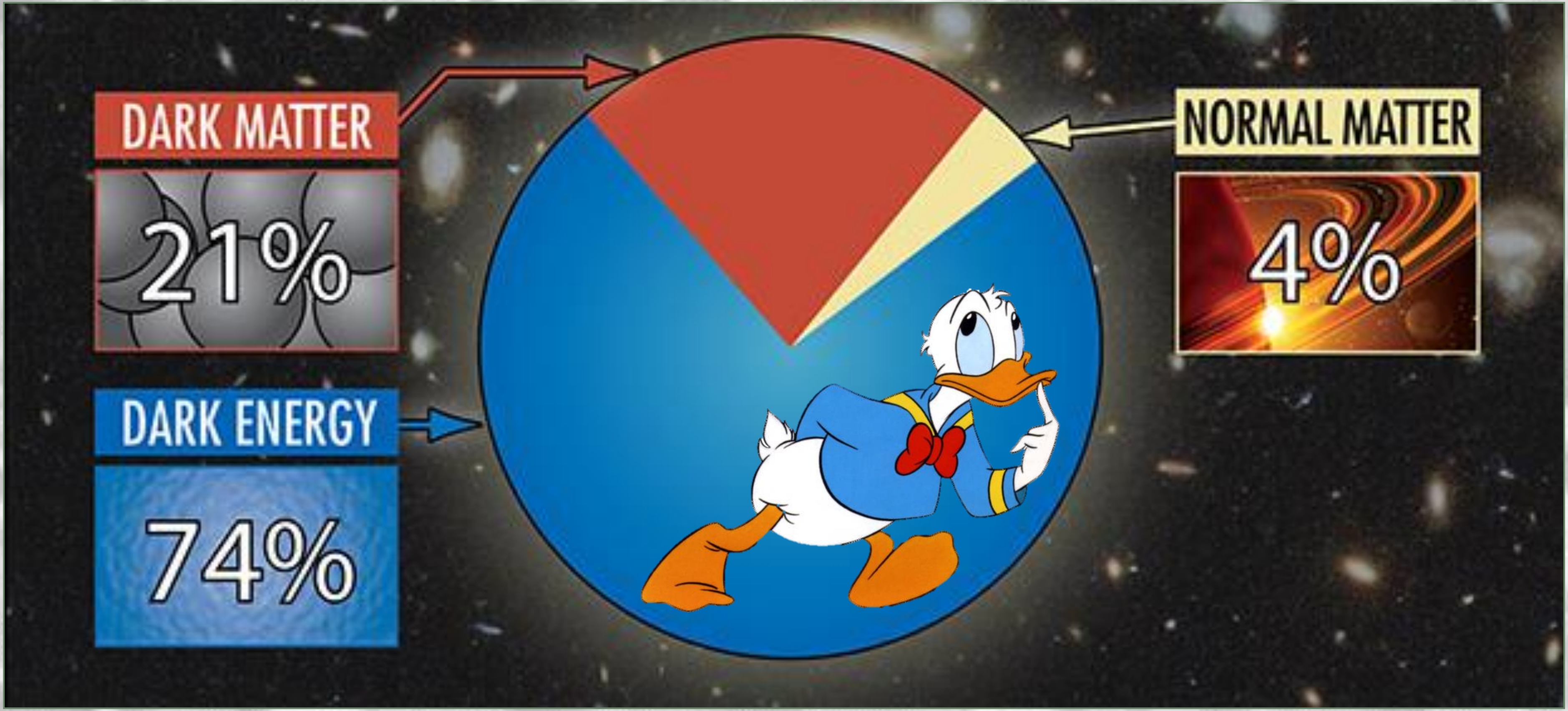

Just the matter which is dark (DM)

About 21% of cosmic matter seems to be in some unknown & exotic "dark" form

- (We believe) it is the gravitational glue holding together galaxies & clusters, and
- It plays a key role in the history & fate of the universe

Yet this matter has not been directly detected

The most popular DM candidates
in terms of detection efforts, are:
neutrinos, WIMPs, MACHOs, and axions

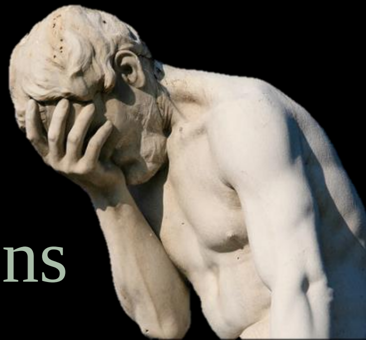

The tricky property: Dark Matter is dark

It is invisible but for the gravitational effects it produces on the visible matter.

That means it must neither emit nor absorb appreciable electromagnetic radiation in any known waveband.

Thus it is called dark matter.

Birth of an idea

Science must begin with myths, and with the criticism of myths.

Karl Popper

What do you blame
when an observation/experiment
does not match the theoretical expectation?

1. Missing ingredients ?
2. Fault in the physical modelling ?

A lesson learned

Discovery of Uranus

Discovery date
13 March 1781

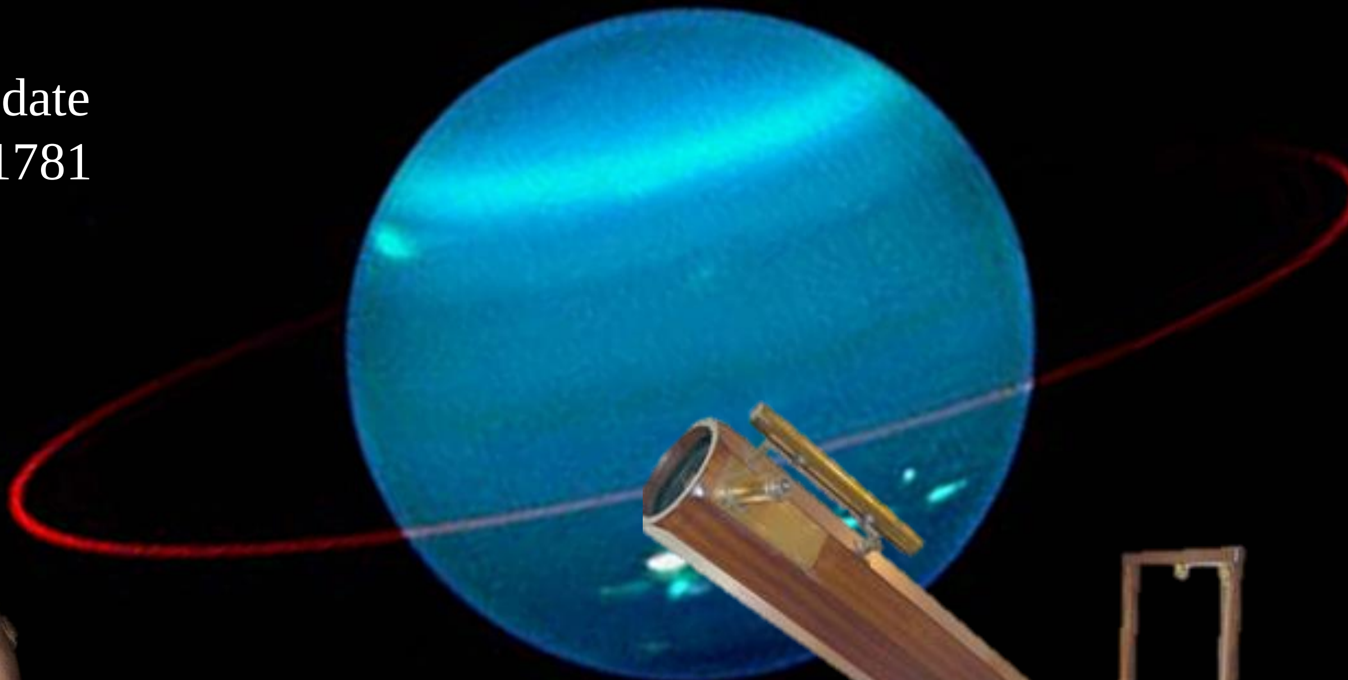

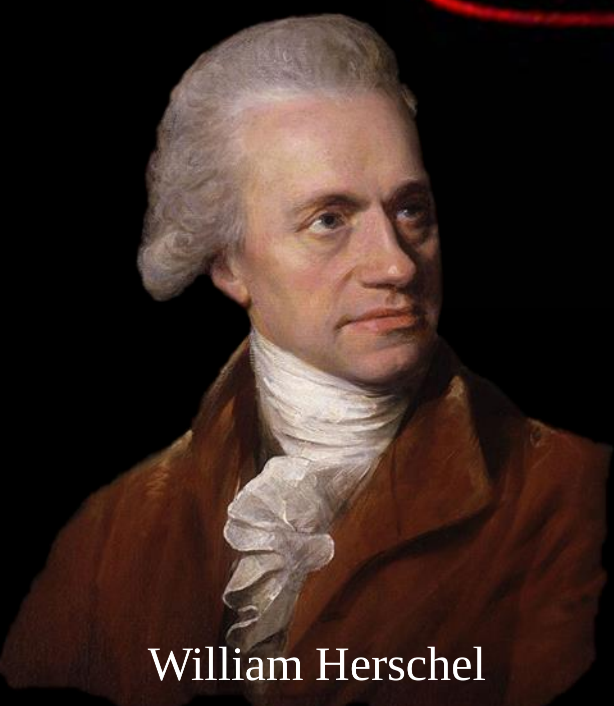

William Herschel

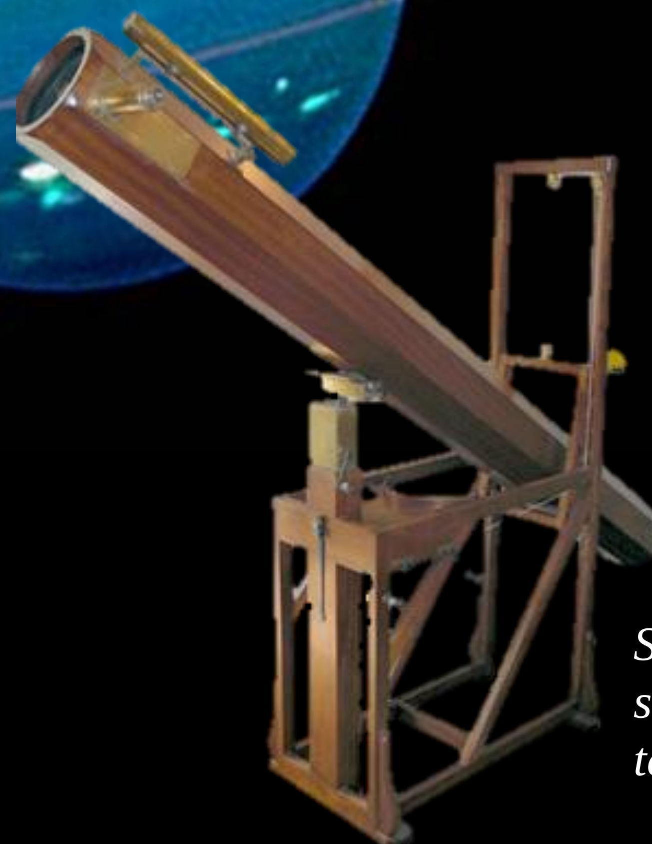

Six inches
seven feet
telescope

Calculation of Uranus orbital parameters

Solution of a *N*-body problem within Newtonian mechanics:

1) law of inertia
2) law of force

with *N* = number of meaningful actors
(Sun + known planets).

The computed speed of Uranus
did not match observations

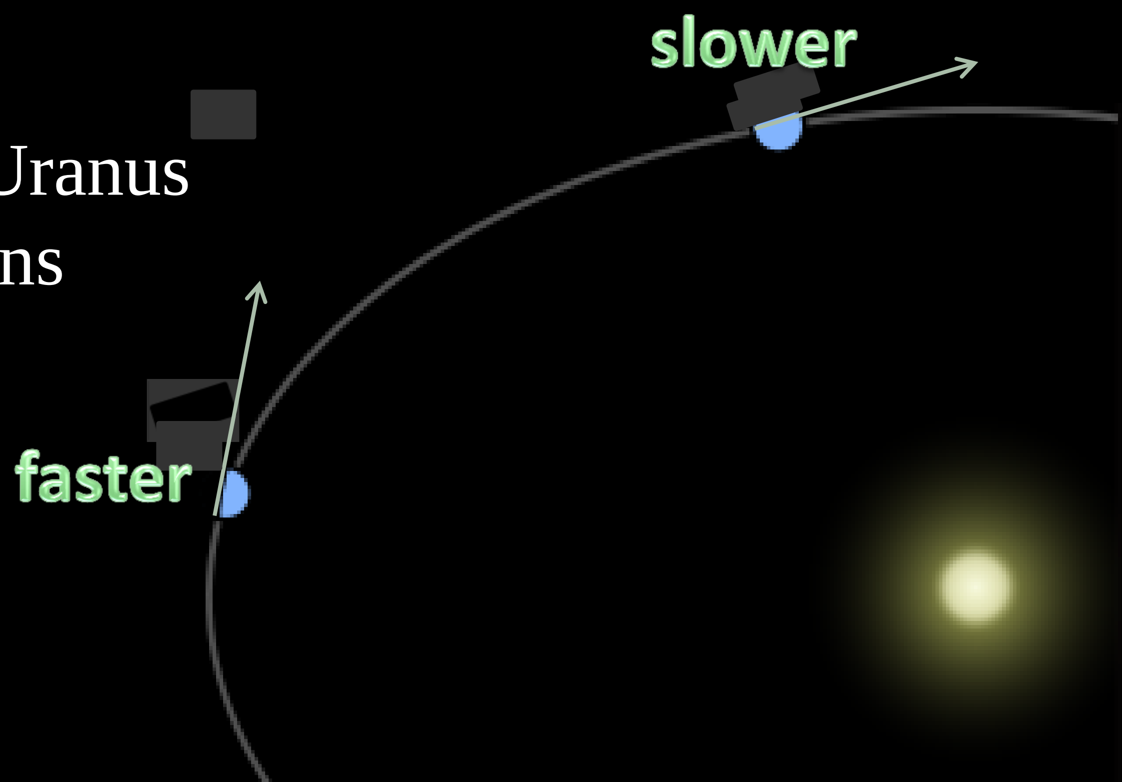

Way out: an unknown body perturbing Uranus

Urbain Le Verrier

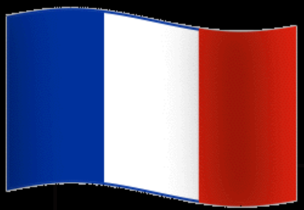

J.C. Adams

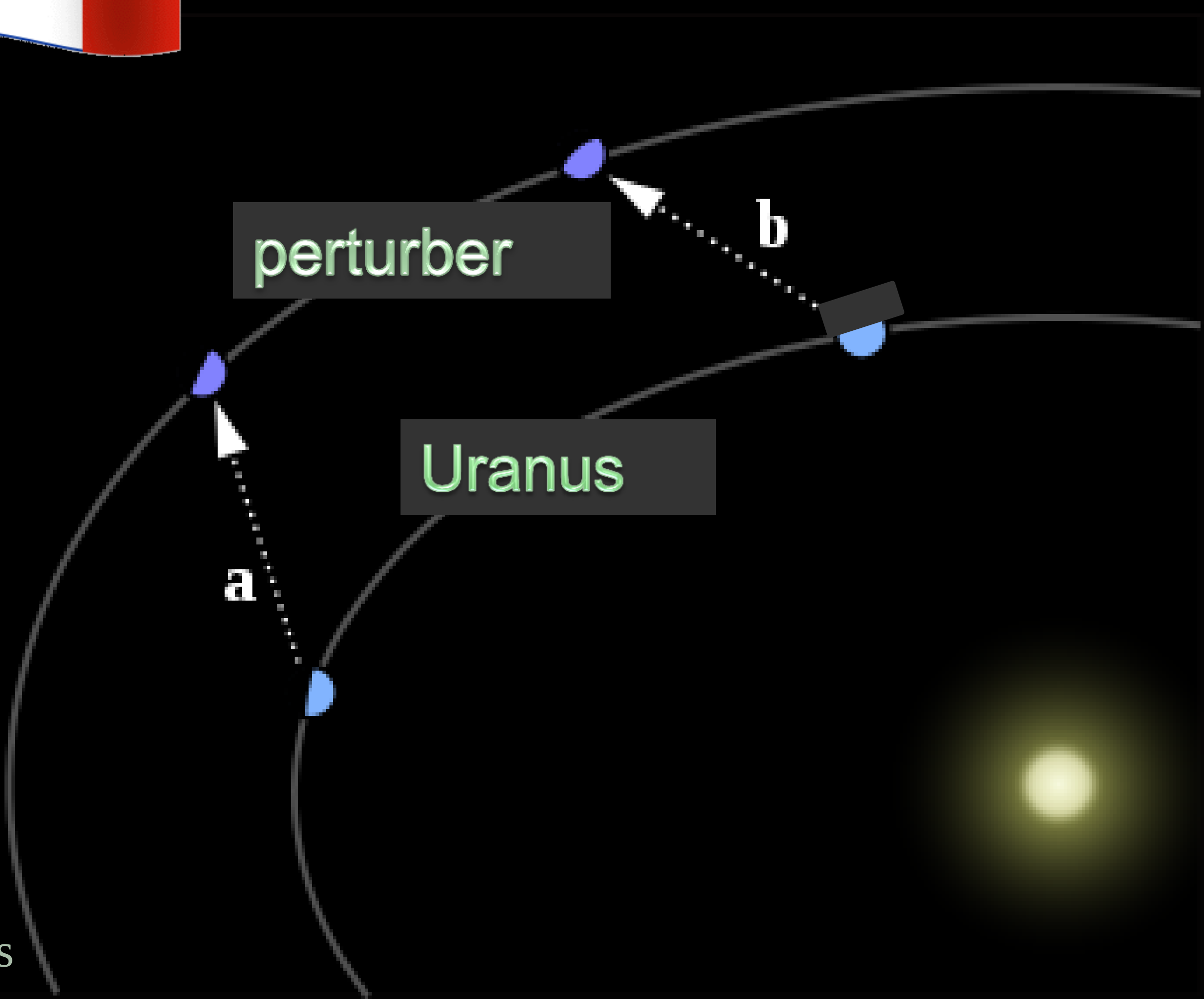

The “dark” ingredient is identified

Discovery of Neptune by J. Galle & H. d'Arrest at Berlin Observatory

«la planète dont le lieu que vous avez [calculé] existe vraiment»

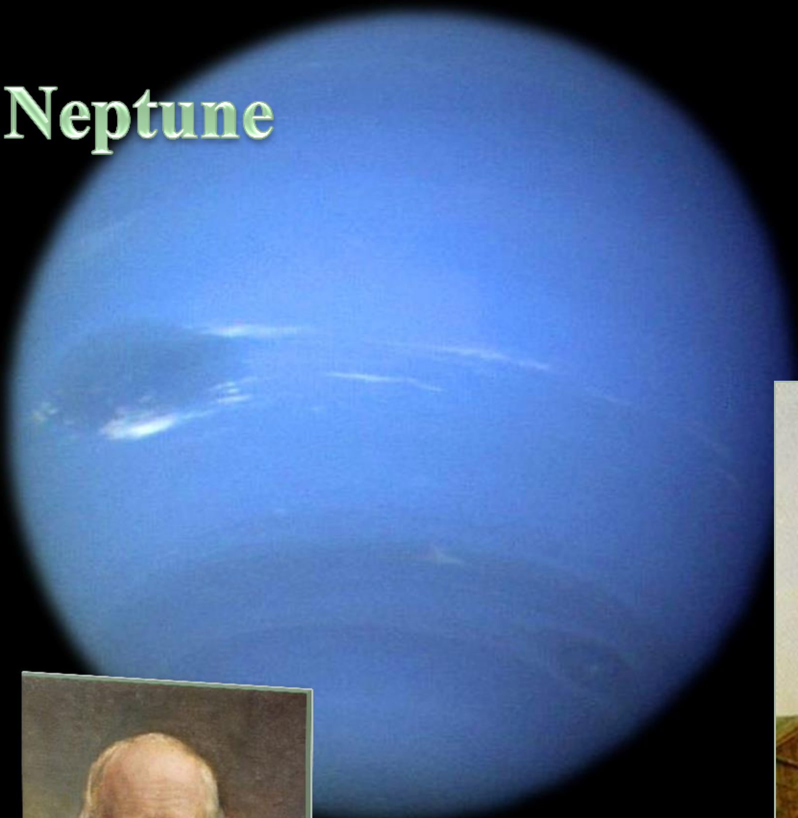

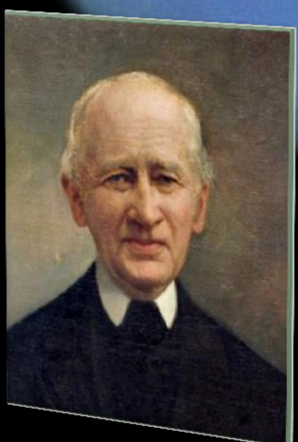

J.Galle

Berlin Observatory

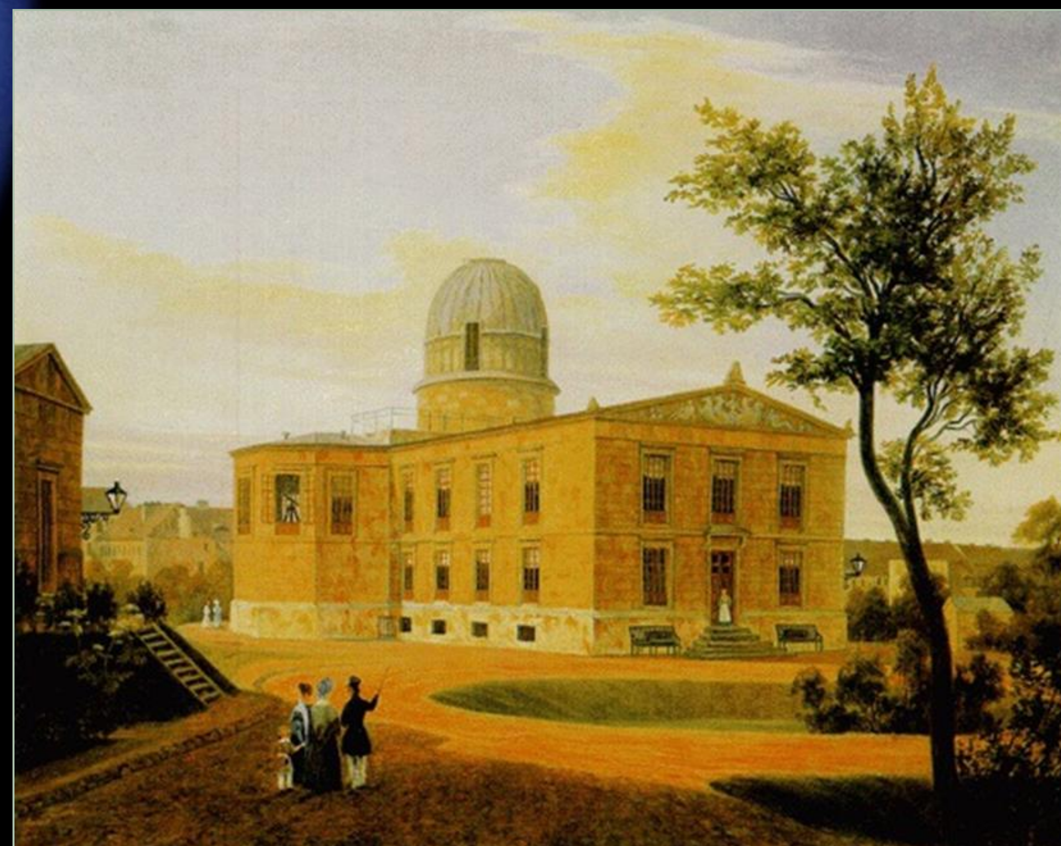

But this is not the rule: a counter-example

Precession of Mercury perihelion

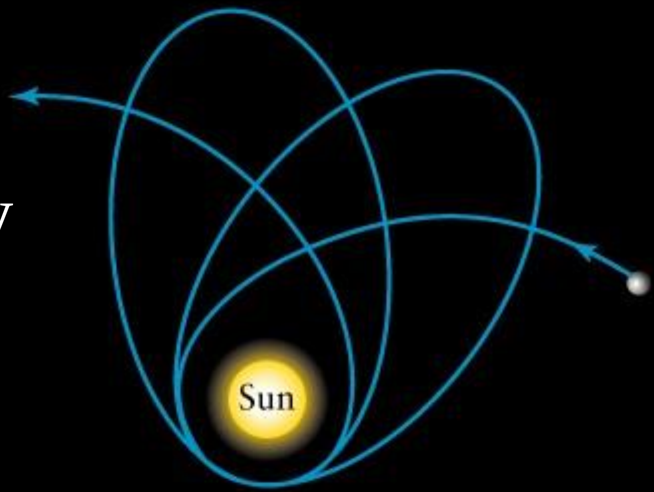

As seen from Earth, the orbit of Mercury precedes by 5600″/century.

Newton's equations, accounting for
 - all the other planets,
 - the slight rotational flattening of the Sun, and
 - the proper inertial reference frame,
predicts a precession of **5557″/century**.

There was a discrepancy of 43″/century (0.78%)

The postman always rings twice

VULCAN

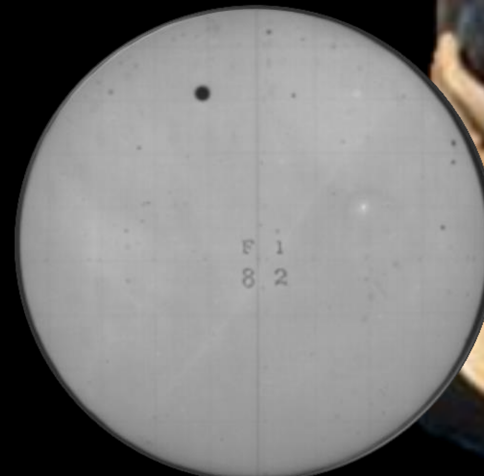

The 1859 “*transit of Vulcan*” may have looked similar to this transit of Venus in a photograph from 1882

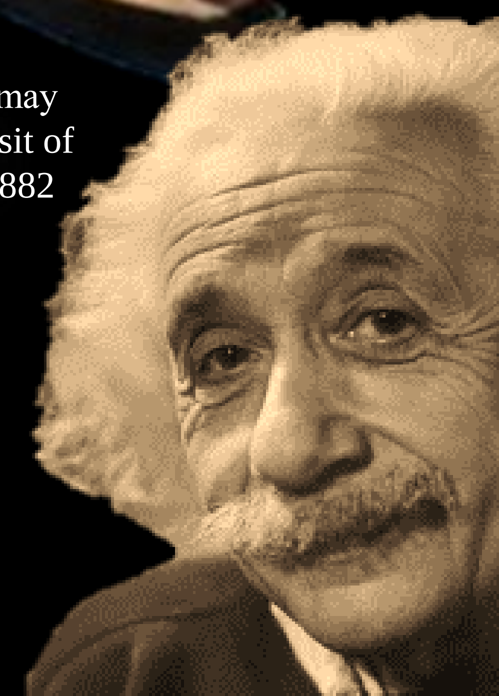

Another new ingredient ????

No, a fault in the theory

Historia magistra vitae est

Cicero's *De Oratore*, II, 36

1932: Solar neighborhood density

Jan H.Oort
(1900-1992)

BULLETIN OF THE ASTRONOMICAL INSTITUTES OF THE NETHERLANDS.

1932 August 17 | Volume VI. | No. 238.

COMMUNICATION FROM THE OBSERVATORY AT LEIDEN.

The force exerted by the stellar system in the direction perpendicular to the galactic plane and some related problems, by *J. H. Oort.*

LEIDEN | 45 | B. A. N. 494

NOTE ON THE DETERMINATION OF K_z AND ON THE MASS DENSITY NEAR THE SUN [1])

BY J. H. OORT

A force K_z has been determined which is consistent with the observations discussed in the preceding article and which at the same time fulfills the requirement that K_z must be due to the attraction by stars and interstellar matter. Our knowledge of the distribution of this attracting mass, though incomplete, is sufficient to put rather stringent conditions on K_z, so that it can be determined much more reliably than if the requirements of Poisson's law are left out of consideration. On the supposition that the z-distribution of the total stellar density is the same as that of the K giants, the variation of K_z with z was found to be like that indicated by crosses in Figure 3. The total mass density at $z = 0$ was found to be 10.0×10^{-24} g/cm^3, or 0.15 solar masses per pc^3, with an estimated uncertainty of about 10%. This density agrees well with that derived by HILL without using Poisson's equation. Its precision is considered to be rather greater. A comparison is made with the results of other recent investigations.
The ratio of mass- to light-density, M/L, in solar units, is 2.4. For the total contents of a cylinder perpendicular to the galactic plane $M/L = 4.2$. The curve in Figure 4, marked K giants, is believed to give a fair representation of the variation of the total star density with z.

The strategic idea

The matter density is measured by sampling a uniform population of stars extending above the disk of the galaxy.

Average velocities of the stars and vertical distances they cover above the disk give a measure of the gravitational restoring force keeping these stars in the disk.

“Oort limit”: lack of visible matter

The density of unseen materia… Milky Way disk
is ≥ 50% of that of the … Oort limit).

WRONG

This additional compon… dark, needs to be nothing very exotic.

It might consist … such as white and even black dwarfs.

N.B. This result has been eventually questioned as the model ignores the pull by the bulge component of the galaxy.

Baryons? Some useful milestones

Unthinkable that missing matter in the Solar area would be non-baryonic.

1932: discovery of the first neutral baryon, the neutron, by James Chadwick

1929: discovery of the expansion of the universe by Edwin Hubble

1926: discovery of the nature of the white nebulae by Edwin Hubble

1937: The "missing mass" in the Coma cluster

Fritz Zwicky
(1898-1974)

THE ASTROPHYSICAL JOURNAL

AN INTERNATIONAL REVIEW OF SPECTROSCOPY AND ASTRONOMICAL PHYSICS

VOLUME 86 | OCTOBER 1937 | NUMBER 3

ON THE MASSES OF NEBULAE AND OF CLUSTERS OF NEBULAE

F. ZWICKY

Helvetica Physica Acta, Vol. 6, p. 110-127, 1933

Die Rotverschiebung von extragalaktischen Nebeln

von **F. Zwicky.**

(16. II. 33.)

Inhaltsangabe. Diese Arbeit gibt eine Darstellung der wesentlichsten Merkmale extragalaktischer Nebel, sowie der Methoden, welche zur Erforschung derselben gedient haben. Insbesondere wird die sog. Rotverschiebung extragalaktischer Nebel eingehend diskutiert. Verschiedene Theorien, welche zur Erklärung dieses wichtigen Phänomens aufgestellt worden sind, werden kurz besprochen. Schliesslich wird angedeutet, inwiefern die Rotverschiebung für das Studium der durchdringenden Strahlung von Wichtigkeit zu werden verspricht.

The Coma cluster of galaxies

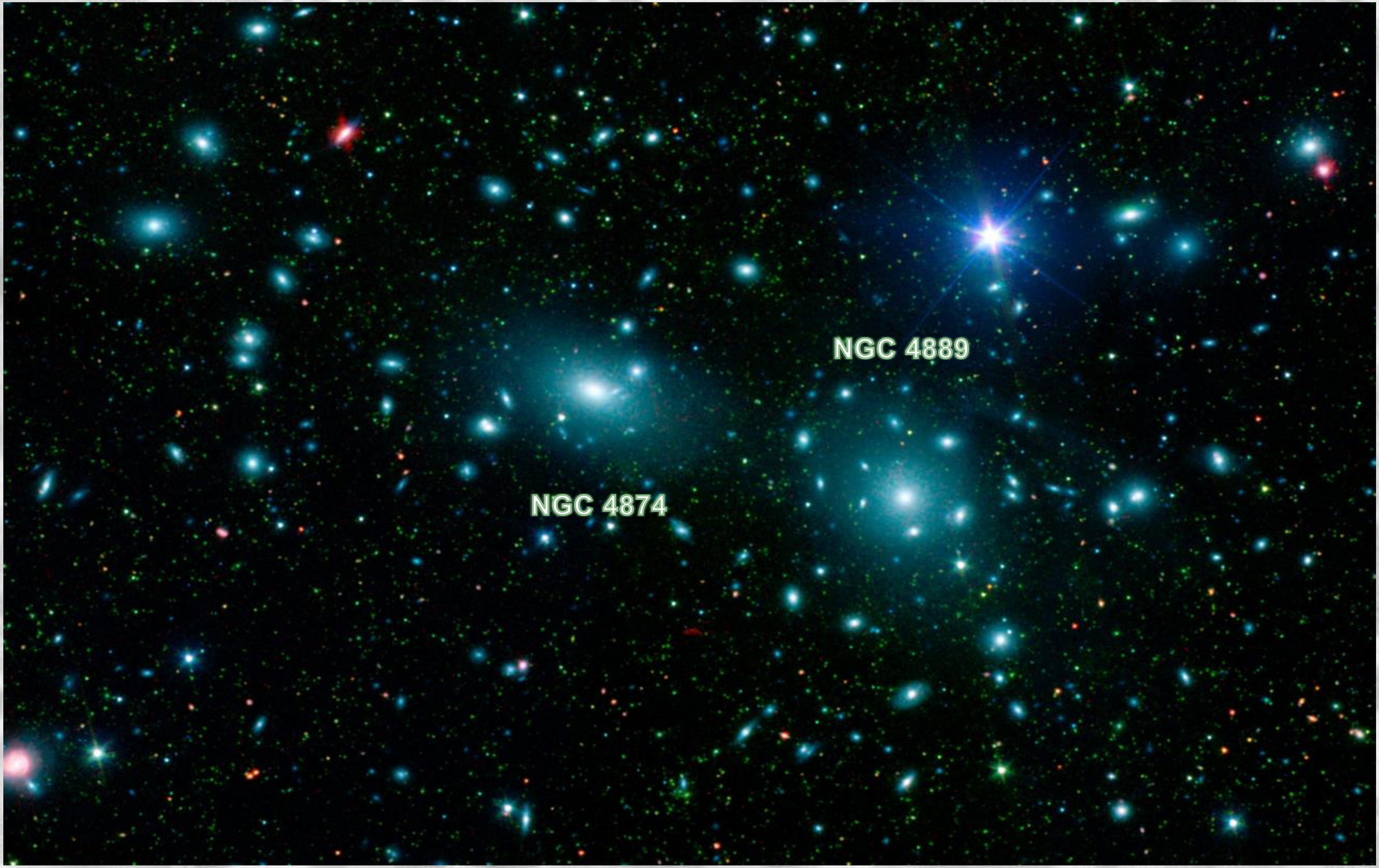

Composite picure from SDSS + Spitzer

The total virial mass

Using the virial theorem with some acrobatic assumptions to account for the geometry of the system and the projection effects:

$$\boxed{M_T = Nm \cong \frac{2Rv^2}{G}}$$

Zwick took: $\sqrt{v^2} = 700$ km/s,

$R = 2\times10^6$ ly,

$N = 1000$,

and obtained:

$M_T > 9\times10^{46}$ gr, or $m > 9\times10^{43}$ gr $= 4.5\times10^{10} M_{Sun}$.

By measuring the luminosity, Zwicky computed mass-to-light ratio γ [$\gamma = 1$ for the Sun].

Plenty of *missing mass*

in the “globular cluster of nebulae”

500 vs. 3

According to (36), the conversion factor γ from luminosity to mass for nebulae in the Coma cluster would be of the order

$$\gamma = 500\,, \tag{37}$$

as compared with about $\gamma' = 3$ for the local Kapteyn stellar system. This discrepancy is so great that a further analysis of the problem is in order. Parts of the following discussion were published several years ago, when the conclusion expressed in (36) was reached for the first time.[5]

Modern value (Lucas & Mamon 2003) is $M/L_{\mathrm{B}} = 351\ h_{70}$

Ignored …; too early

Zwicky's intuitions were not taken seriously by the scientific community.

First of all there were no DM candidates because:

1. gas radiating X-rays and dust radiating in the IR could not yet be observed, and
2. non-baryonic matter was unthinkable.

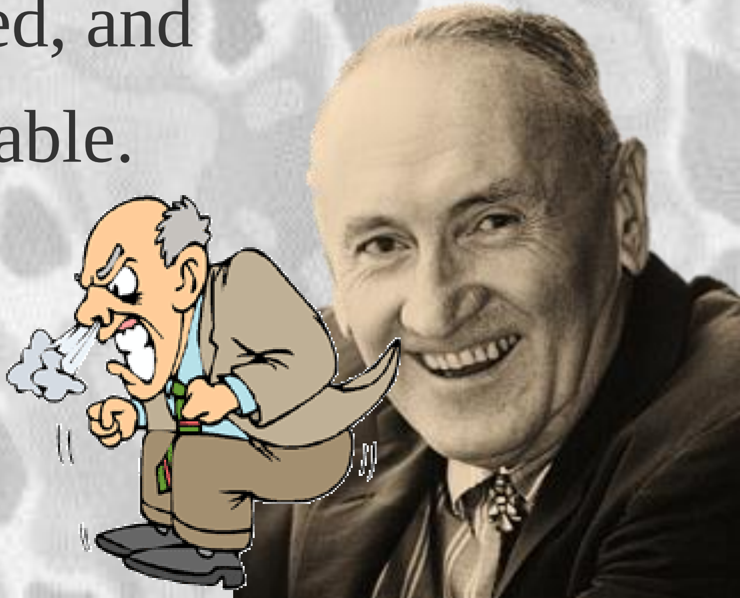

Zwicky's caustic reputation

Zwicky used to call his colleagues
"*spherical bastards*" as they were bastards
from any direction you would look at them, and

in his *Introduction* to a self-published
Catalogue of compact galaxies in 1971
he described the colleagues as
"*scatterbrains, sycophants,*
and plain thieves
. . . [who] doctor their observational data
to hide their shortcomings . . .
[and publish] useless trash in the
bulging astronomical journals".

Zwicky's popularity gradient

Year	No. citations
1955-59	2
1960-64	6
1965-69	5
1970-74	2
1975-89	63
1990-99	71

anvur

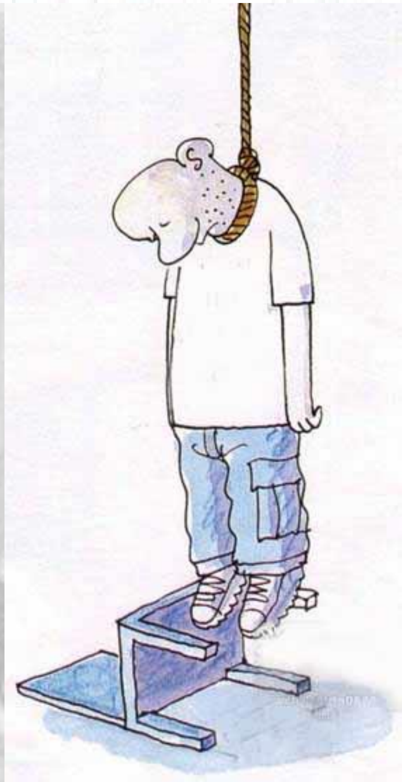

Lesson learned

Since then observations have revised
our understanding of the composition of clusters.

- Luminous stars count for a very small fraction of a cluster mass.
- There is also a baryonic, hot intracluster medium (**ICM**) visible in the X-ray spectrum.
- Rich clusters typically have more mass in hot gas than in stars; in the largest virial systems (e.g. Coma) composition is: 85% DM, 14% ICM, and only 1% stars.

Coma cluster in X-rays

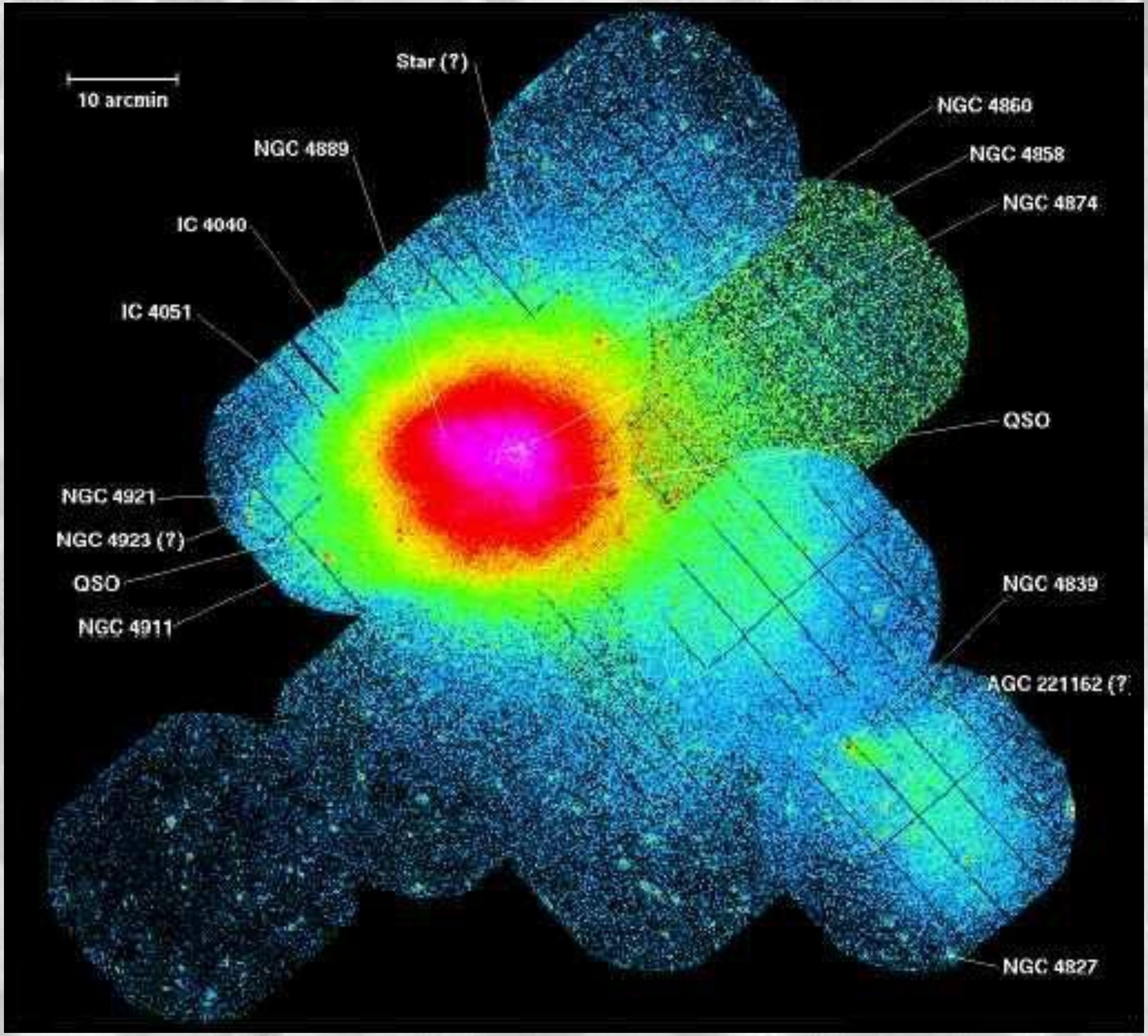

Fritz Zwicky vindicated

Dark matter distribution in the Coma cluster from galaxy kinematics: breaking the mass–anisotropy degeneracy

Ewa L. Łokas[1★] and Gary A. Mamon[2,3★]

Mon. Not. R. Astron. Soc. 343, 401–412 (2003)

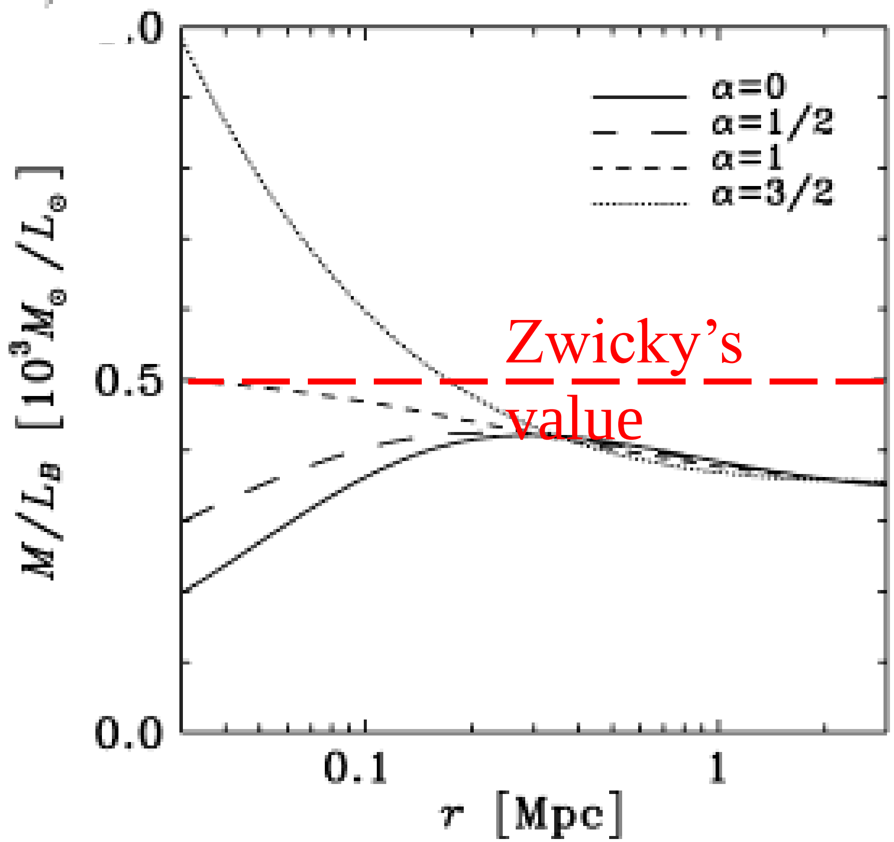

Zwicky’s concern

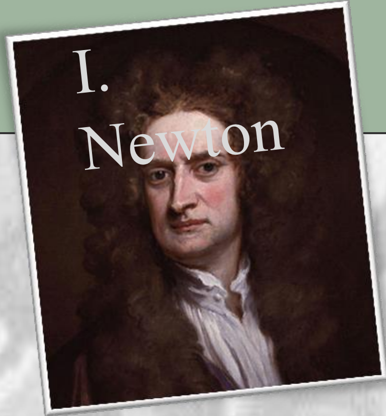

$$\frac{1}{r^2} \ ???$$

In addition it will be n methods which allow
us to determine the relat ernebular material in
clusters as well as in the general field.

It should also be noticed that the virial theorem as applied to clusters of nebulae provides for a test of the validity of the inverse square law of gravitational forces. This is of fundamental interest because of the enormous distances which separate the gravitating bodies whose motions are investigated. Since clusters of nebulae are the largest known aggregations of matter, the study of their mechanical behavior forms the last stepping-stone before we approach the investigation of the universe as a whole.

He had covered his back ….

On the assumption that Newton's inverse square law accurately describes the gravitational interactions among nebulae,

Zwicky's precaution has eventually evolved into new theories of gravity

Mordehai Milgrom

MOND

Robert Sanders

Alexei Starobinsky

$f(R)$

MOND: Modified Newton Dynamics

$$a_N = G\frac{M}{r^2} = \frac{\mathrm{v}^2}{r} \quad \text{where } \bar{a}_N = \mu\left({a}/{a_0} \right)\bar{a}$$

$$\mu\left({a}/{a_0} \right) = \begin{cases} 1 & \text{for } a \gg a_0 \quad \text{classical Newton Dyn: } f = ma \\ {a}/{a_0} & \text{for } a \ll a_0 \quad \text{modified Newton Dyn: } f = ma^2 \end{cases}$$

with $a_0 = 1.2\times 10^{-10}\ \mathrm{m/s^2}$.

Effect:

- modified inertia: $\mu\left({a}/{a_0} \right)\bar{a} = G\frac{M}{r^2}$
- modified force: $\bar{a} = G\frac{M}{\mu\left({a}/{a_0} \right) r^2}$

Phenomenological approach

J.Kepler

Weak vs. strong field regimes

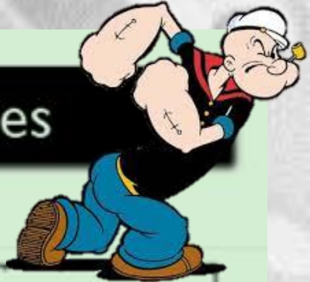

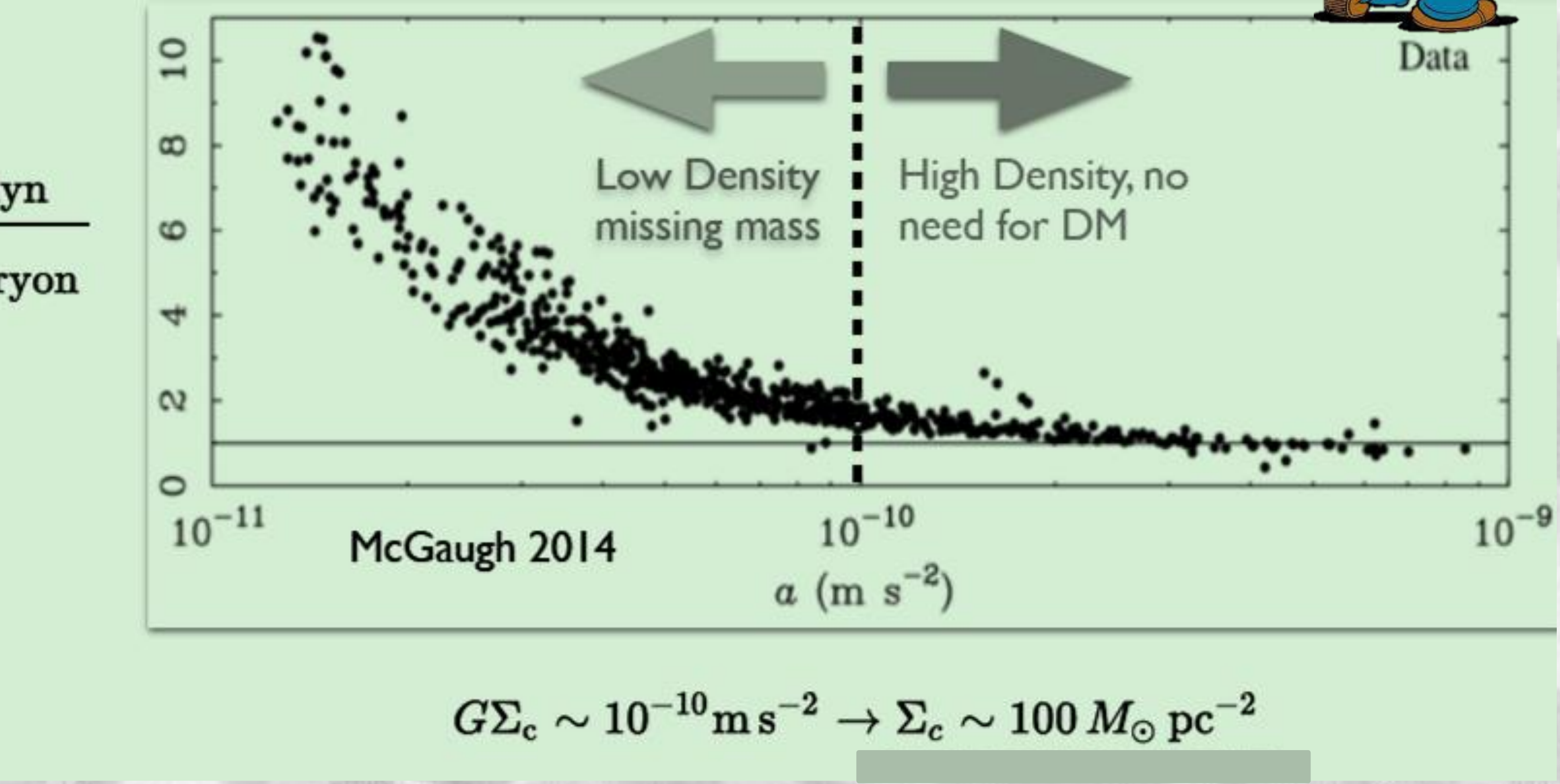

f(R): curvature mimicking gravity

Modified gravity theory geleralizing Einstein's General Relativity.

$f(R)$ gravity is a family of theories defined by a different function of the Ricci scalar R.

$f(R) = R\left(-2\Lambda\right)$ is just General Relativity (and ΛCDM).

Generalized Lagrangian of the Einstein-Hilbert action:

$$S = \int \frac{1}{2\kappa} R\sqrt{g}\ d^4x \quad \rightarrow \quad S = \int \frac{1}{2\kappa} f(R)\sqrt{g}\ d^4x$$

where $\kappa = 8\pi G c^{-4}$ and

$g = \left|g_{\mu\nu}\right|$ is the determinant of the metric tensor.

Focus moved from matter to curvature

Zwicky's survey program

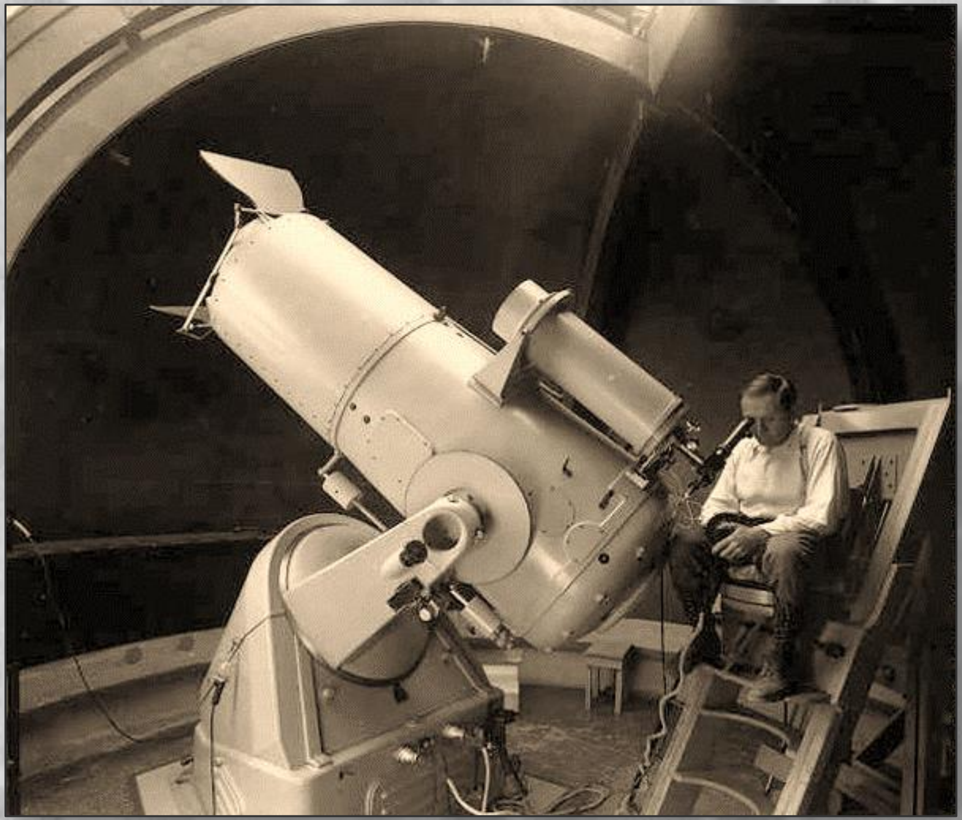

Achievements

- Cluster of galaxies
- Novae
- Supernovae
- Compact galaxies

It is therefore the intention to undertake a series of observations which may throw some light on the problem of the density of internebular matter in clusters, as compared with the density of matter in the general field.

Modern survey telescopes

Modern survey telescopes

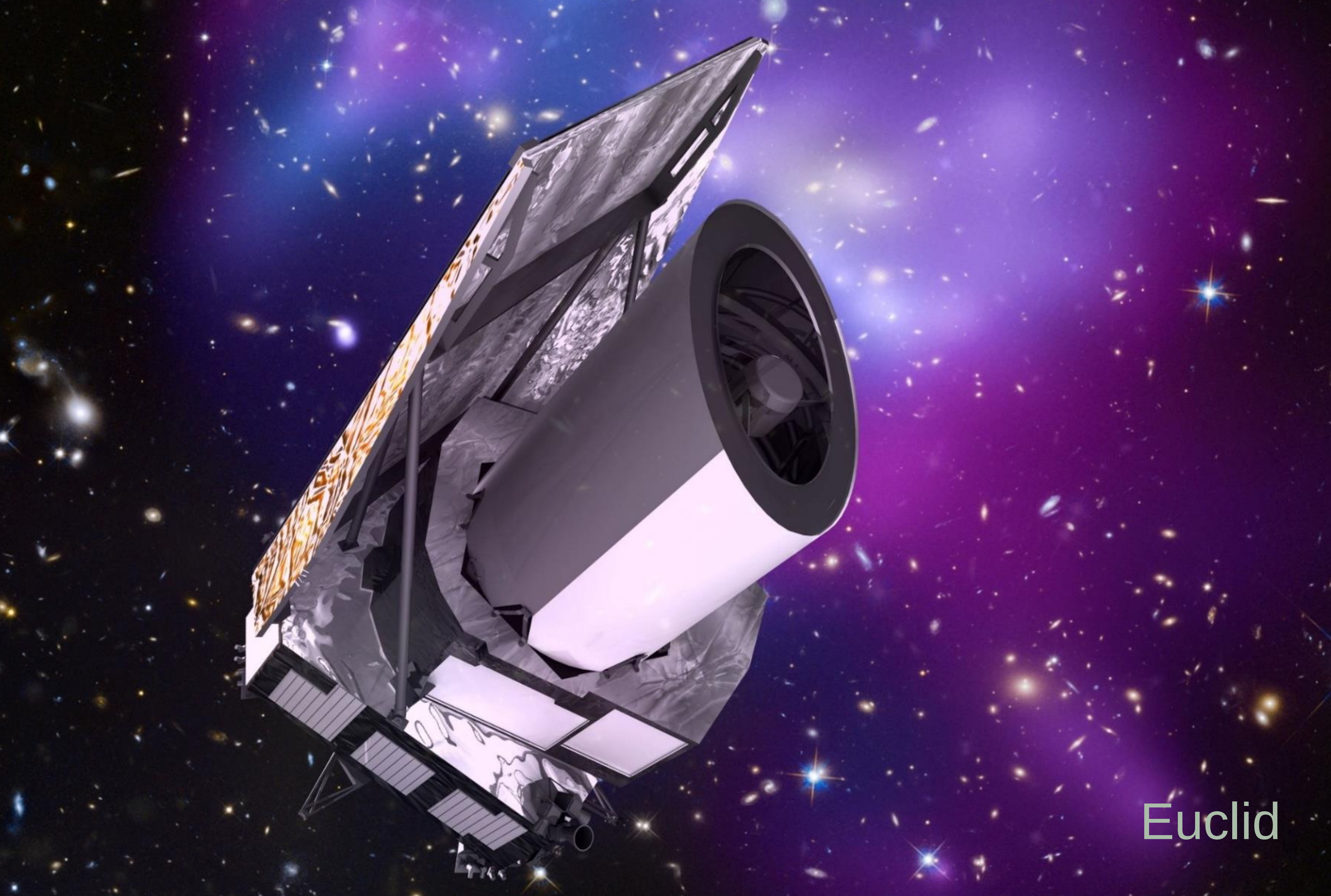

Modern survey telescopes

Zwicky's proposal for gravitational lensing

IV. NEBULAE AS GRAVITATIONAL LENSES

As I have shown previously,[6] the probability of the overlapping of images of nebulae is considerable. The gravitational fields of a number of "foreground" nebulae may therefore be expected to deflect the light coming to us from certain background nebulae. The observation of such gravitational lens effects promises to furnish us with the simplest and most accurate determination of nebular masses.

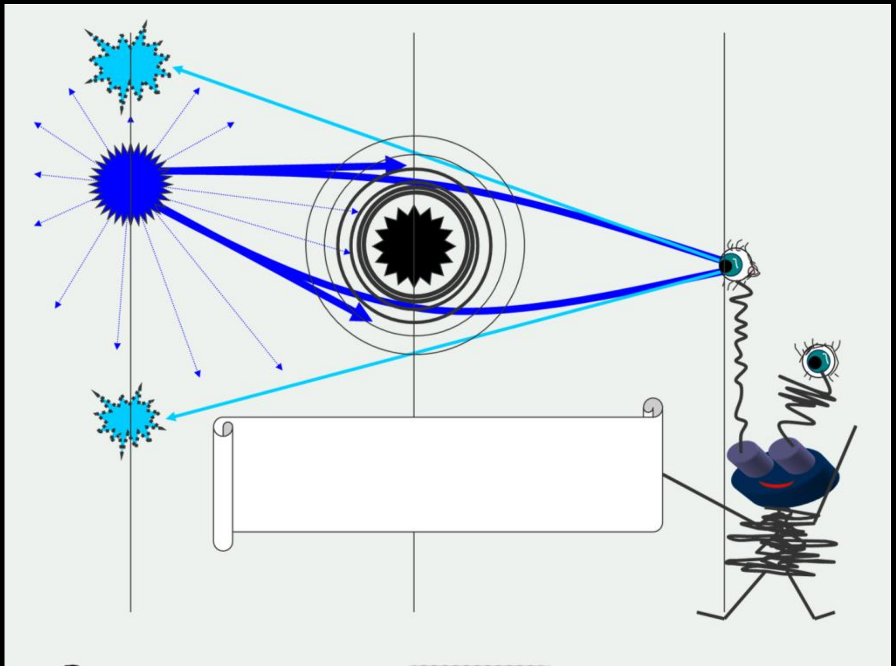

Gravitational lensing regimes

Einstein postulated the equivalence principle with Special Relativity to predict that light rays bend in a gravitational field, even before he developed the concept of curved spacetime.

There are three different regimes:

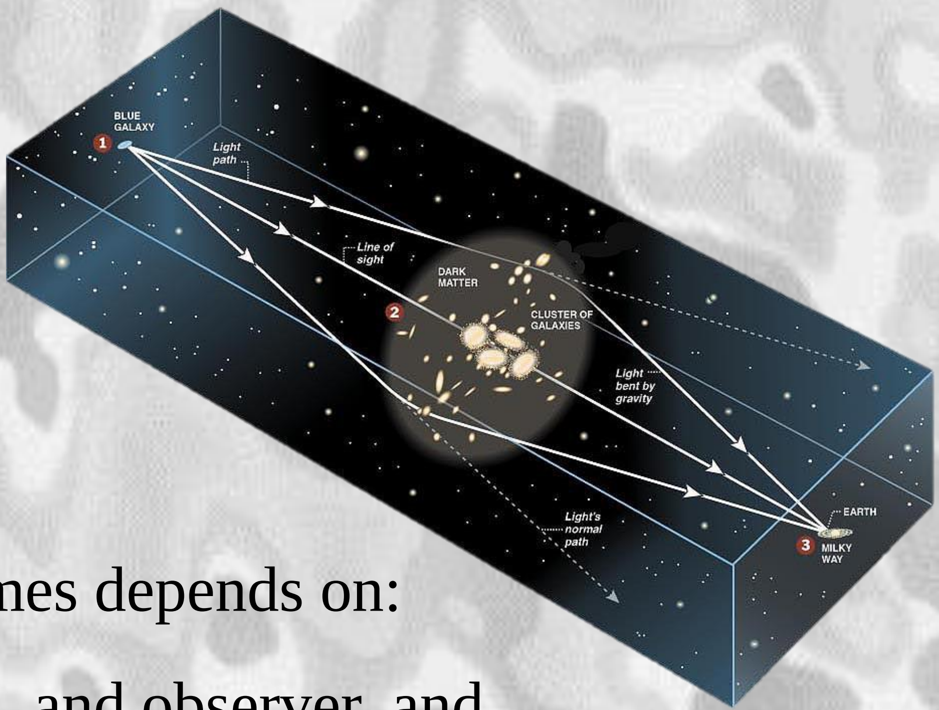

- strong lensing,
- weak lensing,
- microlensing.

The distinction between these regimes depends on:

1. the positions of the source, lens, and observer, and
2. the mass and shape of the lens, which controls how much light is deflected and where.

Gravitational lensing regimes

Strong Lensing:

the lens is very massive and the source is close enough to it.

Weak Lensing:

the lens is not strong enough to form multiple images or arcs. However, the source can still be distorted: both stretched (*shear*) and magnified (*convergence*). Useless for individual sources, but very powerful statistical tool.

Microlensing:

the lensed image that is so small or faint that one doesn't see the multiple images. Additional light bent towards the observer just makes the source appear brighter. (The surface brightness remains unchanged but as more images of the object appear the object appears bigger and hence brighter.)

Strong lensing

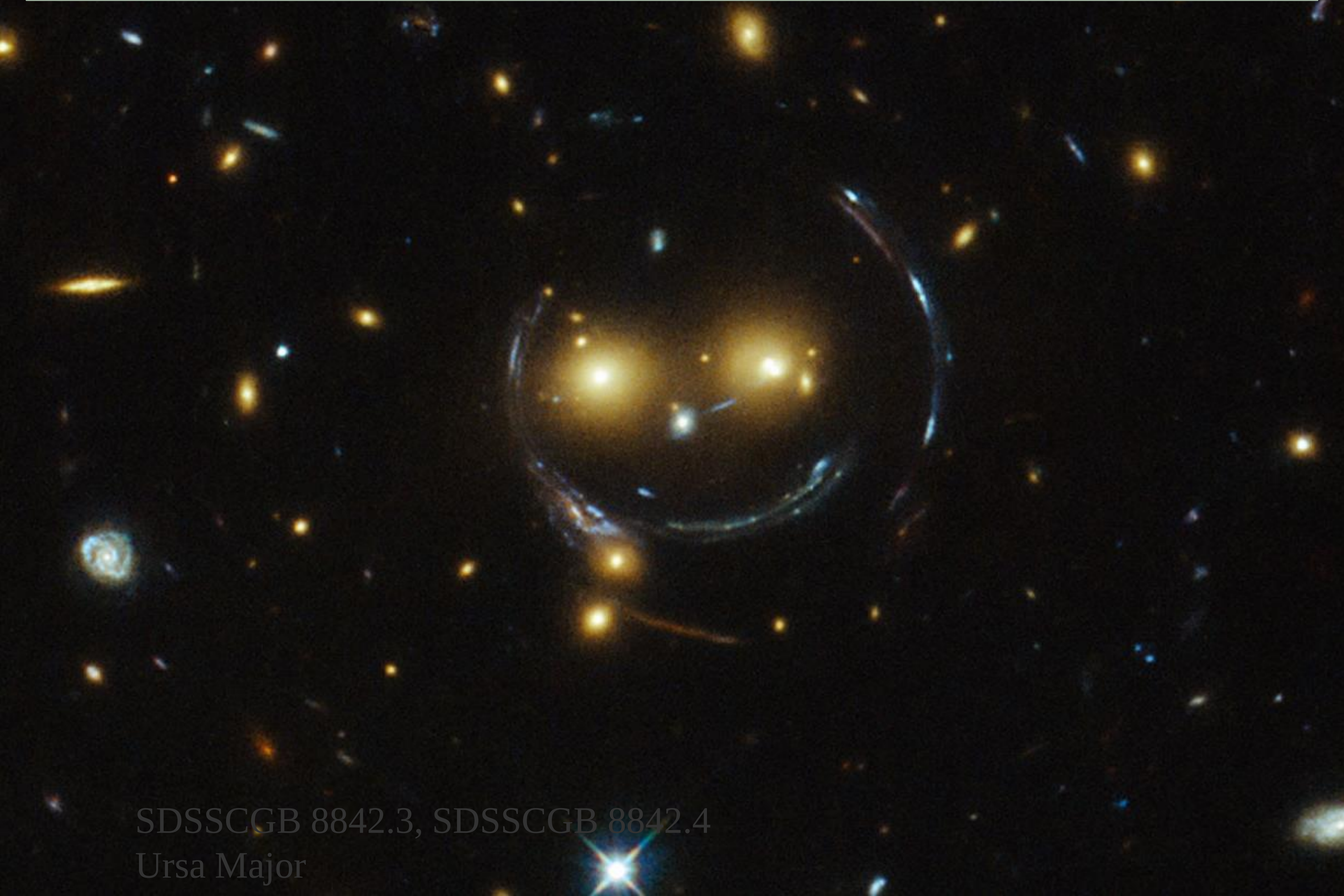

SDSSCGB 8842.3, SDSSCGB 8842.4
Ursa Major

Weak lensing

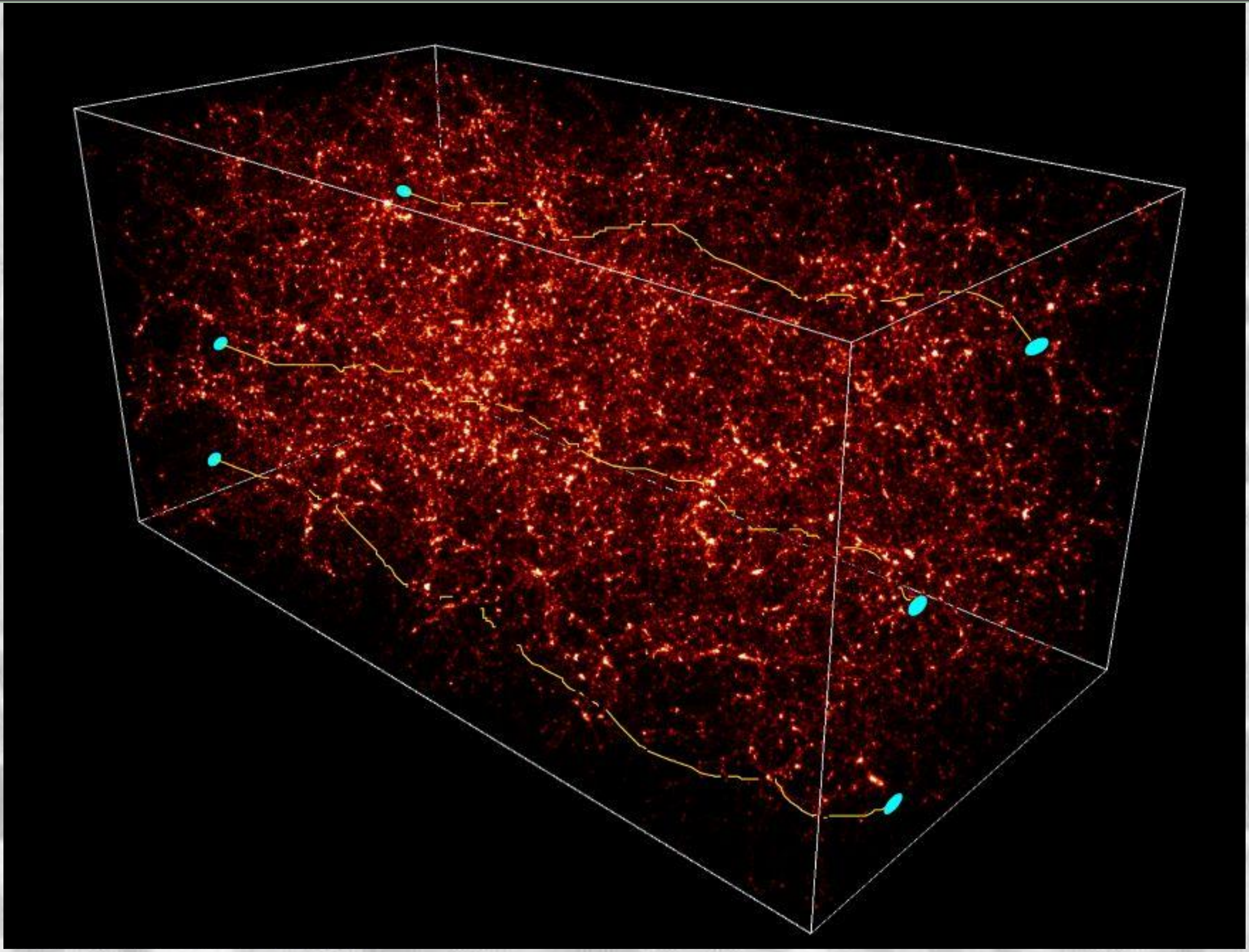

Weak lensing analogy

Weak lensing

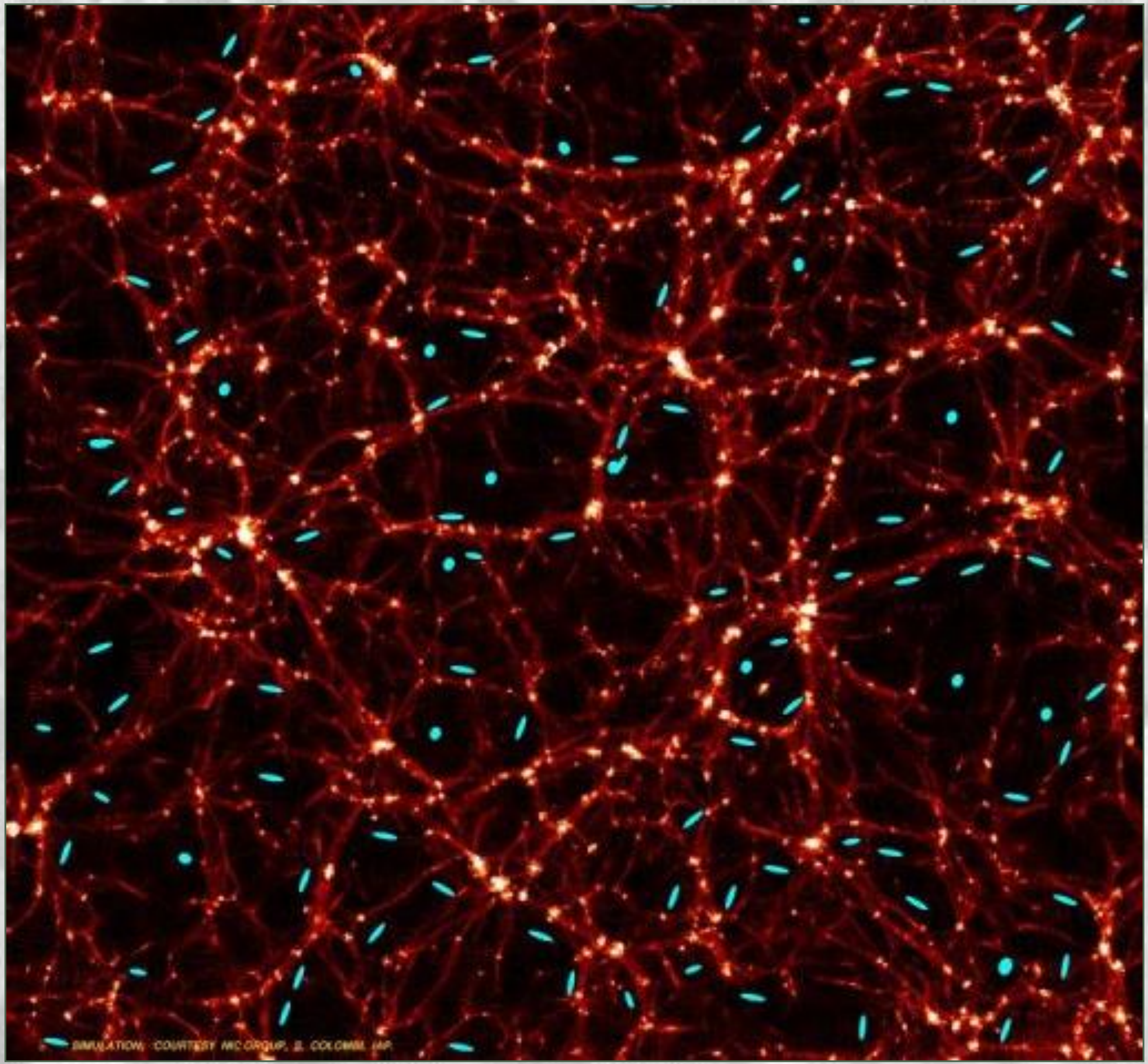

One of the more natural candidates for the halo dark matter are MACHO's, because they are already known to exist. Two experiments reported in 1993 have found strong evidence for the existence of MACHOs. The technique used is gravitational microlensing.

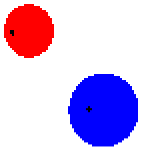

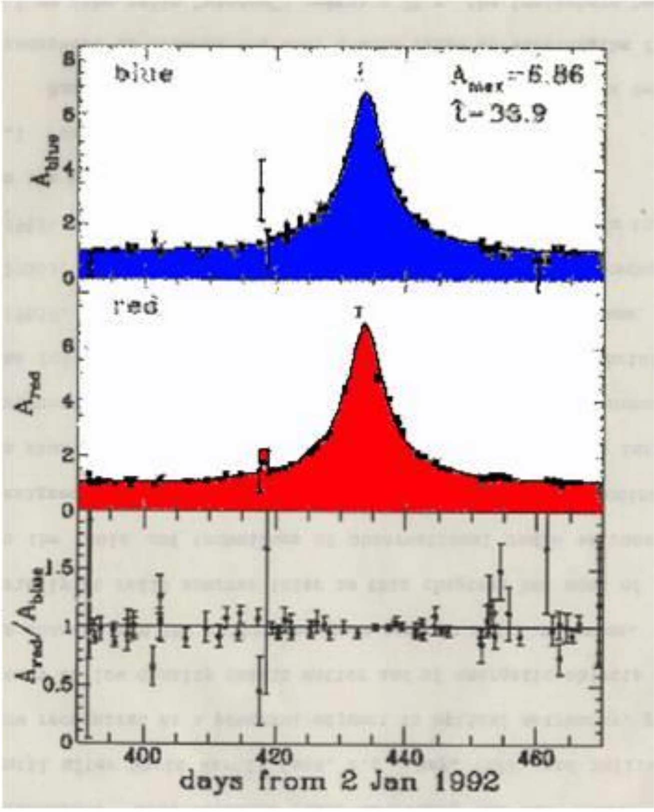

Microlensing on Machos

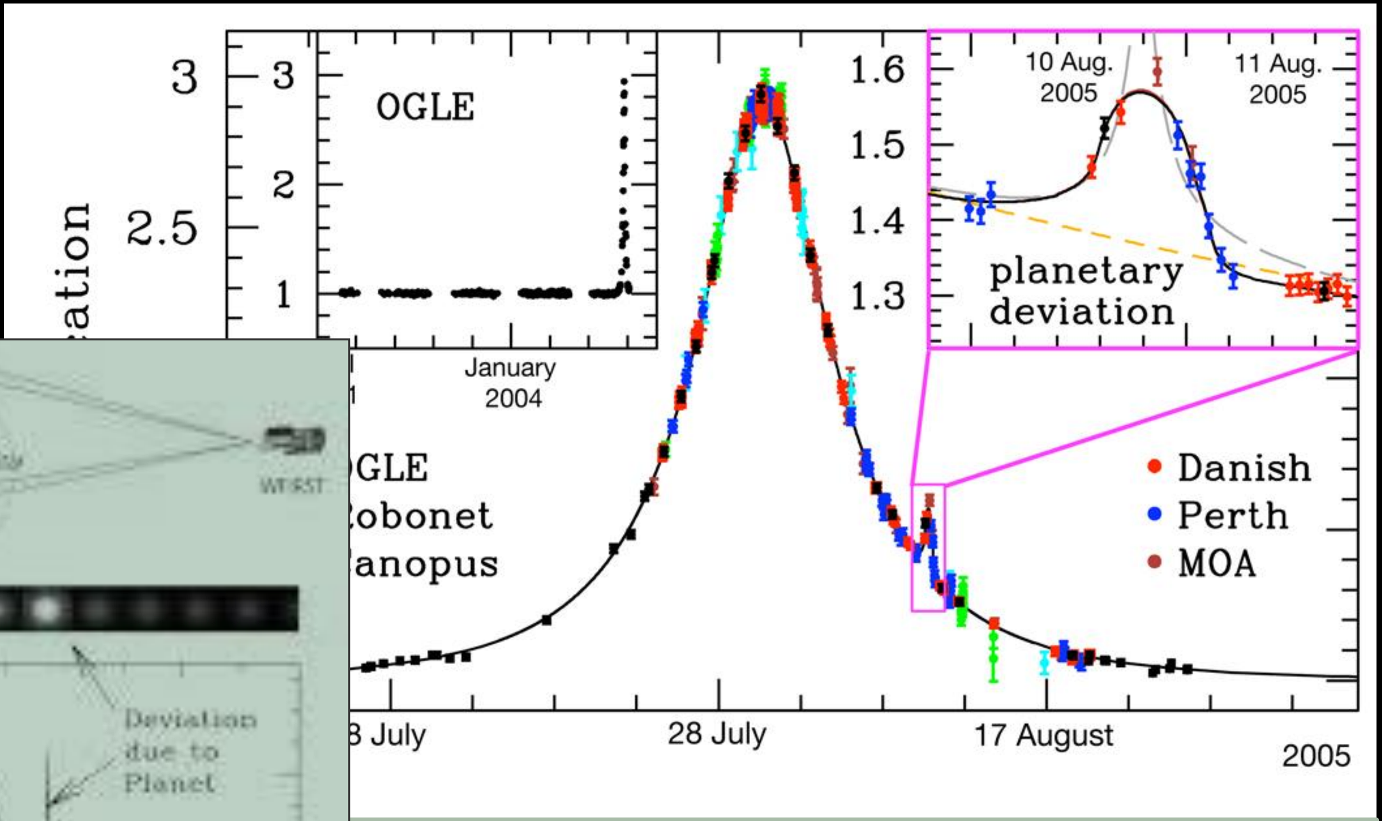

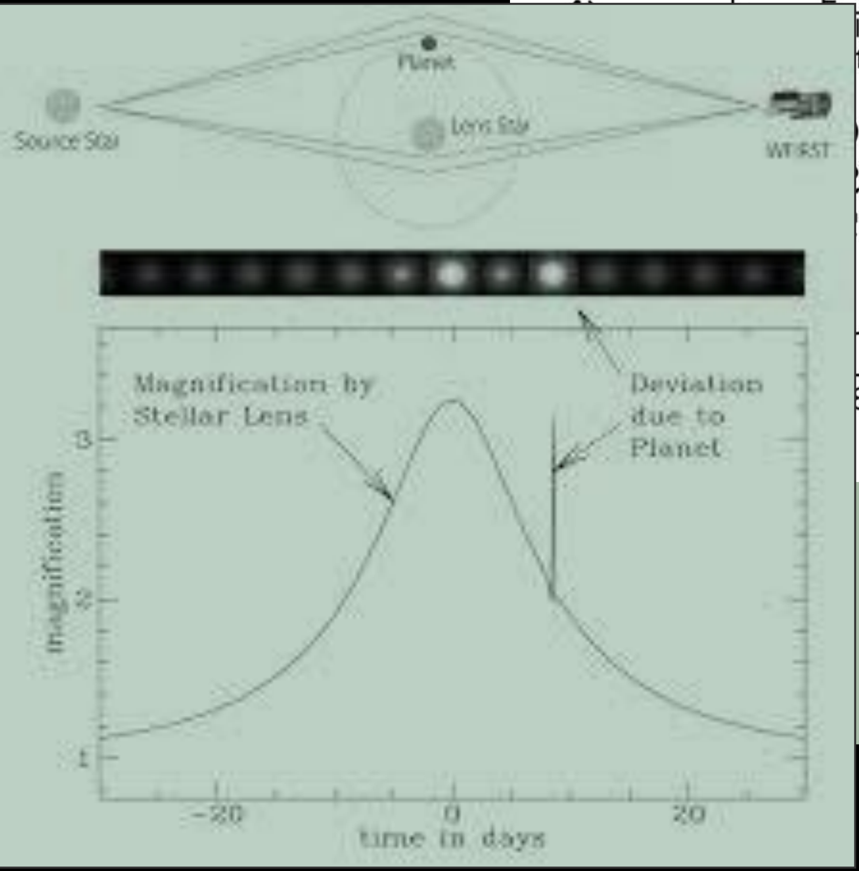

1937: Holmberg’s thesis

A study of double and multiple galaxies

Holmberg was a student of Lundmark at the Lund Observatory. In his dissertation (1937, *Annals of the Observatory of Lund*) he showed that galaxies often appear in groups and pairs, and he realized how it would be possible, using statistics, to determine the masses through the radial velocities of the two components.

Holmberg’s masses of galaxies were just in between Hubble’s and Zwicky’s.

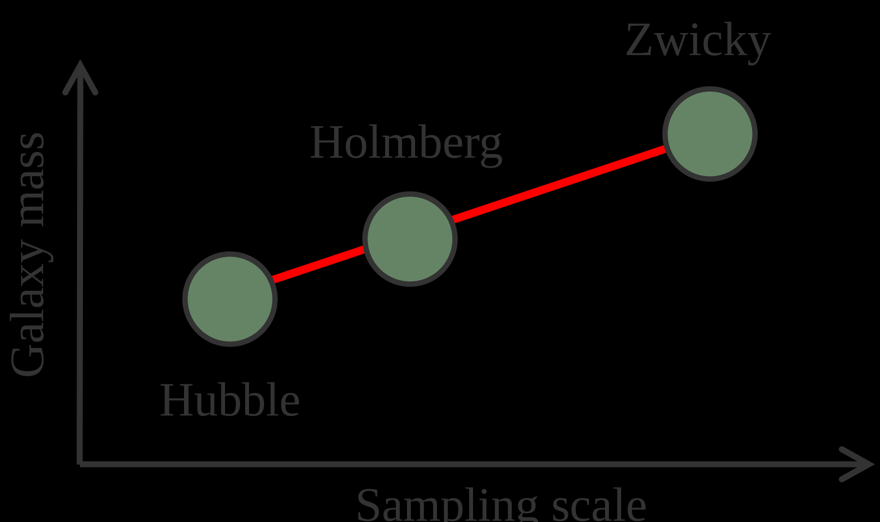

Modern compilation

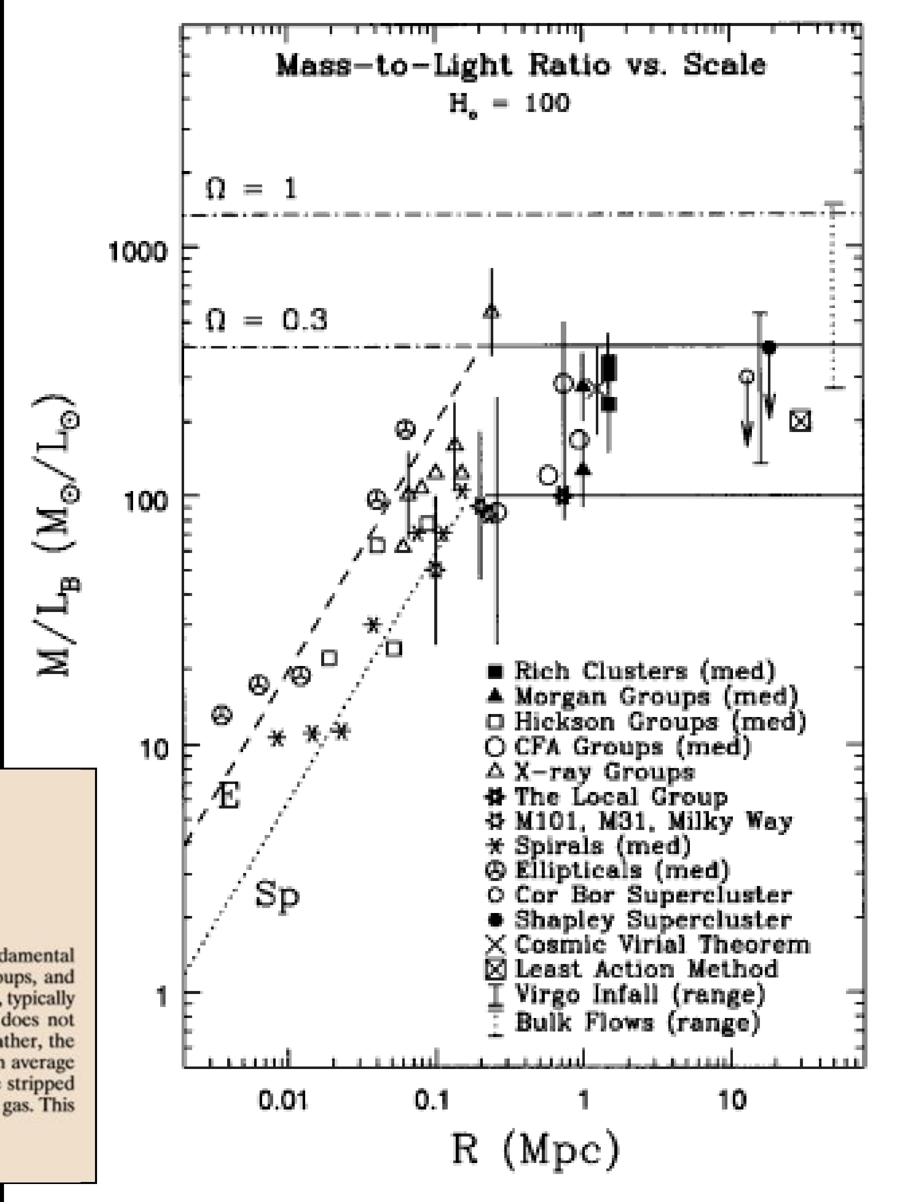

THE ASTROPHYSICAL JOURNAL, 447:L81–L85, 1995

WHERE IS THE DARK MATTER?

NETA A. BAHCALL, LORI M. LUBIN, AND VICTORIA DORMAN
Princeton University Observatory, Princeton, NJ 08544
Received 1995 Mar 27; accepted 1995 May 4

ABSTRACT

How much dark matter is there in the universe and where is it located? These are two of the most fundamental questions in cosmology. We use in this paper optical and X-ray mass determinations of galaxies, groups, and clusters of galaxies to suggest that most of the dark matter may reside in very large halos around galaxies, typically extending to ~200 kpc for bright galaxies. We show that the mass-to-light ratio of galaxy systems does not increase significantly with linear scale beyond the very large halos suggested for individual galaxies. Rather, the total mass of large-scale systems such as groups and rich clusters of galaxies, even superclusters, can on average be accounted for by the total mass of their member galaxies, including their large halos (which may be stripped off in the dense cluster environment but still remain in the clusters) plus the mass of the hot intracluster gas. This conclusion also suggests that we may live in a low-density universe with $\Omega \sim 0.2$–0.3.

The rotation of spiral galaxies

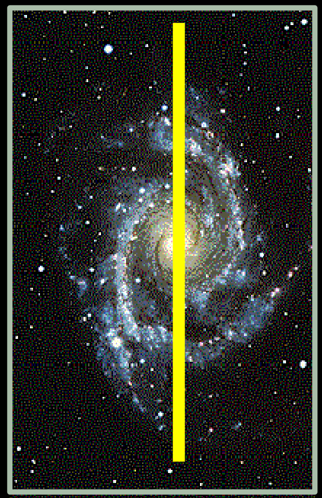

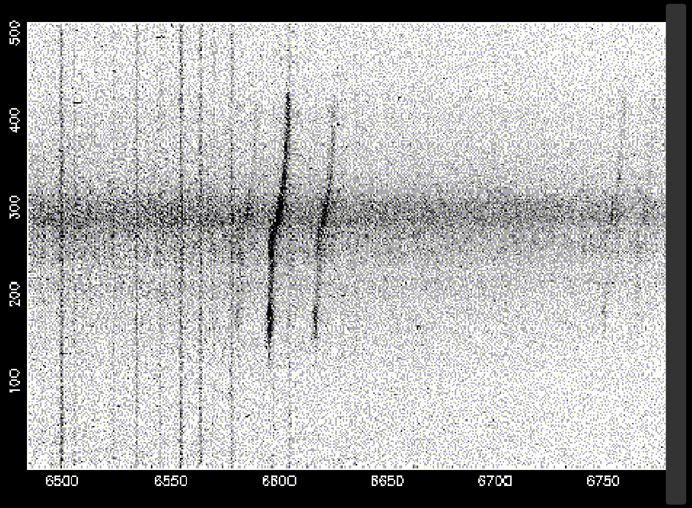

Early pioneers (still unclear nature of the nebulae):

- V. Slipher (1914) detected inclined absorption lines in nuclear spectra of M31 and Sombrero Nebula, and
- M. Wolf (1914) in M81.

- This led G. Pease (1918) to use the Mt. Wilson 60-inch to "investigate the rotation of the great nebula in Andromeda" with exposures of about 80 hours.

The rotation curve

NGC 5426, part of the interacting system Arp 271

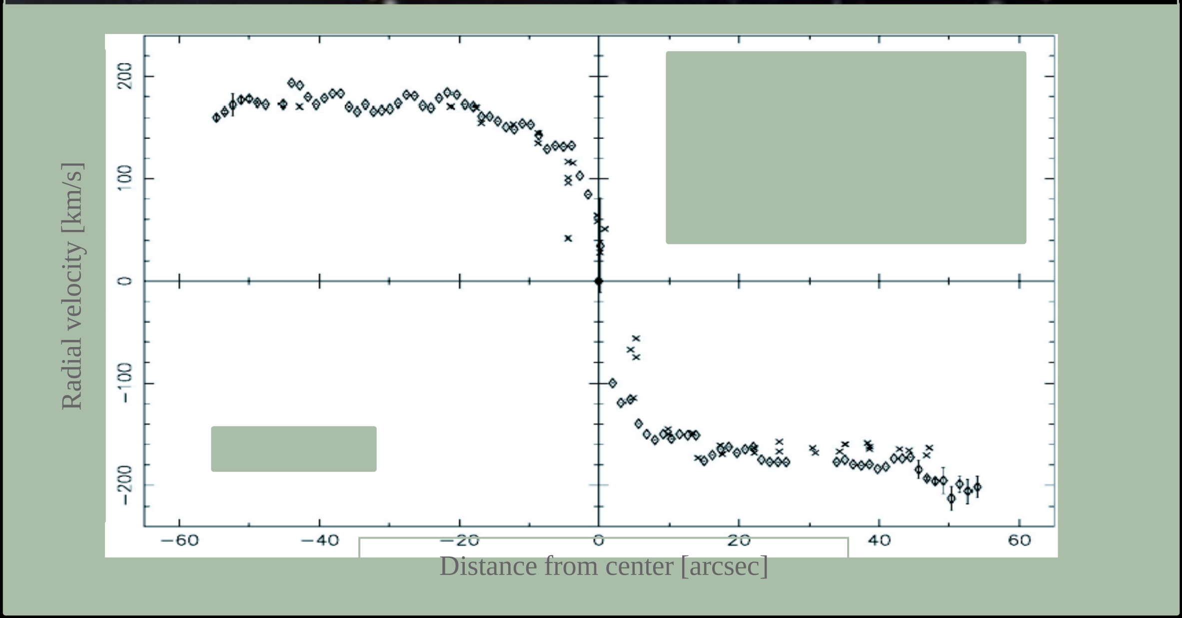

Expected rotation for *M/L = const.*

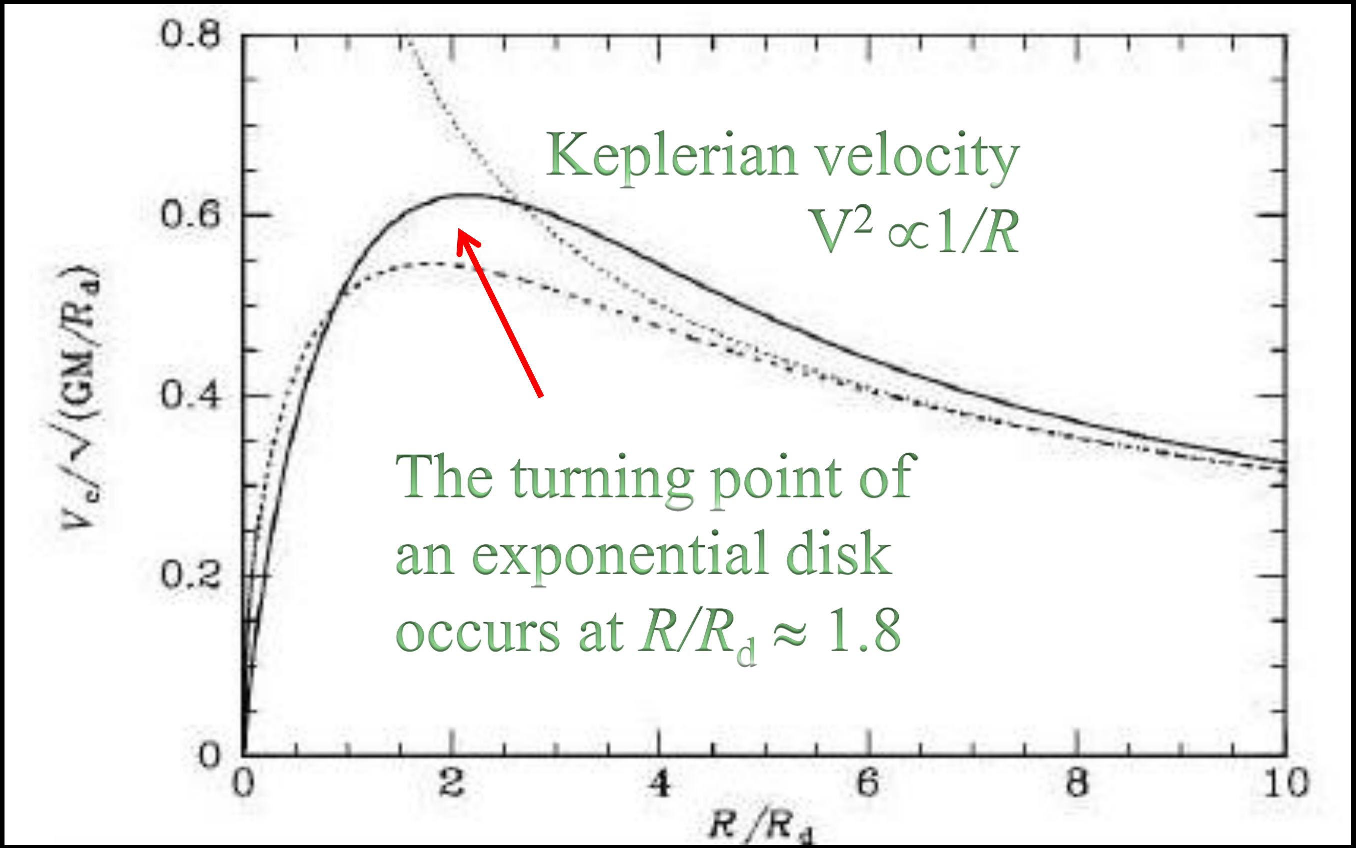

Circular velocity V_C (normalized to R_d) for an exponential disk (solid line), compared to that of an exponential sphere (dashed line) and of a point mass (dotted line), all with the same mass

The coming into play of the 21 cm HI line

H. van der Hulst & J. Oort

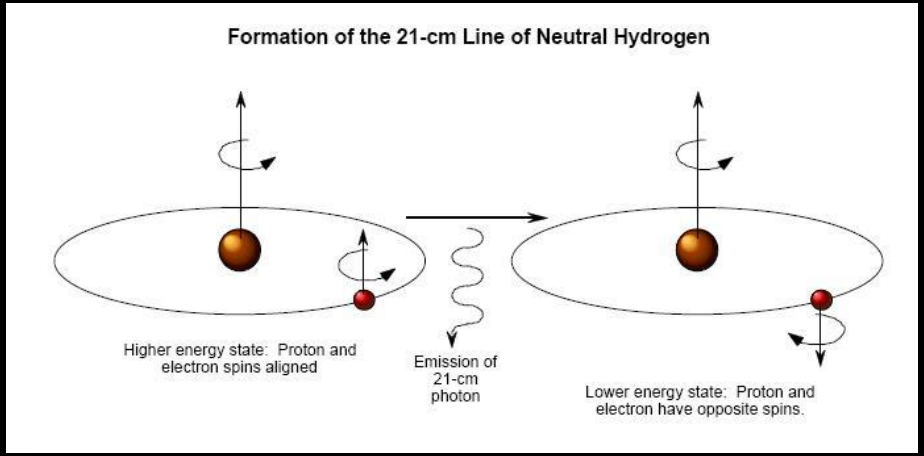

Westerbork Radio Telescope

The HI content of spirals

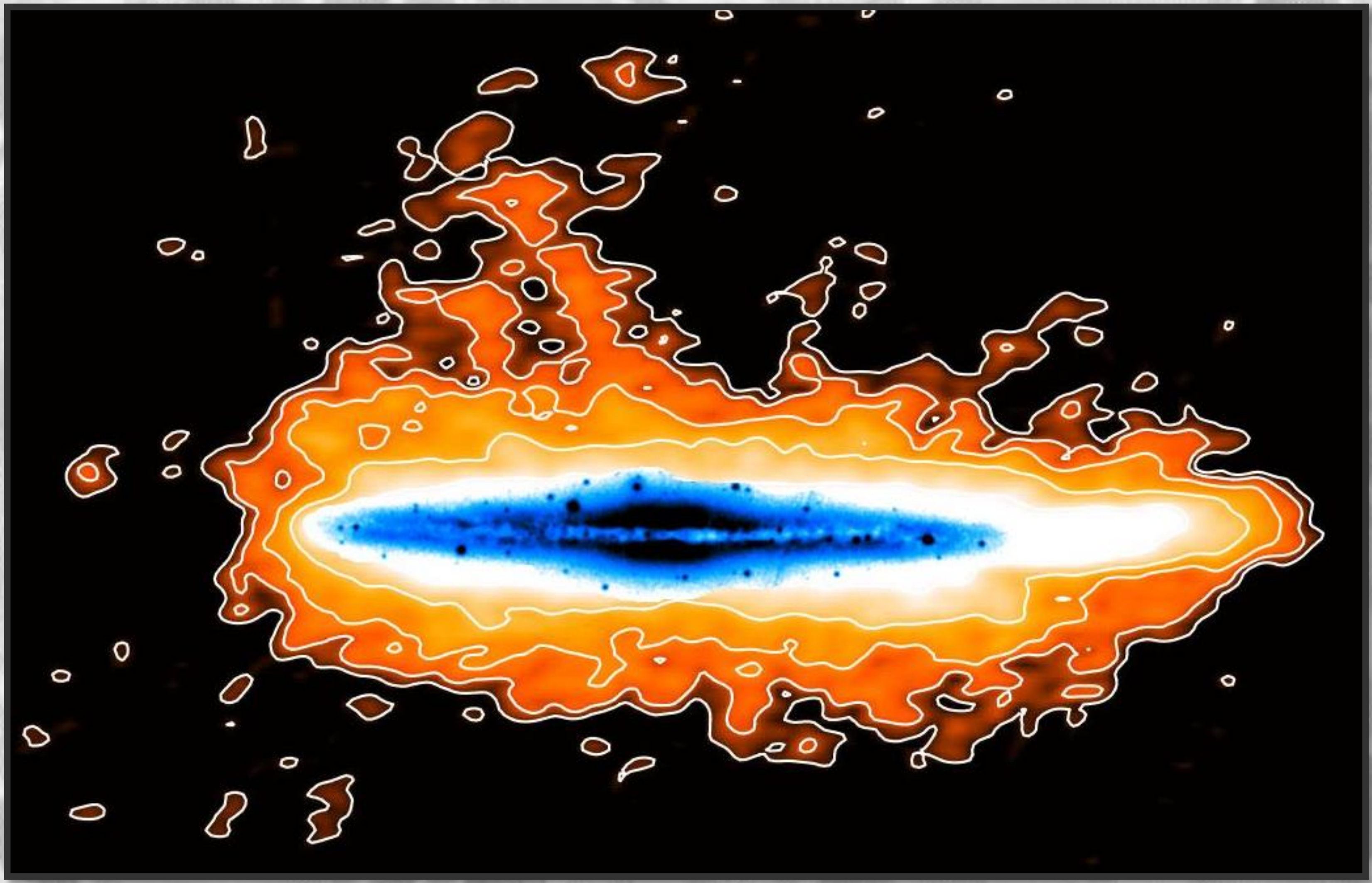

Neutral hydrogen halo of the edge-on spiral galaxy NGC 891
(Oosterloo et al., 2007)

The flat rotation curves from HI

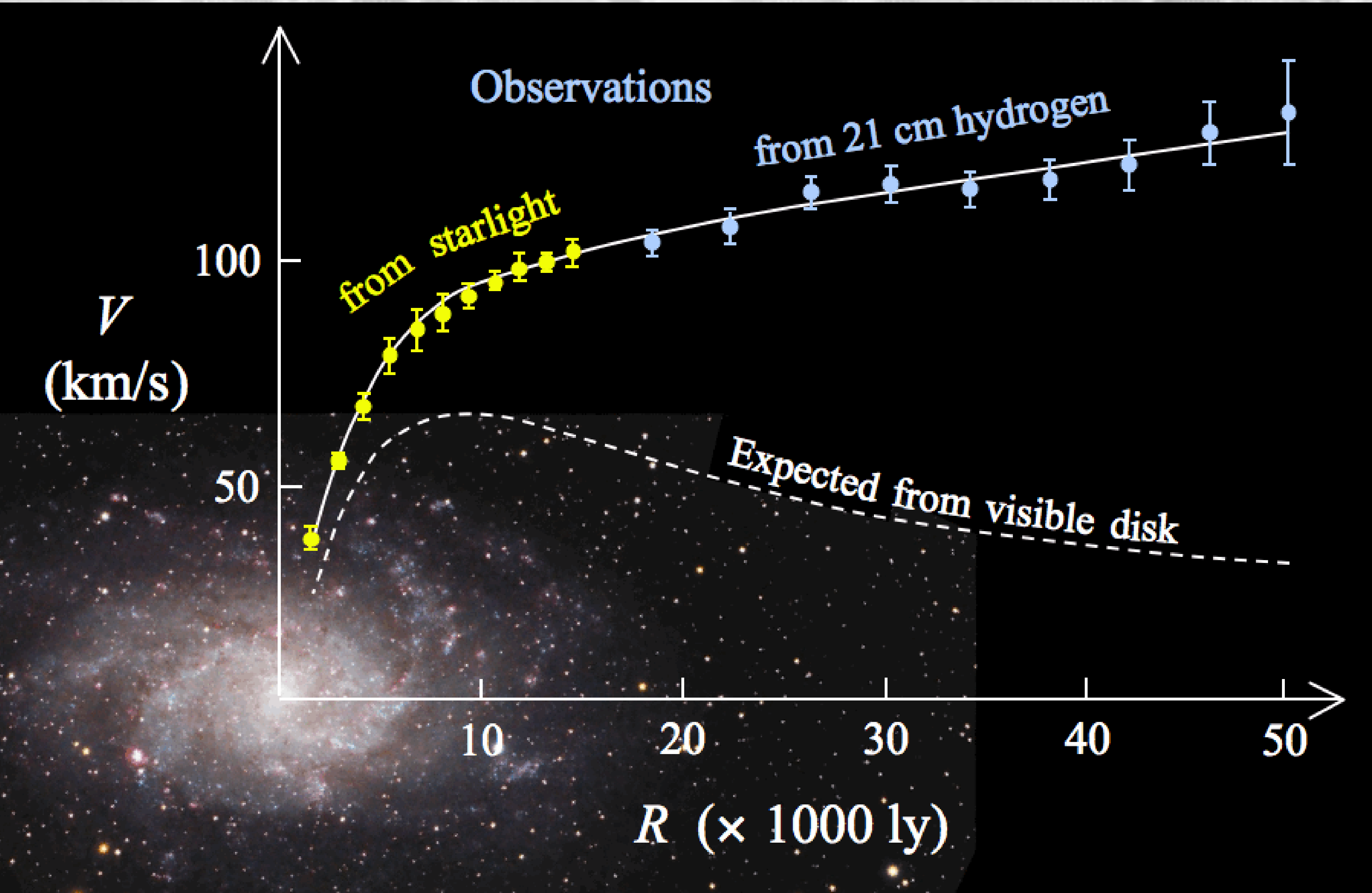

The flat rotation curves from HI

NGC 2403

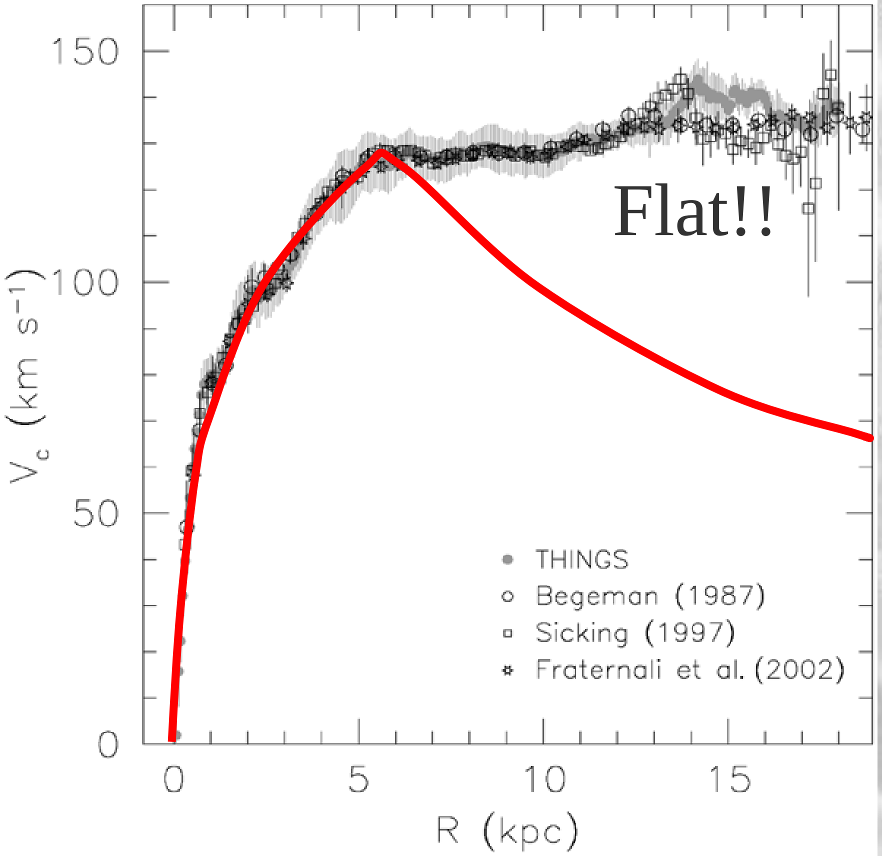

NGC 3198

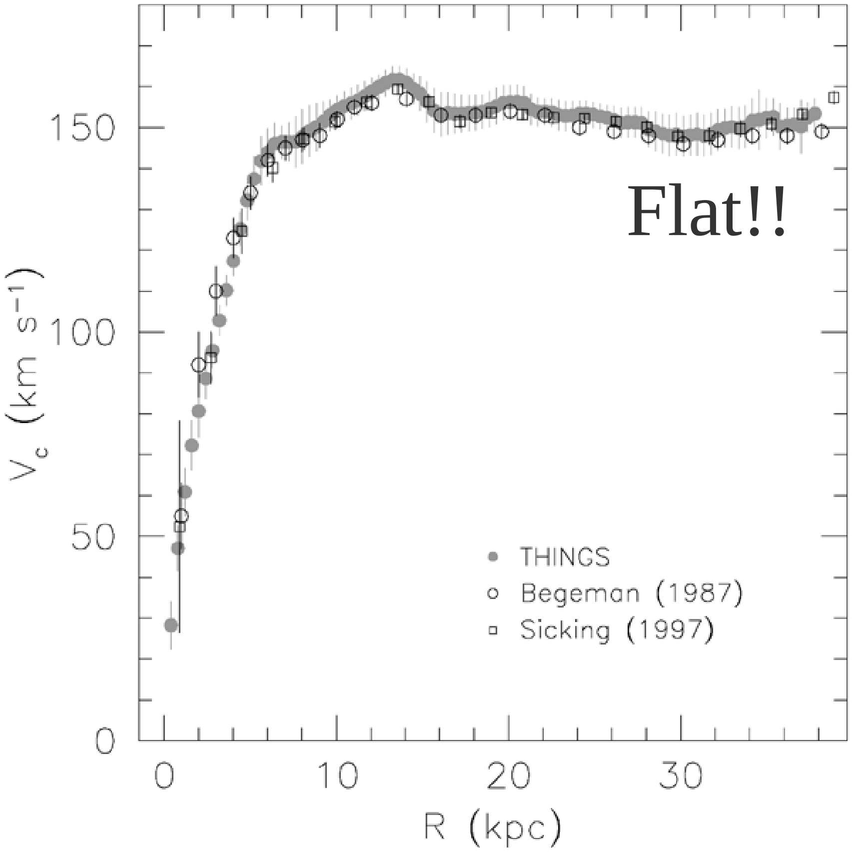

from the virial theorem: $M(r) \propto r$

too steep for the light to cope with it

The flat rotation curves of the Milky Way

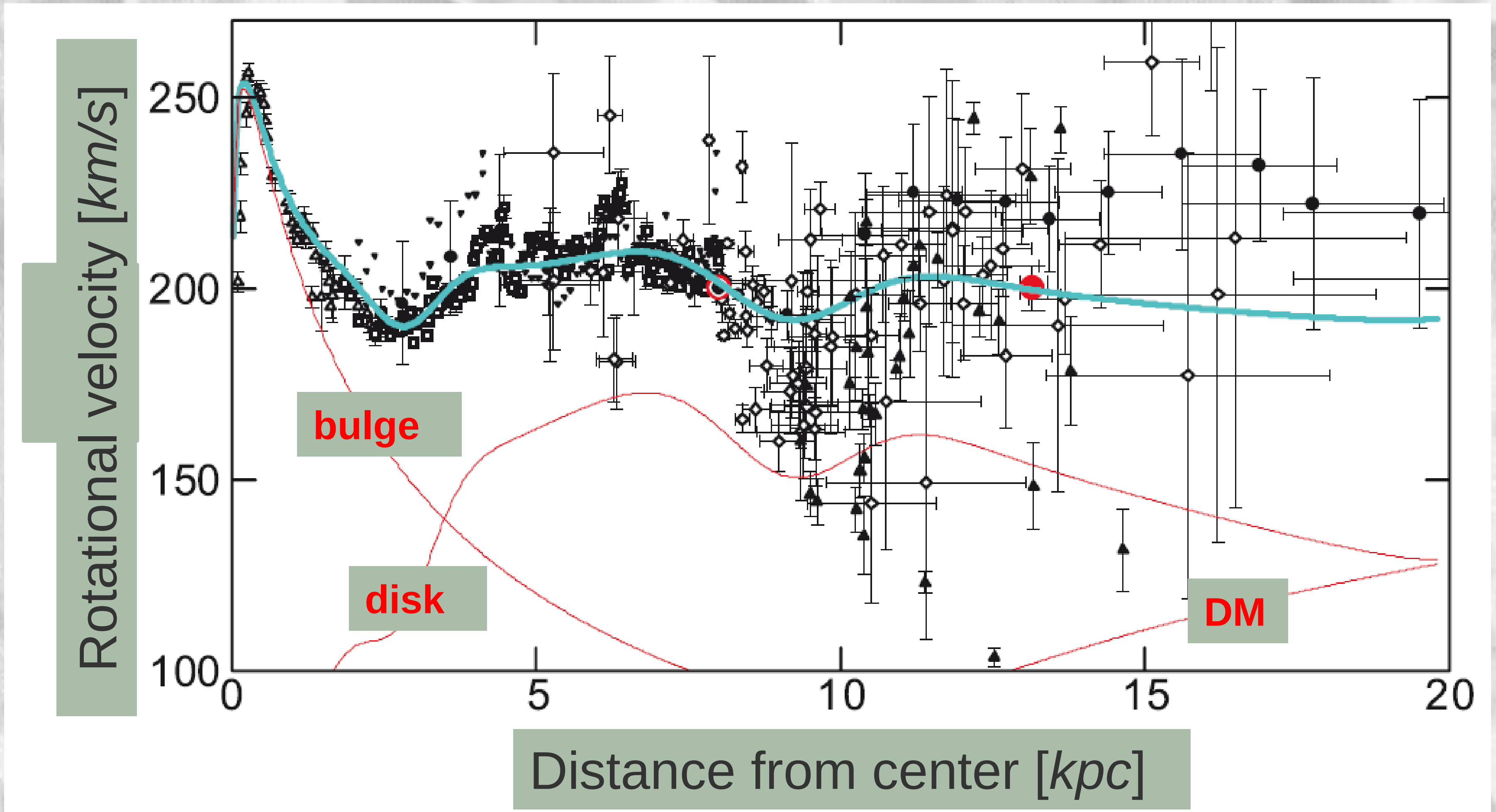

Decomposition of the rotation curve of the Milky Way into the components bulge, stellar disk + interstellar gas, dark matter halo (the red curves from left to right). From Sofue et al. (2009)

1974: the turning point

The majority of astronomers did not become convinced of the need of any Dark Matter in galaxies until:

- Ostriker & Peebles (1973) speculated on stability of disks;
- Ostriker, Peeeble & Yahil (1974) showed that "the mass of spiral galaxies increases almost linearly with radius to nearly 1 Mpc";
- Einasto et al. (1974) provided the dynamical evidence (from hot gas haloes just discovered) that galaxies ought to be surrounded by "massive coronae";
- Ozernoy (1974-1975) argued that the missing mass has to be dispersed in space, and not constrained within individual galaxies.

1973: at least 30% of all spirals are barred.

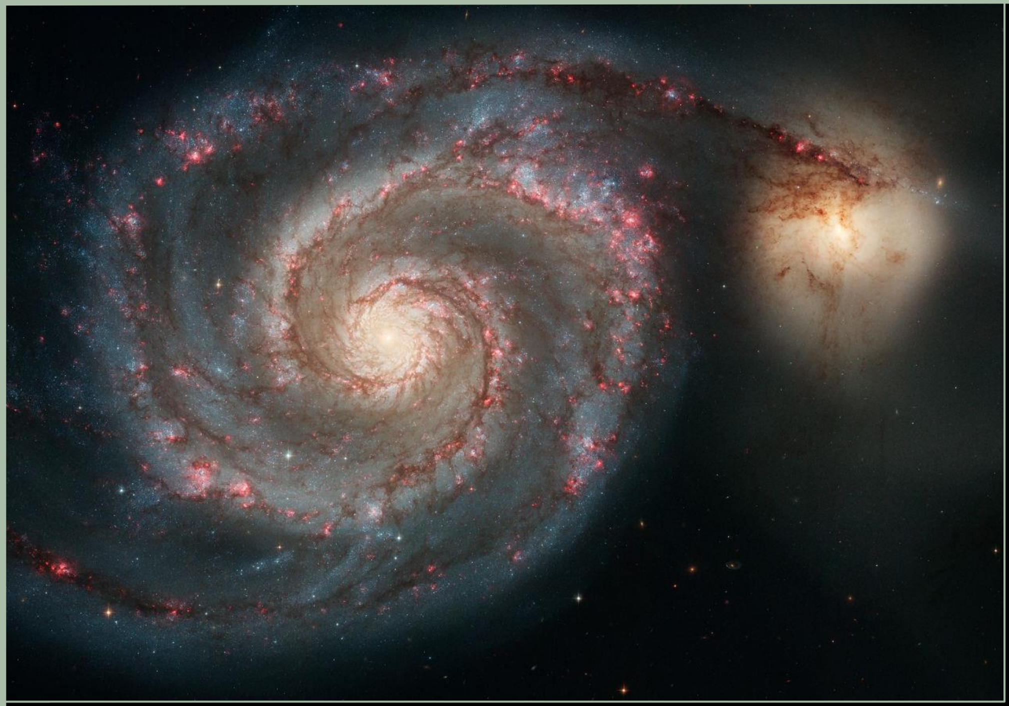

Ostriker & Peebles asked themselves why not all?

THE ASTROPHYSICAL JOURNAL, 186:467–480, 1973 December 1
© 1973. The American Astronomical Society. All rights reserved. Printed in U.S.A.

A NUMERICAL STUDY OF THE STABILITY OF FLATTENED GALAXIES: OR, CAN COLD GALAXIES SURVIVE?*

J. P. OSTRIKER
Princeton University Observatory

AND

P. J. E. PEEBLES
Joseph Henry Laboratories, Princeton University

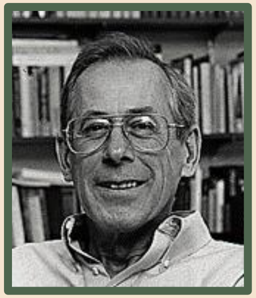

Received 1973 May 29

ABSTRACT

To study the stability of flattened galaxies, we have followed the evolution of simulated galaxies containing 150 to 500 mass points. Models which begin with characteristics similar to the disk of

The solution exists
but is not unique (BT pag. 603).
Also, there are many more barred spirals
than thought then.

then apparently the halo (spherical) mass *interior* to the disk must be comparable to the disk mass. Thus normalized, the halo masses of our Galaxy and of other spiral galaxies *exterior* to the observed disks may be extremely large.

Massive haloes

Letters to Nature

Nature **252**, 111-113 (8 November 1974)

Missing mass around galaxies: morphological evidence

JAAN EINASTO[*], ENN SAAR[*], ANTS KAASIK[*] & ARTHUR D. CHERNIN[†]

1. [*]W. Struve Astrophysical Observatory, Estonian SSR
2. [†]A. Joffe Physical-Technical Institute, Leningrad, USSR

RECENTLY we have obtained convincing empirical indications on the considerable role of hidden matter in the dynamics of single and double galaxies[1]. It seems that this matter is concentrated around massive galaxies, forming their coronas. The total mass of galaxies is about one order of magnitude greater than the mass of their visible parts.

Intergalactic Dark Matter

L. M. Ozernoi,
Akademiia Nauk SSSR, Fizicheskii Institut, Moscow, USSR
Astronomicheskii Zhurnal, 51, 1108, 1974.

Abstract
It is found that the ratio of the virial mass to the observed mass for galaxy systems ranging from pairs up to clusters on the average increases monotonically
with the system dimensions.
It is possible to exclude galaxies as the principal source of 'hidden' mass which is needed for the stationarity of galaxy systems.
It is reasoned that if the hidden mass does exist it should be localized in the intergalactic space.

Sudden paradigm change

BARYONS CRISIS

1. Primordial nucleosynthesis, supported by observations, states that the baryonic density is of the order of $0.04\rho_c$, where the critical density is: $\rho_c = 3H^2/8\pi G$

2. Primordial baryonic fluctuations seen in the CMBR are largely insufficient to drive galaxy formation.

Dark Matter as a life-vest for cosmologists

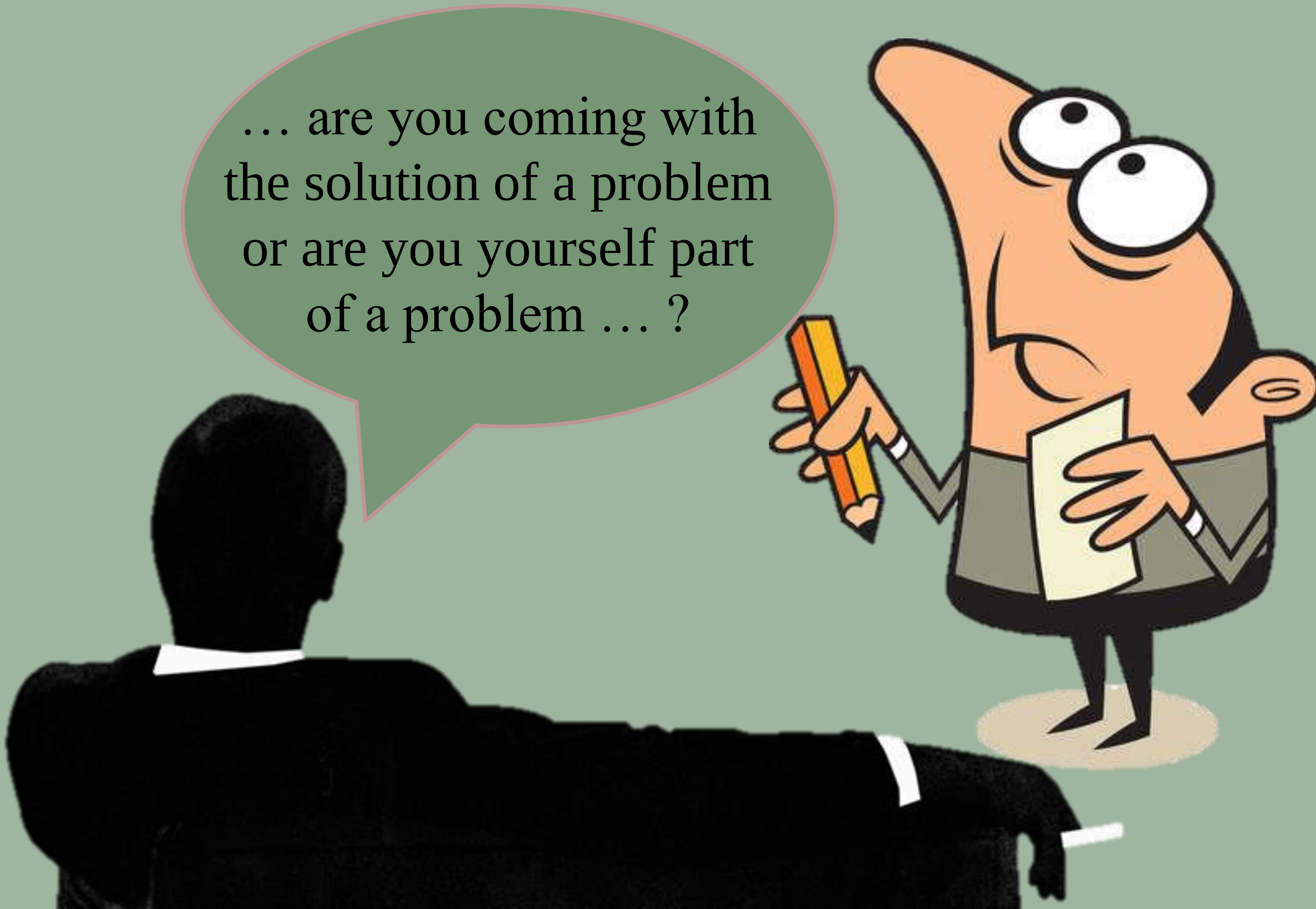

Dark Matter mapped by gravitational lensing

Cosmic shear is the distortion of the shapes of background galaxies due to the bending of light by the potentials associated with large-scale structure.

- For sources at $z_s \sim 1$ and structure at $0.1 < z < 1$, it is a percent level effect which can only be detected statistically.
- Theoretically clean.
- Observationally tractable.

VST KiDS

VST@Paranal

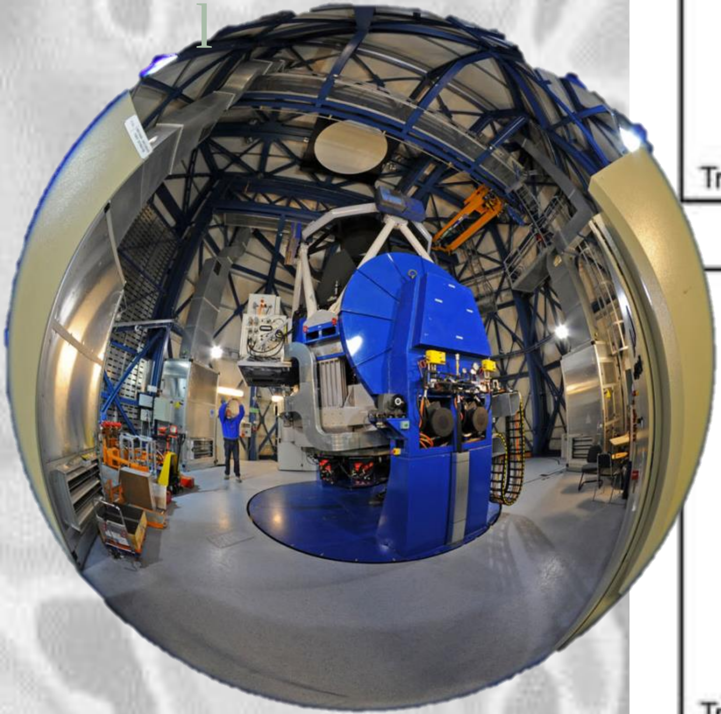

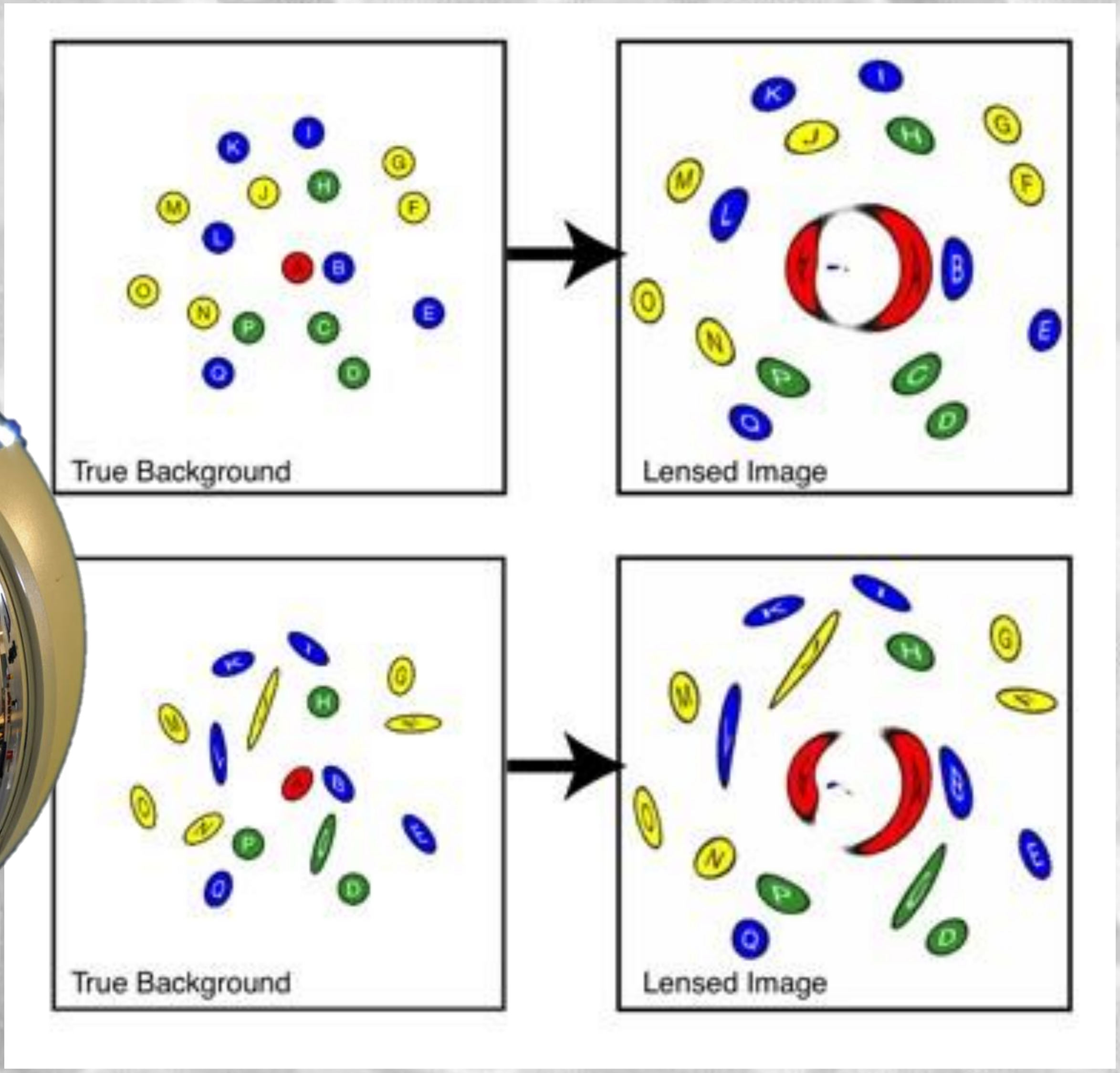

Dark Matter halo mass vs. stellar mass.

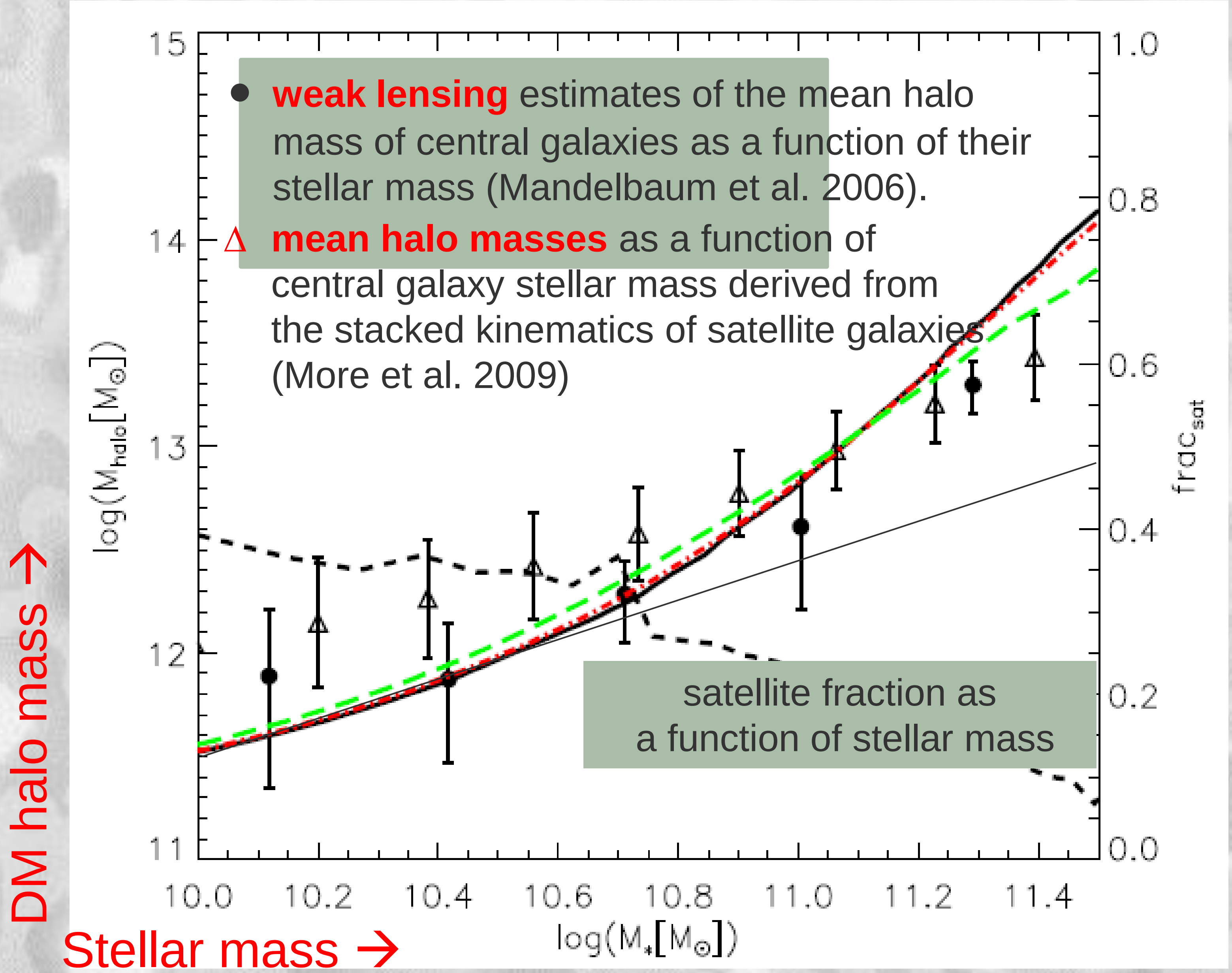

DM evidence: the smoking gun

“*Bullet cluster*” 1E 0657-56: composite image

DM evidence: dissipation vs. indifference

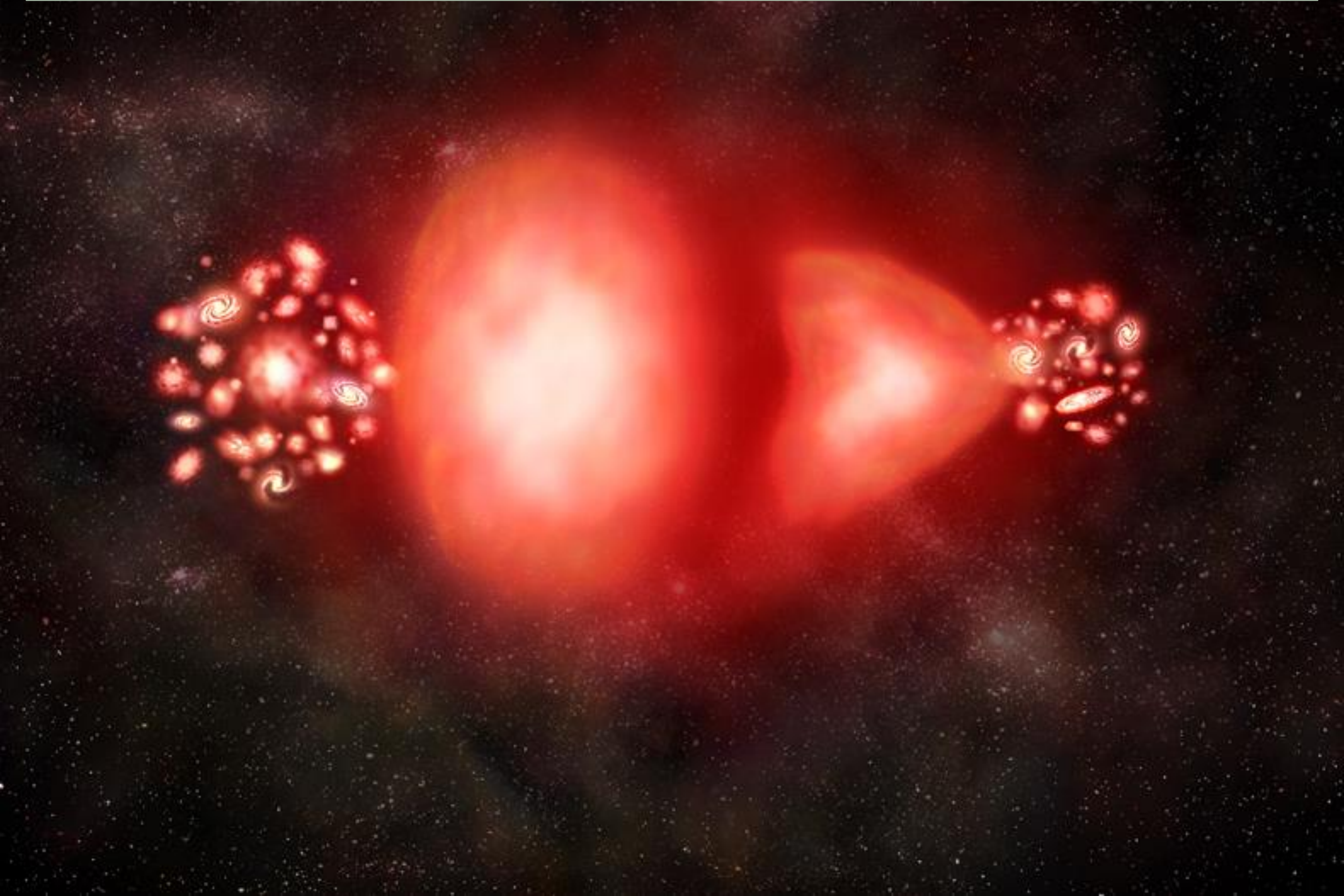

How dark is the Dark Matter?

Is the dark matter self-interacting?

Baryons mapping DM: no self-interaction

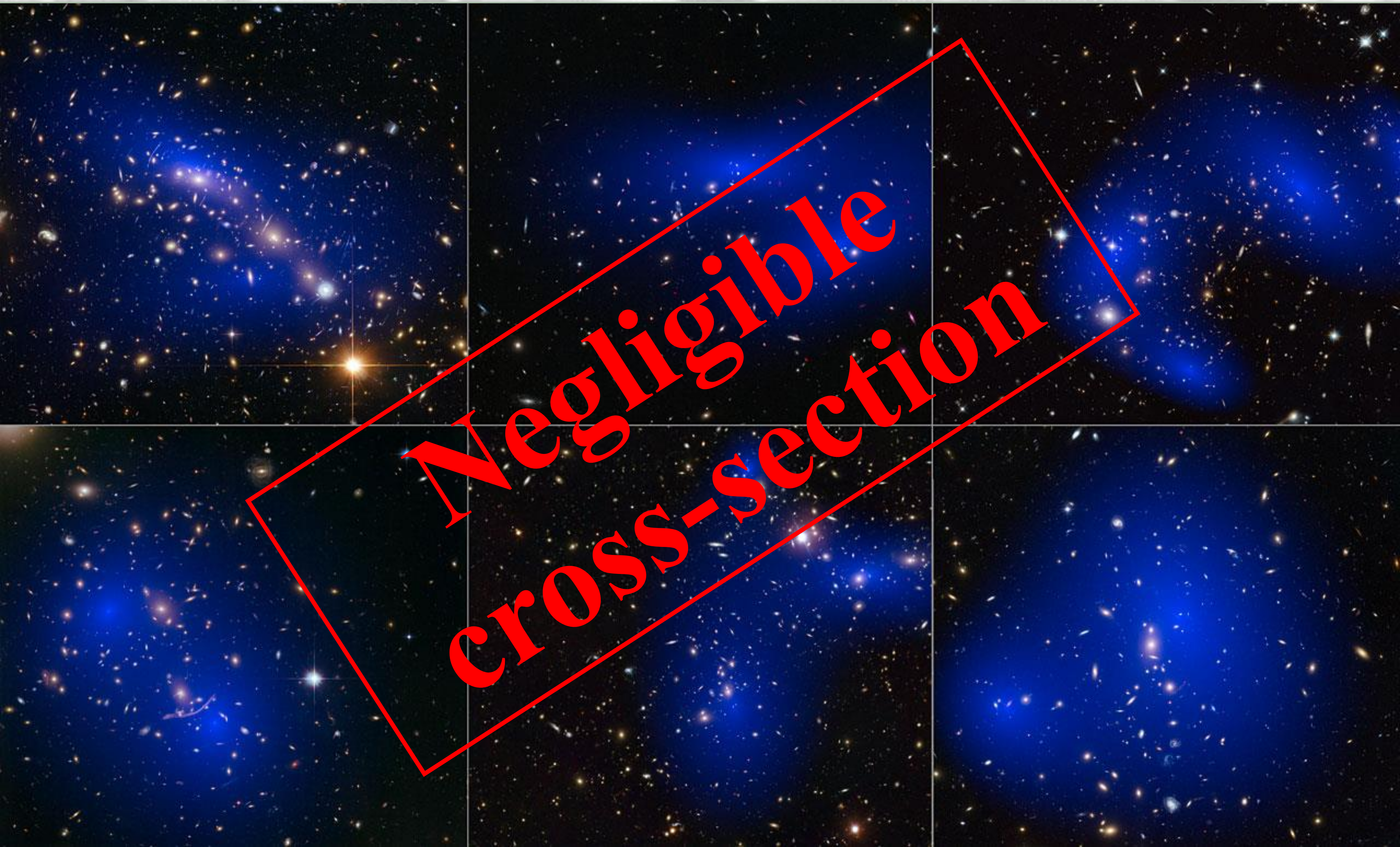

But …

Abell 3827, as taken by Hubble

Multi Unit Spectroscopic Explorer (MUSE)

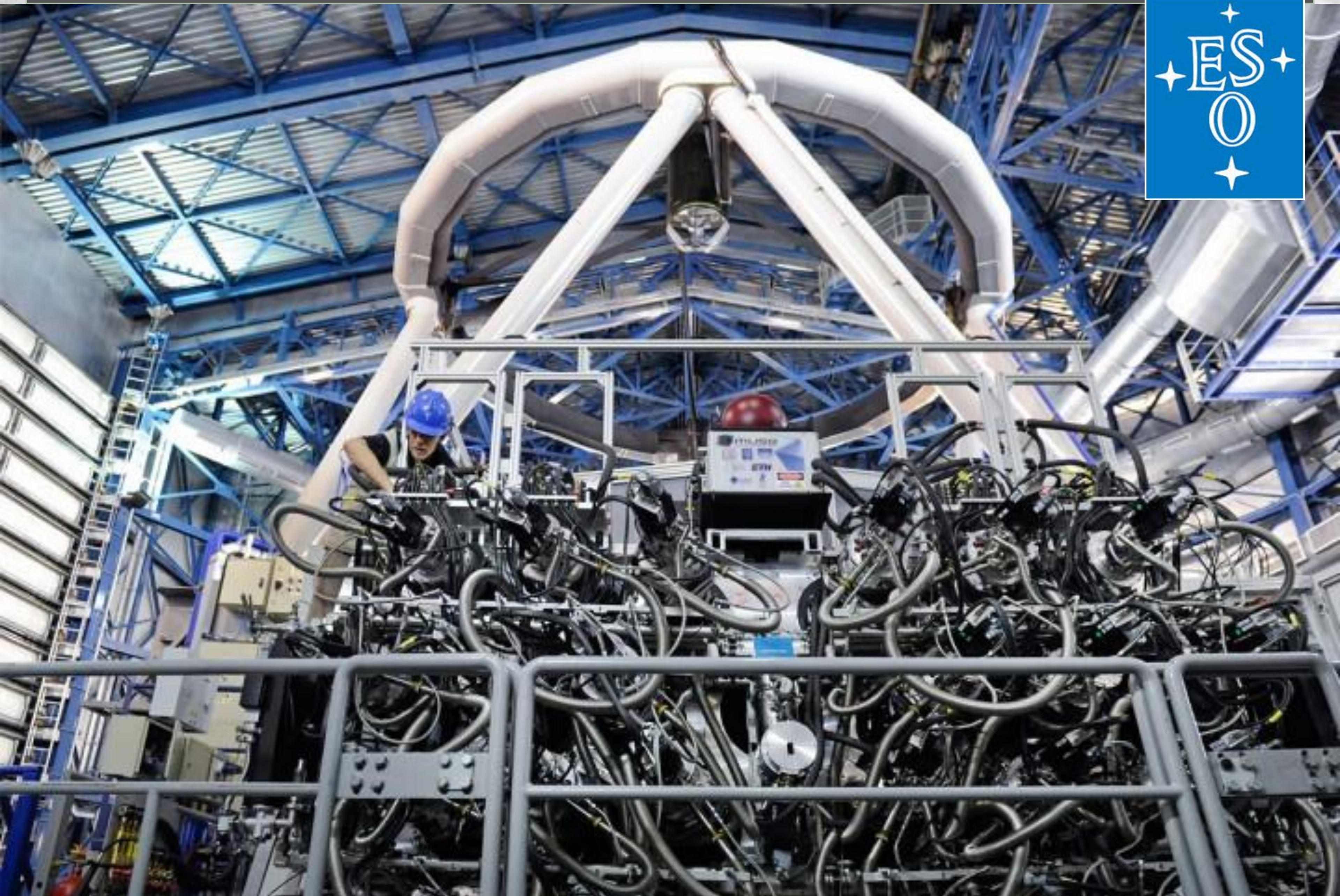

Traces of self-interaction ?

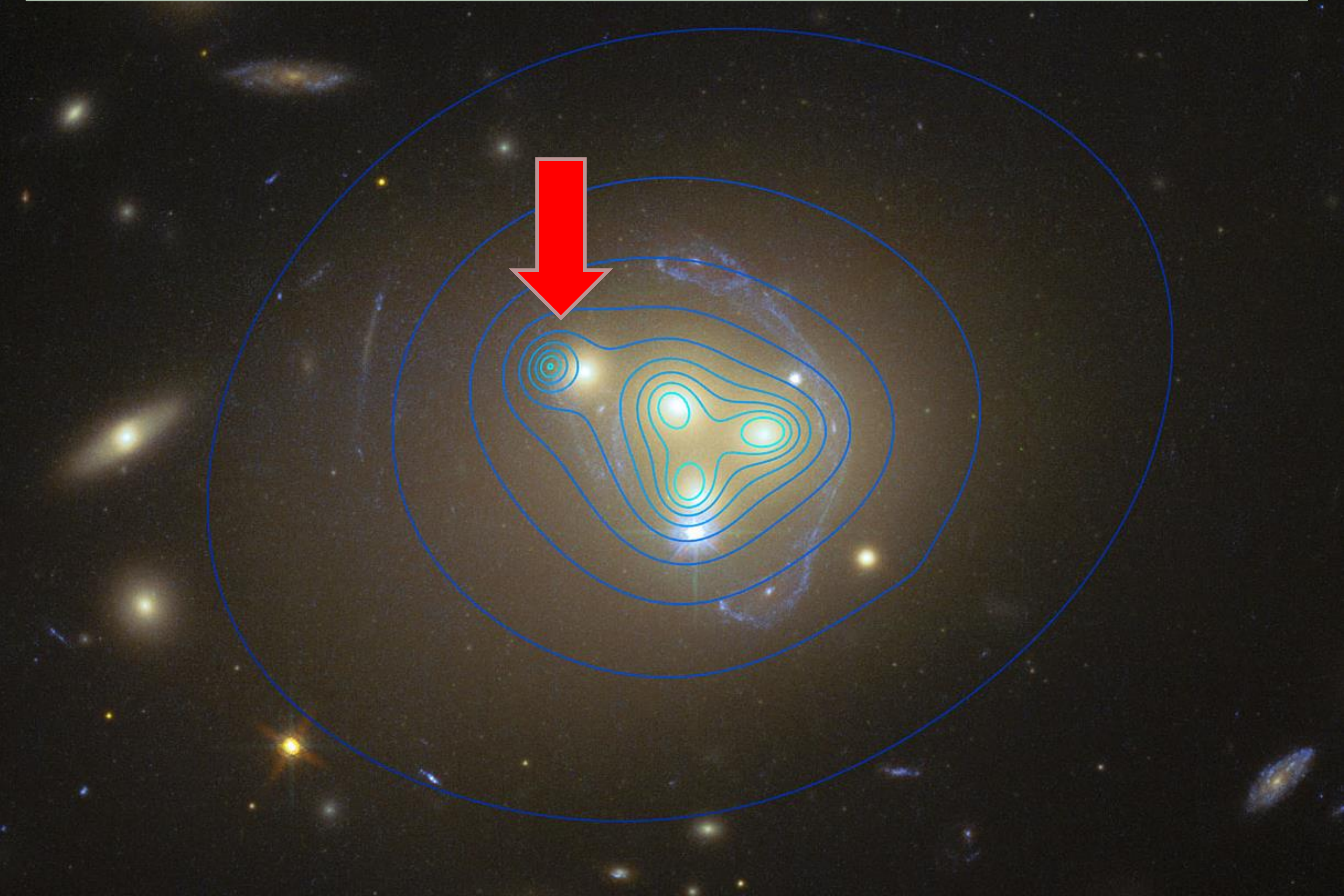

Traces of self-interaction ?

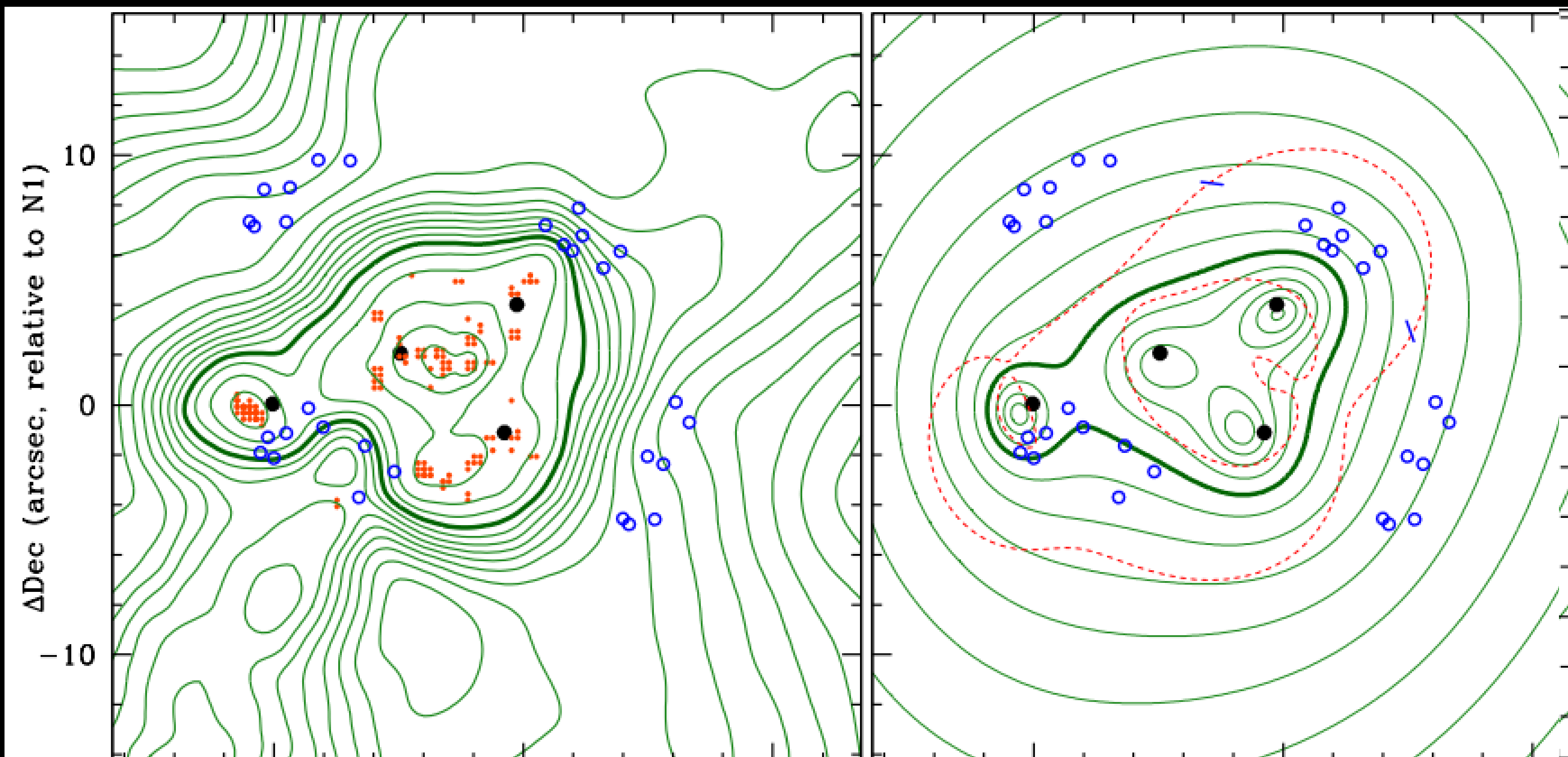

Baryon acoustic oscillations

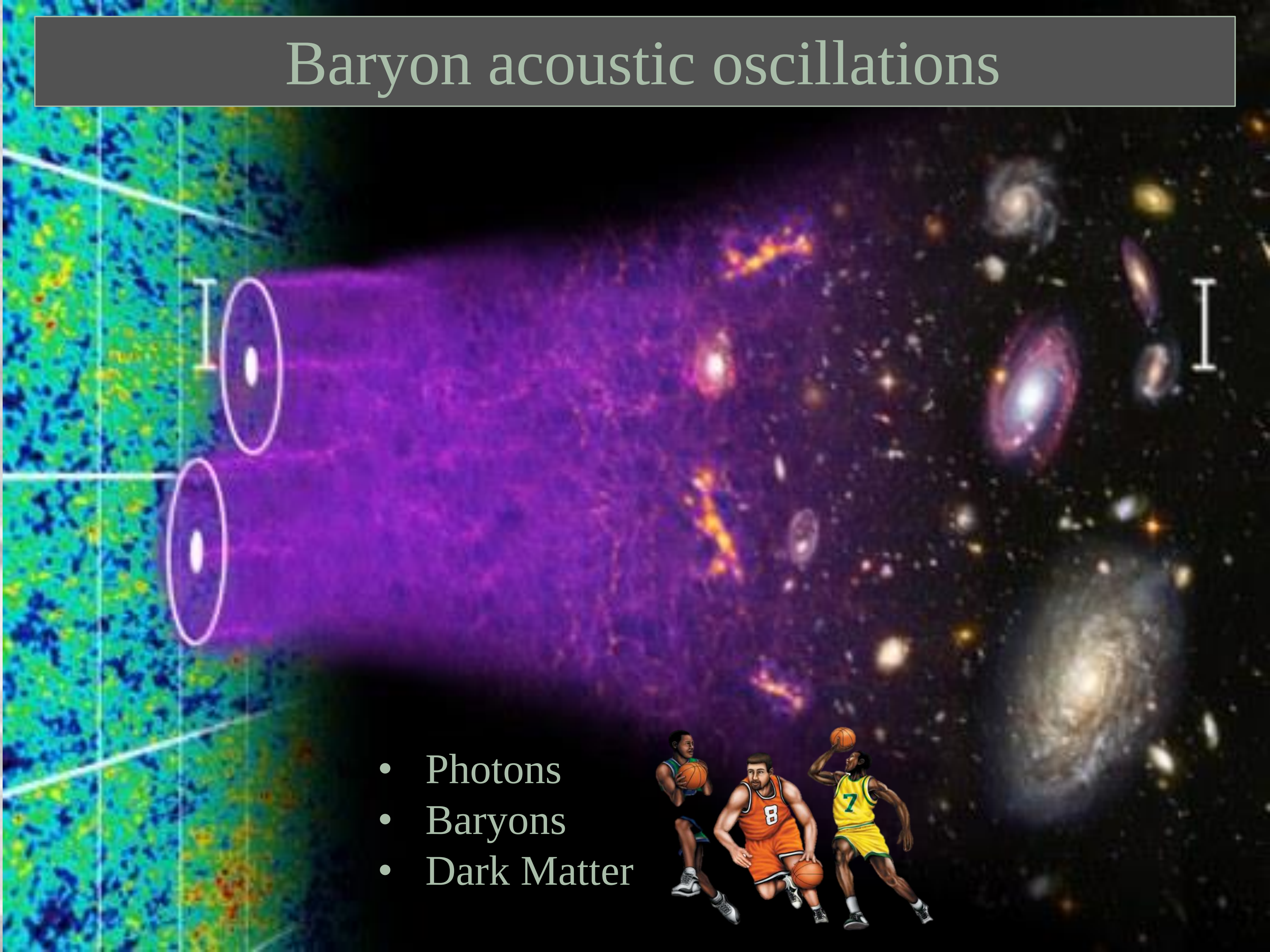

- Photons
- Baryons
- Dark Matter

Concluding … with questions

- Does Dark Matter exist ?
- Remember Vulcan.

- How much is it ?
- Less than originally thought owing to DE.

- What is it ?
- So far God knows.

- Is it self-interacting ?
- Possibly….

Dark Energy

Dark energy is a hypothetical form of matter that fills the space of our Universe and causes of acceleration expansion of our Universe. More is unknown than is known. We know how much dark energy there is because we know how it affects the Universe's expansion. Other than that, it is a complete mystery.

According to the Planck mission data, the total density of the Universe contains 5% of baryons, 27% of dark matter, and 68% of dark energy.

Among several proposed forms for dark energy two are the most attractive: the cosmological constant, a new fundamental physical constant, another explanation for dark energy is that it is a new kind of dynamical energy fluid or field, something that fills all of space but something whose effect on the expansion of the Universe is the opposite of that of matter and normal energy.

Several groups of astronomers published in 1998 results of their observations of SN Ia. The conclusion was that our Universe is expanding with acceleration. The Nobel Prize was awarded for this work in 2011.

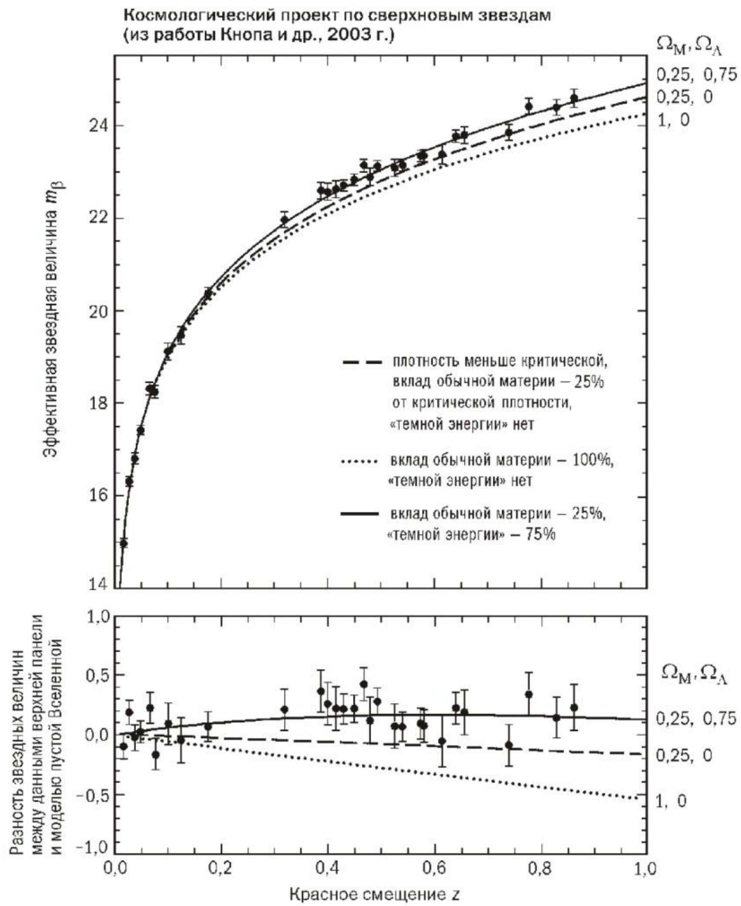

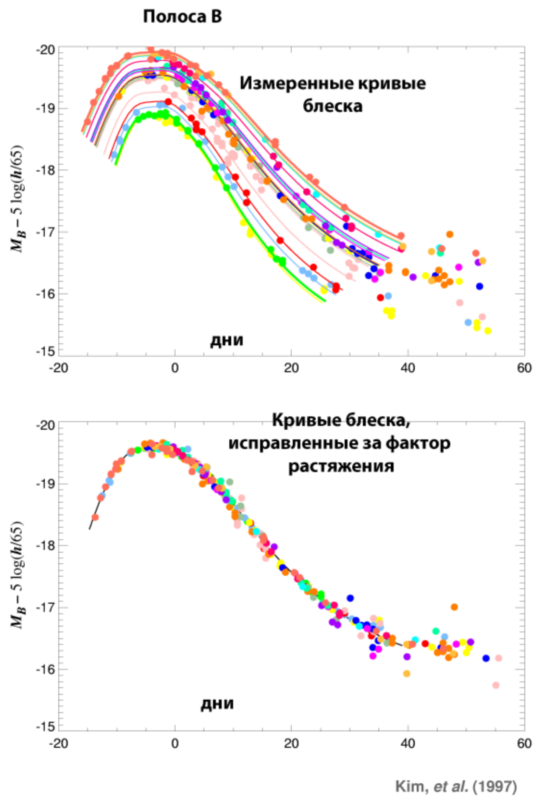

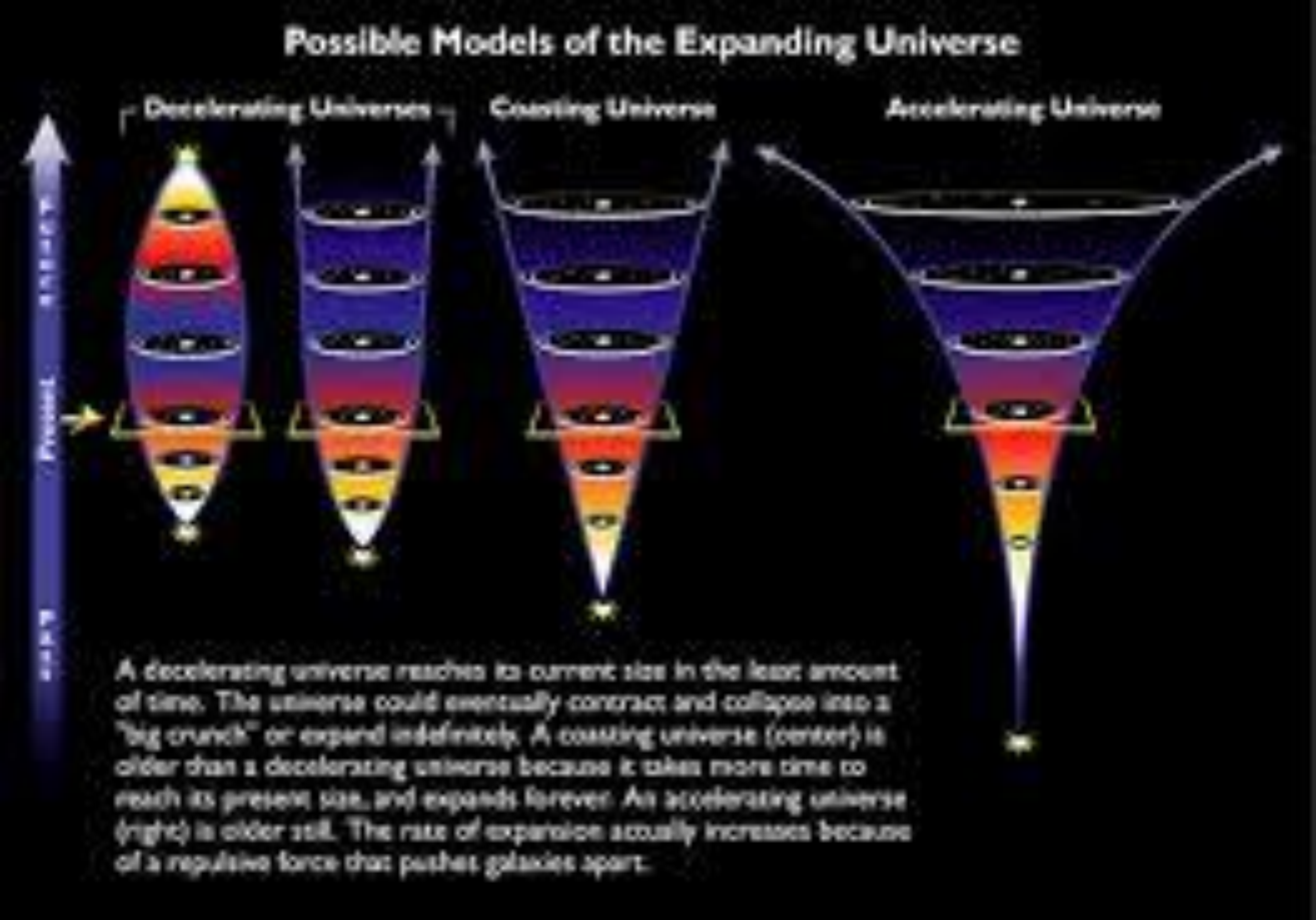
Possible Models of the Expanding Universe
Decelerating Universes
Coasting Universe
Accelerating Universe
A decelerating universe reaches its current size in the least amount of time. The universe could eventually contract and collapse into a "big crunch" or expand indefinitely. A coasting universe (center) is older than a decelerating universe because it takes more time to reach its present size, and expands forever. An accelerating universe (right) is older still. The rate of expansion actually increases because of a repulsive force that pushes galaxies apart.

We see that cosmology really has the status of a respectable science. It has already found definite results forming a solid backbone. It is the status of the Big Bang theory.

Cosmology has definite, well formulated basis, waiting for systematic research. This means that there is no danger of unemployment in cosmology.

Moscow, 1 September 2016

Thank you for attention